Optogenetic approaches to the study of hippocampal long-term plasticity

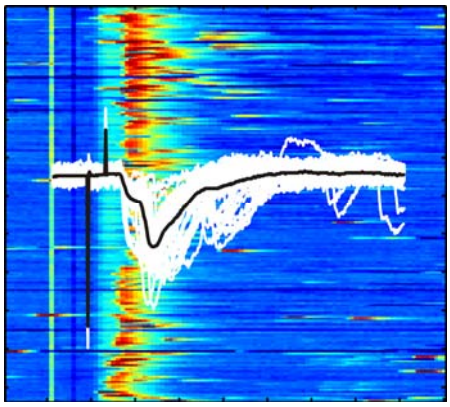

Inauguraldissertation
zur
Erlangung der Würde eines Doktors der Philosophie
vorgelegt der
Philosophisch-Naturwissenschaftlichen Fakultät
der Universität Basel
von

Philipp Schönenberger Lawrence
aus Arbon, Schweiz

Basel, 2011

creative commons

Namensnennung-Keine kommerzielle Nutzung-Keine Bearbeitung 2.5 Schweiz

---

Sie dürfen:

das Werk vervielfältigen, verbreiten und öffentlich zugänglich machen

Zu den folgenden Bedingungen:

Namensnennung. Sie müssen den Namen des Autors/Rechteinhabers in der von ihm festgelegten Weise nennen (wodurch aber nicht der Eindruck entstehen darf, Sie oder die Nutzung des Werkes durch Sie würden entlohnt).

Keine kommerzielle Nutzung. Dieses Werk darf nicht für kommerzielle Zwecke verwendet werden.

Keine Bearbeitung. Dieses Werk darf nicht bearbeitet oder in anderer Weise verändert werden.

- Im Falle einer Verbreitung müssen Sie anderen die Lizenzbedingungen, unter welche dieses Werk fällt, mitteilen. Am Einfachsten ist es, einen Link auf diese Seite einzubinden.
- Jede der vorgenannten Bedingungen kann aufgehoben werden, sofern Sie die Einwilligung des Rechteinhabers dazu erhalten.
- Diese Lizenz lässt die Urheberpersönlichkeitsrechte unberührt.

Quelle: http://creativecommons.org/licenses/by-nc-nd/2.5/ch/ Datum: 3.4.2009

Genehmigt von der Philosophisch-Naturwissenschaftlichen Fakultät

auf Antrag von

Dr. Thomas G. Oertner, Prof. Dr. Silvia Arber, Prof. Dr. Dominique Muller

Basel, den 14. Dezember 2010

Dekan

Prof. Dr. Martin Spiess

TABLE OF CONTENTS

1. SUMMARY

Synaptic plasticity is one of the cellular mechanisms thought to underlie learning and memory formation. Enormous progress has been made in the last two decades concerning the molecular mechanisms of plasticity induction and expression for both long-term potentiation (LTP) and long-term depression (LTD). LTP and LTD, together with so-called homeostatic plasticity that keeps overall activity levels near a certain set point, are experimental models for the processes that are thought to enable neuronal circuits to adapt to changing requirements and to store information. Electrophysiological approaches allow inducing synaptic plasticity with high reliability, which is ideal to study the precise molecular pathways involved in changing synaptic strength. However, it remains unclear how stable these changes in synaptic strength are. A better understanding of the long-term stability of synaptic plasticity will be crucial to better understand the relationship between synaptic plasticity and memory formation. The present thesis consists of three main parts. In the first part we explore the resolution limits of optogenetic stimulation, which relies on the activation of the light-gated ion channel channelrhodopsin-2 (ChR2) by blue light. In the second part we characterize the photocycle of an engineered ChR2 variant with very slow channel kinetics and show that light-induced firing can alter gene expression in stimulated neurons. In the third part we present a novel class of ChR2 variants that enormously improves the reliability of optogenetic neuronal stimulation and will allow delivering plasticity-inducing stimuli to genetically targeted neurons in a non-invasive manner.

Part I: Spatial resolution of ChR2 activation

We investigate the spatial resolution of ChR2 excitation by one-photon activation using focal laser illumination. Interestingly, resolution in hippocampal slice culture and dissociated hippocampal cells is best at minimal light intensities. At high light intensities, focal saturation of excitation and increased out-of-focus ChR2 activation degrade spatial selectivity of channel stimulation. We show that a trade-off between photocurrent amplitude and the local specificity of ChR2 activation determines the spatial precision of optical action potential (AP) induction. Furthermore, local stimulation allows to induce APs with more physiological shapes that wide-field illumination.

Part II: Photocycle of bi-stable channelrhodopsins and effect of light-controlled firing on immediate early gene expression

The so-called bi-stable channelrhodopsins have open channel state lifetimes of seconds to minutes. We show that the photocycle of the ChR2(C128A) variant is branched. Accumulation of desensitized channel in a long-lived non-conducting state leads to progressive reduction of photocurrent amplitudes. Vigorous burst firing can be elicited by ChR2(C128A) activation even with minimal light intensities, but the number of bursts is limited by photocurrent run-down. Finally, we show that high-frequency AP firing mediated by the C128A mutant can induced c-Fos expression in a cell-autonomous manner, which may be exploited to identify light-responsive neurons or to induce expression of foreign proteins under control of the c-fos promoter with precise timing and single cell specificity.

Part III: High-efficiency channelrhodopsins for high-frequency spiking and optical control of synaptic plasticity

Optogenetic control of synaptic plasticity has been hindered by the large cell-to-cell variability in the reliability of optical AP induction. We characterize the novel ChR2(T159C) mutation that dramatically increases photocurrents. When introduced in a wild-type background, the TC mutation generates very large photocurrents and sensitizes neurons to very low light intensities. Because TC can trigger several APs in response to a single light pulse, we combined the TC mutation with the previously reported E123T mutation to increase channel speed. ChR2(E123T/T159C), or simply ET/TC, combines large photocurrents with rapid channel kinetics and allows triggering single APs with high reliability up to 60 Hz. In contrast to currently used channelrhodopsins, the rapid ET/TC kinetics are preserved even at depolarized membrane potentials, which speeds up membrane repolarization after AP firing and allows high-frequency spiking even during plateau depolarizations in pyramidal neurons. In conclusion, the novel TC variants will greatly improve the reliability of optogenetic plasticity induction and enable us to investigate the long-term fate of changes in synaptic strength.

2. INTRODUCTION

2.1 Synaptic plasticity

The capacity to generate new neurons in the adult brain is very limited and thus is very unlikely to underlie learning and memory formation. Santiago Ramón y Cajal therefore already at the end of the 19th century proposed that memories are stored in the synaptic connections between neurons, where electrical and chemical signals are exchanged (Jones, 1994). In 1949, the Canadian psychologist Donald Hebb proposed an elegant model how strengthening of existing synapses in response to correlated firing of pre- and postsynaptic neurons can implement associative learning in neuronal assemblies (Hebb, 1949). Over the last 45 years, different forms of synaptic plasticity, i.e. strengthening or weakening of synapses, have been observed in various brain regions, and synaptic plasticity has become the most important experimental paradigm for the cellular mechanisms thought to underlie learning and memory formation.

2.1.1 Forms of synaptic plasticity

Long-term potentiation

Long-term potentiation (LTP) is the persistent enhancement of synaptic strength and can be induced in a large number of brain regions. LTP has been studied extensively at the hippocampal Schaffer collateral (SC)-CA1 synapse. The induction of LTP in the CA1 area of the hippocampus depends on activation of NMDA receptors and strong postsynaptic Ca2+ influx (reviewed in Malenka & Bear, 2004). Since NMDA receptors are blocked by Mg2+ ions at hyperpolarized membrane potentials, the postsynaptic neuron has to be depolarized by strong synaptic input or precisely timed back-propagating action potentials (bAPs) to allow strong Ca2+ influx and LTP induction (Markram *et al.*, 1997; Bi & Poo, 1998; Malenka & Bear, 2004; Holbro *et al.*, 2010). Ca2+ influx triggers a molecular signaling cascade that enhances synaptic transmission, first by phosphorylation of synaptic AMPA receptors (AMPARs) to increase single channel conductance (Barria *et al.*, 1997), and then by insertion of new AMPARs into the postsynaptic density (Song & Huganir, 2002). Both of these LTP expression mechanisms belong to the so-called early phase of LTP expression (E-LTP) that lasts 60 or so minutes and are independent of protein synthesis. In

contrast, late LTP (L-LTP) which maintains potentiated synaptic transmission over several hours depends on activation of kinase signaling pathways as well as gene transcription and protein synthesis (Kelleher *et al.*, 2004). Interestingly, with the induction and expression of L-LTP, synapses do not enter a new stable state. Instead, enhanced synaptic transmission seems to be actively maintained and can be destabilized by synaptic activity (Fonseca *et al.*, 2006a; Fonseca *et al.*, 2006b). This activity-dependent destabilization of L-LTP is reminiscent of memory reconsolidation, i.e. the destabilization of memories by retrieval (Nader *et al.*, 2000), and underlines the potential role of LTP and specifically L-LTP in memory formation. However, studies of L-LTP have generally focused on the first few hours after LTP induction and the potential role of LTP in long-lasting memories has remained unclear (see below).

Long-term depression

Long-term depression (LTD) of synaptic transmission can be induced at hippocampal SC-CA1 synapses and in many other parts of the brain. CA1 pyramidal neurons can express NMDAR-dependent LTD (NMDAR-LTD) and metabotropic glutamate receptor-dependent LTD (mGluR-LTD) (Oliet *et al.*, 1997). Under certain conditions, still other forms of LTD in CA1 area may be expressed (Kamsler *et al.*, 2010). Induction of NMDAR-LTD requires activation of synaptic NMDARs, rises in postsynaptic Ca2+ levels, and protein phosphatase activation (Malenka & Bear, 2004). Hippocampal NMDAR-LTD is expressed by dephosphorylation and rapid internalization of postsynaptic AMPARs (Luthi *et al.*, 1999; Banke *et al.*, 2000). mGluR-LTD at CA1 synapses, in turn, depends on activation of group 1 mGluRs that are located in the perisynaptic zone surrounding the ion tropic receptors of the PSD (Lujan *et al.*, 1996) and trigger removal of AMPARs from the spine surface (reviewed in Luscher & Huber). In immature CA1 neurons mGluR-LTD can additionally be expressed by a presynaptic mechanism that reduces vesicle release probability (Bellone *et al.*, 2008).

Homeostatic plasticity

A number of mechanisms employed by CNS neurons ensure that overall electrical activity over timescales of hours to days is kept near a certain set point. Such homeostatic plasticity (HP) prevents neuronal circuits from falling totally silent if input is reduced and protects neurons from harmful hyperexcitation. HP can act on local or global scales and depends on a large diversity of induction and

expression mechanisms that are thought to collectively balance Hebbian plasticity (Pozo & Goda, 2010). Experimentally, HP is generally induced by chronic pharmacological manipulation of electrical activity (Turrigiano *et al.*, 1998; Kim & Tsien, 2008). Similar to LTP and LTD, some forms of HP induction depend on postsynaptic Ca2+ signaling (Ibata *et al.*, 2008) and can be expressed by changes of AMPAR content of synapses (Turrigiano *et al.*, 1998). In addition, HP can be expressed by modification of presynaptic vesicle pool size and pool partitioning (Burrone *et al.*, 2002; Kim & Ryan, 2010; Rose *et al.*, unpublished) or modulation of intrinsic excitability (Desai *et al.*, 1999).

Structural synaptic plasticity

With the advent of advanced microscopy techniques that allow investigation of neurons in live tissue over minutes to hours, structural changes that parallel functional synapse modifications have been discovered. In 1999, several studies demonstrated that LTP-inducing stimuli trigger the formation of new spines (Engert & Bonhoeffer, 1999; Maletic-Savatic *et al.*, 1999; Toni *et al.*, 1999), and more recently it was demonstrated that LTP stabilizes potentiated spines and leads to clustering of new synapses in their vicinity (De Roo *et al.*, 2008). Importantly, potentiation of single spines by two-photon glutamate uncaging induces rapid spine volume increase, which may be a general morphological correlate of enhanced synaptic transmission (Matsuzaki *et al.*, 2004; Harvey & Svoboda, 2007). Despite the recent demonstration of single-spine LTD (Holbro *et al.*, 2009), a clear-cut morphological counterpart of LTD still needs to be identified. LTD induction by extracellular stimulation of an unknown population of axons enhances bouton turnover and leads to spine retraction for several hours (Nagerl *et al.*, 2004; Bastrikova *et al.*, 2008; Becker *et al.*, 2008). However, the relationship between these slow and long-lasting morphological rearrangements and functional LTD, which is expressed immediately after induction, remains unclear. Structural reorganization accompanying homeostatic plasticity in mammalian CNS neurons has received less attention. Ultrastructural studies suggest that prolonged pharmacological modulation of electrical activity can affect pre- and postsynaptic elements. For example, chronic AMPAR blockade induces a correlated increase in active zone area and PSD size, suggesting that pre- and postsynaptic components remain precisely matched during functional homeostatic adaptation (Murthy *et al.*, 2001).

2.1.2 Implication of synaptic plasticity in learning and memory formation

Three main lines of evidence suggest that synaptic plasticity at least partly underlies learning and memory formation in vivo (see below). First, some experimental paradigms inducing rapid behavioral changes are accompanied by modifications of synaptic transmission in brain structures that support altered behavior. This synaptic plasticity seems to be causally related to the behavioral changes. Second, functional adaptations to altered sensory input or during learning are tightly correlated with structural remodeling and spine formation in several brain areas. Third, pharmacological or genetic manipulations that interfere with LTP or LTD impair learning and memory and seem to block in vivo synaptic plasticity and structural remodeling.

In vivo interference with synaptic plasticity impairs learning

Addiction can be regarded as a pathological form of reward-driven learning and seems to depend on synaptic plasticity in the mesolimbic dopaminergic system (Kauer & Malenka, 2007). For example, cocaine induces NMDAR-dependent LTP-like potentiation of synapses onto dopaminergic neurons in the ventral tegmental area (Ungless *et al.*, 2001). Preventing this cocaine-evoked synaptic plasticity by genetic ablation of NMRAR function in dopaminergic VTA neurons reduces addictive behavior and suggests a causal link between synaptic potentiation and behavioral changes (Engblom *et al.*, 2008). Hippocampus-dependent spatial learning also depends on NMDAR activation. Blockade of NMDARs by a selective antagonist suppresses LTP in vivo and severely impairs place learning (Morris *et al.*, 1986). Likewise, NMDAR-dependent LTP and spatial learning are blocked by NMDAR knockout specifically in the hippocampal CA1 area (Tsien *et al.*, 1996). A recent study suggested that the formation of long-term spatial memory depends on NMDAR-LTD rather than LTP by selective manipulation of either synaptic potentiation or depression in a Morris water maze task (Ge *et al.*, 2010). Together, these and many other studies strongly suggest that NMDAR-dependent synaptic modifications analogous to LTP and LTD underlie the formation of hippocampal spatial memories.

Structural remodeling and synapse formation accompany functional adaptations and learning

Repeated two-photon imaging of dendrites and dendritic spines has revealed that the fine-structure of cortical neurons in vivo is surprisingly dynamic with continuous spine formation and elimination even

under baseline conditions (Grutzendler *et al.*, 2002; Trachtenberg *et al.*, 2002). Altered sensory experience enhances spine turnover and can selectively stabilize new spines (Holtmaat *et al.*, 2006). Importantly, new spines rapidly form synapses and might thus contribute to functional remodeling of neural circuits (Holtmaat *et al.*, 2006; Knott *et al.*, 2006). Similar spine formation and persistent stabilization has been observed after monocular deprivation or motor learning, corroborating the potential role for structural plasticity and formation of new synapses in adaptive reorganization of cortical circuits (Hofer *et al.*, 2009; Yang *et al.*, 2009). A formal proof that structural plasticity and synaptogenesis are required for functional adaptation has not been provided and might require selective manipulation of the activity of newly formed and - in fact – removed synapses, which is technically not feasible. However, the potential role of structural plasticity in functional adaptation has been further strengthened by the observation that in an αCaMKII autophosphorylation deficient mouse model that lacks functional adaptations to altered somatosensory experience, there is no experience-dependent stabilization of new spines in the barrel cortex (Wilbrecht *et al.*, 2010). In wild-type mice, in contrast, experience-dependent potentiation of whisker responses is associated with structural changes in the barrel cortex. Thus, it seems that functional changes and structural reorganization do not simply correlate, but instead structural modifications may indeed at least in part provide the physical basis to encode new representations and memories.

2.1.3 Long-term evolution of functional and structural synaptic modification

How does a synapse evolve after LTP or LTD induction? How stable are changes in synaptic strength and what factors determine stability? Strong evidence suggests that modification of existing synapses and formation of new synaptic contacts are key mechanisms underlying learning and memory formation (see above). However, what happens long (i.e. days or weeks) after induction synaptic plasticity is largely unknown and thus it remains uncertain how synaptic plasticity can provide the physical basis to store long-lasting memories. In vivo LTP induced simultaneously in large numbers of synapses can persist for weeks and is accompanied by alterations in the spine actin cytoskeleton (Fukazawa *et al.*, 2003). Initially, existing spines seem to be potentiated, but it is possible that at later stages new synaptic contacts are formed that will be the basis for increased synaptic strength. On the structural level, postsynaptic spines have been identified as an important substrate for circuit remodeling (Holtmaat *et al.*, 2006; Hofer *et al.*,

2009; Yang *et al.*, 2009). In these studies, the presynaptic partners are unknown and functional parameters could not be measured.

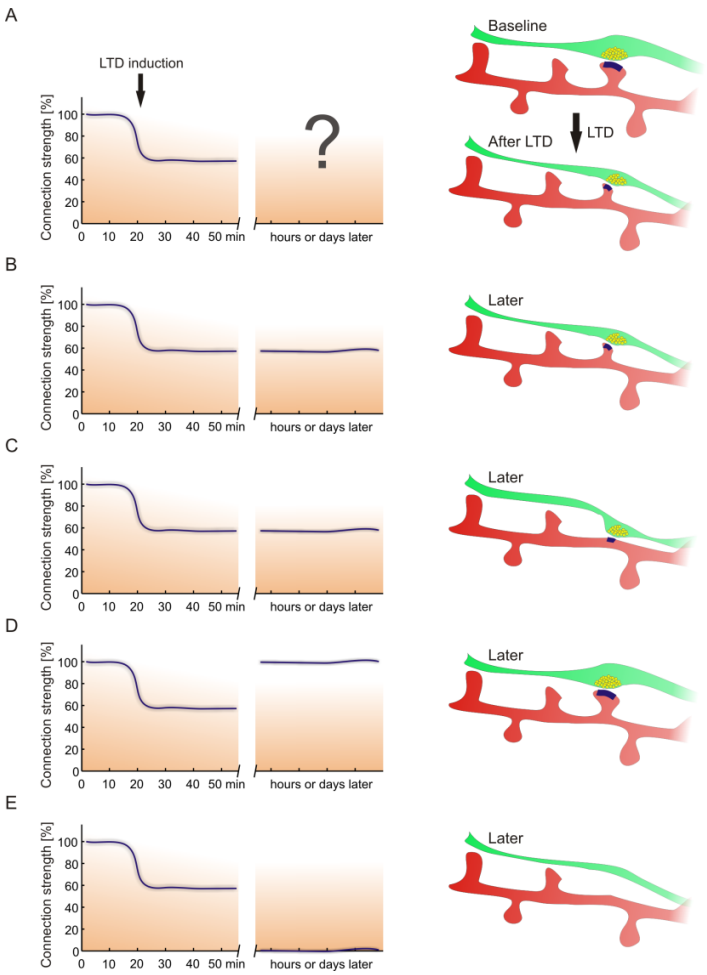

Figure 1. Possible scenarios of the stability of LTD at individual synaptic connections over extended periods of time. *(A) Left: A synaptic connection consists of a presynaptic bouton containing neurotransmitter vesicles and the corresponding spine carrying the postsynaptic density (PSD). For clarity, a single synaptic connection is depicted, although connections between a pair of neurons may consist of several synapses. In response to an LTD inducting stimulus, the efficacy of synaptic transmission is depressed. This functional change in synapse strength may be accompanied by structural remodeling, e.g. a correlated shrinkage of pre- and postsynaptic structures. (B) The depressed state may be maintained for many hours or days without any further structural rearrangement. (C) Further structural changes such as spine loss and formation of a shaft synapse may occur while transmission efficacy is stable. (D) If LTD is not actively maintained, synaptic strength may revert to the baseline state over extended periods of time. In parallel, pre- and postsynaptic elements may recover to their original size. (E) Finally, a depressed synapse may be removed altogether if it is not potentiated again after a certain period of time.*

The small structural modifications observed after learning or manipulations of sensory experience suggest that memories are encoded by changing a relatively small number of synapses on a given neuron. To understand the contribution of changes in synaptic transmission to long-term circuit reorganization, it is therefore important to investigate synaptic plasticity on the level in unitary synaptic connections between identified pairs of neurons. Currently, our knowledge about functional synaptic changes and associated structural modifications after plasticity induction are largely limited to 30 – 60 min after plasticity induction, which corresponds to the time window accessible to patch-clamp recordings (Matsuzaki *et al.*, 2004; Harvey & Svoboda, 2007; Holbro *et al.*, 2009). LTD, for example, is generally stable for up to 60 min after induction and may be accompanied by shrinkage of pre- and postsynaptic elements (Fig. 1A). Hours or days later, these functional and structural changes may persist

(Fig. 1B), but structural reorganization may continue, while the depressed state is maintained (Fig. 1C; and see Nagerl *et al.*, 2004). Alternatively, homeostatic or other mechanisms might revert depressed synapses to their baseline state (Fig. 1D) or depressed synapses may be removed altogether after some period of time (Fig. 1E). Furthermore, modifications in synaptic transmission may spread to neighboring spines or induce the formation of new synaptic contacts, for example in the vicinity of a modified synapse (Harvey & Svoboda, 2007; De Roo *et al.*, 2008). To investigate these potential late processes at single synaptic connections, non-invasive plasticity induction for example by optical approaches would be needed to study functional and possible structural changes at any time point after plasticity induction.

2.2 Channelrhodopsin

2.2.1 History

The first attempt to depolarize genetically targeted neurons with light stimulation relied on the activation of endogenous ion channels by a light-activated signaling cascade consisting of three proteins borrowed from the Drosophila phototransduction cascade (Zemelman *et al.*, 2002). While this system - dubbed chARGe – demonstrated the potential value of non-invasive control of neural activity it was complicated and operated on timescales that were too slow to trigger individual action potentials (APs). An important break-through was achieved in 2005, when channelrhodopsin-2 was first expressed in hippocampal neurons, enabling the induction of single APs with brief blue light pulses (Boyden *et al.*, 2005).

Let us go back about a hundred years.

Already at the beginning of the 20th century, single-celled green algae such as *Chlamydomonas reinhardtii* were popular model systems to study phototaxis, i.e. the capability of living organisms to detect the direction of a light source and move toward or away from it. Together with information on light intensity, phototaxis allows organisms to avoid harmful very intense light or to find locations in their environment that are optimally suited for photosynthesis. In 1916, the pigmented eye spot of unicellular algae was identified as the light-sensing organelle (Mast, 1916). It then took about another

80 years until Georg Nagel cloned the two genes encoding the proteins that detect light in the *Chlamydomonas* eye spot and start the signaling cascade ultimately controlling phototactic behavior (Nagel *et al.*, 2002; Nagel *et al.*, 2003). The two proteins were named channelrhodopsin-1 (ChR1) and channelrhodopsin-2 (ChR2) and they both are directly light-gated ion channels. Already in the first two seminal publications, Nagel and colleagues expressed ChR1 and ChR2 in heterologous cells and demonstrated their ability do depolarize cells upon activation with blue light. The next step into neurons marked the beginning of a new area of neuroscience (Boyden *et al.*, 2005).

2.2.2 Biophysical properties

ChR2, which has become the most widely used channelrhodopsin in neuroscience, is an inward-rectifying cation channel that allows the flux of protons, sodium and potassium ions, and - to a weaker extent – divalent cations through the channel pore (Fig. 2; Nagel *et al.*, 2003). The single-channel conductance of ChR2 is too low to be measured directly by patch-clamp recordings. Several studies employing stationary noise analysis reported single-channel conductances in the range of 50 fS – 250 fS (Bamann *et al.*, 2008; Lin *et al.*, 2009). This is about two orders of magnitude lower than the single-channel conductance of voltage-gated sodium and potassium channels or many ligand-activated channels, which typically is in the range of 5 pS to 50 pS (Hille, 1992). Kinetics is another important channel property. Upon absorption of a blue photon, ChR2 opens within 1 ms – 2 ms and remains in the open conducting state for about 10 ms (Bamann *et al.*, 2008; Ritter *et al.*, 2008). Completion of the photocycle and return to the dark-adapted state takes several seconds, resulting in a photocurrent reduction during continuous illumination or repeated stimulation at elevated frequencies.

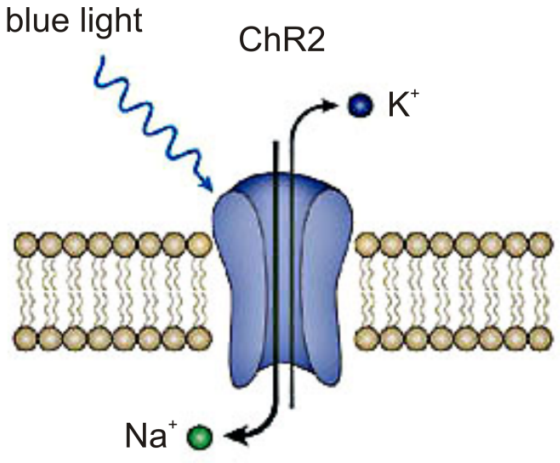

Figure 2. Schematic of channelrhodopsin-2 (ChR2). *ChR2 is a light-gated cation channel from the green algae Chlamydomonas reinhardtii. Adapted from Zhang et al., 2007.*

2.2.3 Currently used channelrhodopsin variants

Like for GFP, a rapidly growing number of ChR2 variants have been reported. For neuroscience, only a limited number is of interest. ChR2(H134R) is widely used for in vivo applications and carries a gain-of-function mutation that increases photocurrents (Nagel *et al.*, 2005). A slight slowdown in channel kinetics, which may be the reason for enhanced photocurrents, reduces the precision of AP induction with this channelrhodopsin variant (Lin *et al.*, 2009) and data presented in this dissertation). Faster channel speed was achieved by a glutamate-to-threonine conversion at position 123, which also brought about a strong reduction of photocurrent amplitudes (Gunaydin *et al.*, 2010). Combination of the E123T and the H134R mutations increased photocurrent amplitudes again and allowed firing cortical interneurons, but at the same time partly cancelled the improvement in channel kinetics (Gunaydin *et al.*, 2010; Lin, 2010). Finally, the so-called bi-stable C128X channelrhodopsins constitute a fundamentally different class of optogenetic tools, since they allow depolarization of neurons for several minutes with brief activation pulses, but are not suitable for the control of single action potentials (Berndt *et al.*, 2008). Experiments presented in this thesis have revealed that the photocycle of the bi-stable ChR2 variants is branched, leading to rapid channel desensitization upon repeated stimulation (see below).

2.2.4 Application in fundamental neuroscience

ChR2 has found a diverse range of applications in neuroscience. The key advantages of ChR2-mediated photostimulation over electrical stimulation techniques are the possibility to selectively activate genetically defined neuronal populations and to stimulate individual neurons in a non-invasive manner to investigate activity-dependent processes in non-perturbed neurons. Using cell type-specific photostimulation, a number of studies have provided important insight into the contribution of particular cellular subpopulations to circuit function and behavior such as the modulation of breathing by specialized astrocytes or the generation of rhythmic locomotor-like activity in the spinal cord by glutamatergic interneurons (Gourine *et al.*, 2010; Hagglund *et al.*, 2010). On the level of single-cell physiology, ChR2 has been used to map the fine-scale organization of different afferents impinging on the dendritic tree of cortical neurons or to potentiate individual visually identified spines in intact neurons without affecting the intracellular milieu and second messenger systems by whole-cell patch clamping (Zhang *et al.*, 2008; Petreanu *et al.*, 2009).

2.2.5 Application in medical neuroscience

Optical methods to stimulate and inhibit neuronal activity hold great promise for clinical application, because a large number of neurological and psychiatric diseases at least partly involve altered activity patterns in specific neuronal populations. Altered activity may not be the underlying cause of disease, but pharmacological or electrical modulation of electrical activity and neurotransmitter action can alleviate disease symptoms in diverse conditions such as schizophrenia, anxiety disorders, or Parkinson's disease (Kane & Correll, ; Stevens & Pollack, 2005; Kringelbach *et al.*, 2007). Several studies have demonstrated the potential utility of so-called optogenetic approaches in animal models of disease. A very early potential application was the restoration of vision in light-insensitive retinas. ChR2 expression in specific bipolar cells in the retina has successfully re-established a certain level of responses to visual stimuli in blind mice (Lagali *et al.*, 2008). More recently, the hyperpolarizing chloride pump halorhodopsin has been used to reactivate cone photoreceptors that had lost their light-sensing outer segments, resulting in an impressive restoration of retinal circuit function (Busskamp *et al.*, 2010). Parkinson's disease has been another focus for potential clinical use of optogenetics. Optical stimulation of direct-pathway neurons in the dorsal striatum alleviated disease symptoms in an animal model of the Parkinson's (Kravitz *et al.*, 2010), whereas another study identified the neural circuitry underlying the beneficial effect of deep brain stimulation in Parkinson's disease (Gradinaru *et al.*, 2009). Together, these studies demonstrate the potential of optical methods to both understand mechanisms of disease and develop novel therapeutic strategies in brain disease.

3. AIM OF THE THESIS

Non-invasive induction of synaptic plasticity would open the door to investigate the stability of changes in synaptic transmission between identified pairs of neurons over substantially prolonged periods of time compared to traditional electrophysiological approaches. Long-term aspects are important since there is a large temporal gap between functional changes in synaptic strength that can be studied for minutes or hours using electrophysiology, and memories which can last for a lifetime (see Fig. 3). The aim of my thesis was to refine optogenetic stimulation methodology to a degree that enables the non-invasive control of synaptic plasticity and thereby allows investigating processes occurring long after the initial plasticity induction.

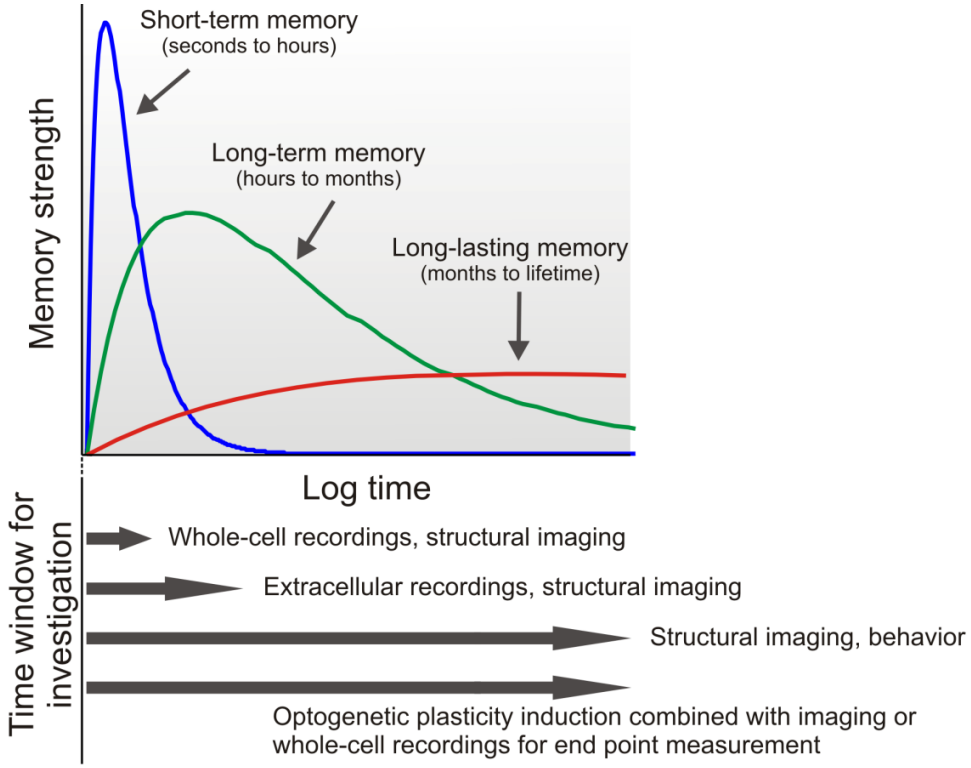

Figure 3. Phases of memory and time windows accessible to different approaches to monitor synaptic plasticity. *Top: Memory can be divided into several phases lasting from seconds to an organism's lifetime. Bottom: Different experimental approaches allow obtaining functional or structural information about synapses over different time scales. Combination of optogenetic plasticity induction with structural imaging and later functional measurements using electrophysiology would allow monitoring changes in synaptic structure and function long after a plasticity-inducing stimulus. Based on McGaugh, 2000.*

In a separate project I investigated the factors that determine and limit the resolution of optogenetic stimulation. Local activation of light-responsive proteins may enable spatio-temporal control of chemical and electrical signaling in living cells with much higher accuracy than pharmacological approaches. This will allow researchers to investigate signal integration in a physiological context where cells can receive several inputs in different subcellular domains. Furthermore, local activation of ChR2 allows specifically stimulating individual neurons in groups of ChR2-expressing cells and may allow controlling neurotransmitter release at individual presynaptic boutons. Thus, optogenetic manipulation of subcellular processes, which so far has not been a focus of optogenetic research, holds great potential for cellular neurophysiology and the study of chemical as well as electrical signaling in living cells in general.

4. PUBLICATIONS

Part 4.A

Optimizing the spatial resolution of Channelrhodopsin-2 activation

Philipp Schoenenberger, Åsa Grunditz, Tobias Rose, and Thomas G. Oertner

Brain Cell Biol. 2008 Aug;36(1-4):119-27. Epub 2008 Jul 25.

Abstract

Over the past few years, the light-gated cation channel Channelrhodopsin-2 (ChR2) has seen a remarkable diversity of applications in neuroscience. However, commonly used wide-field illumination provides poor spatial selectivity for cell stimulation. We explored the potential of focal laser illumination to map photocurrents of individual neurons in sparsely transfected hippocampal slice cultures. Interestingly, the best spatial resolution of photocurrent induction was obtained at the lowest laser power. By adjusting the light intensity to a neuron's spike threshold we were able to trigger action potentials with a spatial selectivity of < 30 µm. Experiments with dissociated hippocampal cells suggested that the main factor limiting the spatial resolution was ChR2 current density rather than scattering of the excitation light. We conclude that subcellular resolution can be achieved only in cells with a high ChR2 expression level and that future improved variants of ChR2 are likely to extend the spatial resolution of photocurrent induction to the level of single dendrites.

Introduction

The light-gated channel Channelrhodopsin-2 (ChR2) is a versatile tool for the controlled activation of neurons. The temporal precision of light-induced action potential generation can be as good as 1 ms (Boyden et al., 2005), but the spatial resolution limit of ChR2 activation has not been systematically explored. Spatial specificity of light stimulation can be achieved by two methods: Selective expression of ChR2 in a subset of cells (Adamantidis et al., 2007), or restriction of the illumination to a small region of tissue or even to a single cell (Wang et al., 2007). Different strategies for introducing ChR2 into neurons have been used: Viral transfection (Adamantidis *et al.*, 2007; Aravanis *et al.*, 2007; Zhang *et al.*, 2008), *in utero* electroporation (Petreanu *et al.*, 2007; Huber *et al.*, 2008), and the generation of *Thy1* transgenic mice (Arenkiel *et al.*, 2007; Wang *et al.*, 2007). Most of these techniques produce a relatively high density of ChR2 expressing cells, and it is not clear whether individual cells can be activated by focused illumination under these conditions.

Here we use particle-mediated gene transfer to achieve a low density of transfected neurons in organotypic slice cultures, allowing us to explore the spatial resolution limit of ChR2 activation in detail. We used a focused laser beam to generate current and spike maps of ChR2 expressing cells. Surprisingly, spatial resolution improved with reduced laser power, which made it possible to map the position of a single cell and the orientation of the main apical dendrite, but not the location of fine dendrites. Degradation of the laser focus due to light scattering in the tissue was not a limiting factor in our experiments. Furthermore, we show that the previously described after-depolarization (Zhang & Oertner, 2007) is much reduced with focused illumination, indicating that a blue laser might be the ideal light source to mimic the properties of naturally occurring action potentials.

Methods

Cell culture and transfection

Hippocampal slice cultures from rats (Sprague Dawley) were prepared at postnatal day 4-5 as described (Stoppini et al., 1991), according to the rules of the Federal Veterinary Office of Basel-Stadt. After 7 days in culture, we used a Helios gene gun (Bio-Rad) to co-transfect individual cells with DNA encoding ChR2-

YFP (K. Deisseroth) and tdimer2 (dimeric RFP, R.Y. Tsien), each subcloned into a neuron-specific (synapsin1) expression vector. Dissociated hippocampal cultures were prepared as previously described (Fischer et al., 1998) and transfected using lipofectamine (Invitrogen).

Electrophysiology and Photostimulation

The recording setup was based on a BX-51 microscope equipped with a LUMPlan 60x 0.9NA water immersion objective (Olympus) and a cooled CCD camera (Sensicam QE). A secondary camera port was used to couple in 488 nm light (Melles Griot 543 argon ion laser) via single-mode optical fiber (MFD = 3.2 µm). Acousto-optic modulator (AA Opto-Electronic) and position of the motorized stage (Sutter Instrument) were controlled by custom software written in MATLAB (The MathWorks). To avoid successive illumination of neighboring points, we used a step-back pattern (1-5-2-6-3-7...) for mapping. To monitor the time course of the light stimulus, we used a photomultiplier tube below the condenser to detect a small fraction of the blue excitation light transmitted through the preparation. Laser power was measured at the back aperture of the objective (LaserCheck, Coherent). For patch-clamp recordings, we used an Axopatch 200B amplifier (Molecular Devices) and MP-225 manipulators (Sutter Instrument). Experiments were conducted at room temperature 1-3 weeks after transfection. Artificial cerebrospinal fluid (ACSF) for slice cultures contained (in mM) 119 NaCl, 26.2 $NaHCO_3$, 11 D-glucose, 2.5 KCl, 4 $MgCl_2$, 4 $CaCl_2$, 1.0 NaH_2PO_4. ACSF was complemented with 1 µM TTX, 10 µM NBQX for voltage-clamp experiments; 10 µM bicuculline, 10 µM dCPP, and 10 µM NBQX in current-clamp experiments to block $GABA_A$, NMDA and AMPA receptors. Cell-attached recordings were performed under the same conditions as the current clamp experiments, pipettes contained 150 mM NaCl. Glass pipettes for patch-clamp recordings were filled with intracellular solutions containing (in mM): 135 potassium gluconate, 10 HEPES, 4 $MgCl_2$, 4 Na_2-ATP, 0.4 Na-GTP, 10 Na_2-phosphocreatine, and 3 ascorbate for current-clamp experiments; 135 cesium methanesulfonate, 10 HEPES, 4 $MgCl_2$, 4 Na_2-ATP, 0.4 Na-GTP, 10 Na_2-phosphocreatine, and 5 glutathione for voltage-clamp. Recordings in dissociated cells were performed with solutions as described (Skeberdis et al., 2006).

Data analysis

Data were analyzed with custom software written in MATLAB. To generate color coded 2D maps, we used MATLAB's *surf* function with interpolated shading. Numerical values are given as mean ± SD.

Results

Characterization of laser-induced photocurrents

To measure the spatial selectivity of ChR2 activation, we measured laser-induced photocurrents in pyramidal neurons voltage-clamped at -65 mV. Recordings were performed in ACSF containing TTX and NBQX to isolate light-induced currents. Arc lamp stimulation with blue excitation light (EGFP filterset, 470/40 exciter) induced large photocurrents (3.3 ± 0.9 nA, n = 5 cells). For laser stimulation at 488 nm, the end of a single-mode optical fiber was imaged into the center of the visual field (see methods). Scanning was achieved by computer-controlled movements of the motorized microscope stage on which recording chamber and patch-clamp manipulators were mounted. Compared to wide-field illumination, laser-evoked photocurrents were much smaller (0.7 ± 0.2 nA), even at high laser intensities (350 µW at the back aperture of the objective), indicating that only a small fraction of the total ChR2 present in the membrane was activated by the focused laser light (Fig. A.1a). The relationship between laser power and current amplitude was linear below 10 µW but sublinear for higher laser powers (Fig. A.1b). The sublinear characteristic suggests that ChR2 became saturated within the laser focus. Fluorescence emitted from the YFP-label of ChR2 showed less saturation with increasing laser power (Fig. A.1b) due to its much faster photocycle: A single fluorescent protein can emit >2000 photons / ms (Kubitscheck et al., 2000), whereas ChR2 takes several seconds to return to the ground state (Bamann et al., 2008). Therefore, YFP fluorescence is proportional to ChR2 currents only at very low light intensities.

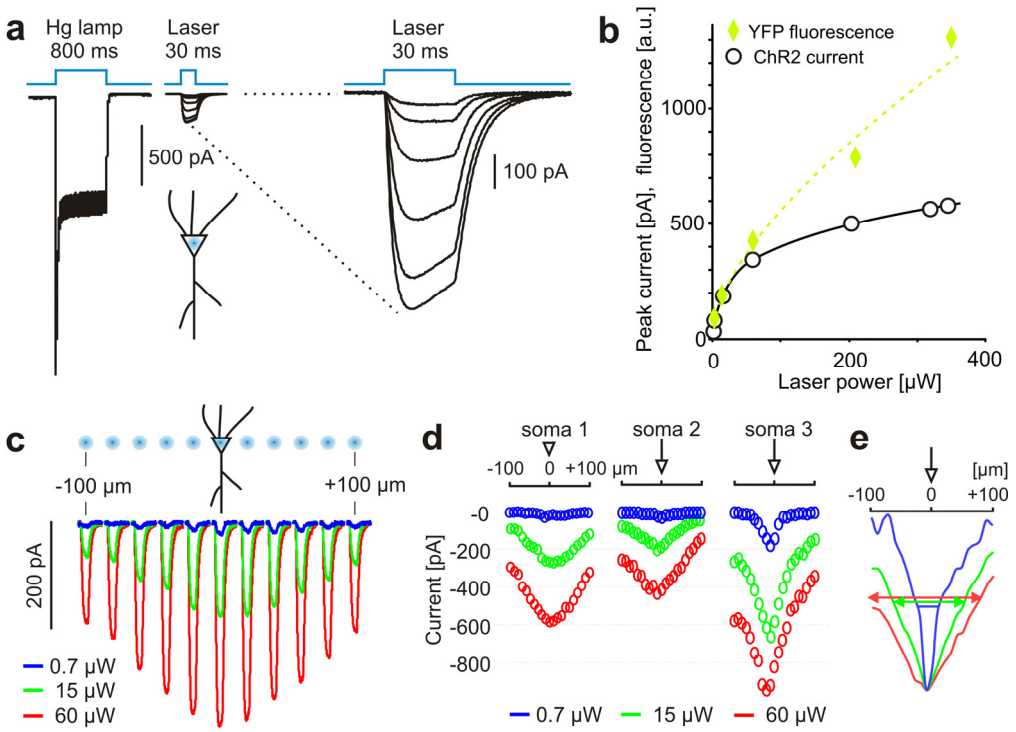

Fig. A.1. Induction of photocurrents by laser stimulation of ChR2. *(a) Comparison of ChR2 currents during wide-field stimulation (Hg arc lamp, 0.8 mW) and focused laser stimulation at the soma (note different time scales). (b) Relationship between photocurrent amplitude and laser intensity shows strong saturation at laser powers > 20 µW. Integrated fluorescence of ChR2-YFP (green diamonds, arbitrary units) shows less saturation for the same range of laser intensities. (c) Currents evoked by a series of laser pulses with 10 µm steps. For clarity, only every second current trace and schematic laser spot are shown. (d) Peak photocurrent amplitudes with respect to laser position. Three different cells were stimulated as in (c) at 3 laser intensities. (e) Peak-normalized photocurrents (n = 3 cells). Full-width at half maximum activation (35 µm, 115 µm, 180 µm) depends on laser intensity.*

Next we explored the spatial resolution of photocurrent generation. Pyramidal neurons were voltage-clamped and laser-induced currents were recorded while the cells were moved in 10 µm steps along a line perpendicular to the orientation of the apical dendrite (Fig. A.1c). The length of the scanned line was 200 µm and the soma was positioned in the middle. Stimulation pulses were applied with intervals of 5 s to allow for recovery of ChR2-mediated currents. The photocurrents reached maximum amplitude when the soma was in the center of the laser spot and decreased with increasing distance from the laser beam (Fig. A.1c). Surprisingly, at laser powers of 15 µW or more, large photocurrents were induced even at a distances >100 µm lateral from the soma (Fig. A.1d). As a measure for the spatial resolution of photocurrent generation, we used the full width at half maximum current (FWHM) for different laser intensities (Fig. A.1e). Interestingly, spatial resolution was best at the lowest stimulation intensity (FWHM = 35 µm at 0.7 µW, 115 µm at 15 µW, ~180 µm at 60 µW, *n* = 3). Taken together, our data

indicate that laser illumination activates a small fraction of the total membrane-bound ChR2, and that the spatial resolution of laser stimulation depends on laser intensity.

Laser intensity and illuminated area

To better understand the effect of laser intensity on spatial resolution, we made use of the fact that both the chromophore (all-trans retinal) and the YFP label of ChR2 are excited by the 488 nm laser line. Therefore, at low laser power, YFP fluorescence can be used as a reporter of the spatial extent of ChR2 activation. In the center of the laser beam, however, the relationship between YFP fluorescence and photocurrent will not be linear due to stronger saturation of ChR2 (Fig. A.1b). We focused the laser on the soma of a ChR2-YFP expressing cell and captured YFP fluorescence excited at different laser intensities (Fig. A.2a). The membrane area with detectable YFP fluorescence increased as a function of laser intensity, which is best seen in intensity profiles measured across the soma (Fig. A.2b). With 350 µW laser power, we detected fluorescence from dendrites up to 80 µm from the laser focus (data not shown). To measure the intensity profile of the excitation beam, we imaged the fluorescence excited in a thin film of fluorescein solution. The profile was symmetric with FWHM = 2.7 µm (independent of laser power in the tested range of 10 – 60 µW) and long tails (Fig. A.2c). From these findings, we conclude that the membrane area generating ChR2-mediated photocurrents increases as a function of laser intensity. In the laser focus, the photocycle of ChR2 is likely to become saturated, thus the current will not scale with laser power at medium to high intensities. The recruitment of more and more distal ChR2 channels with increasing laser power explains the apparent loss in spatial resolution (Fig. A.1 c-e).

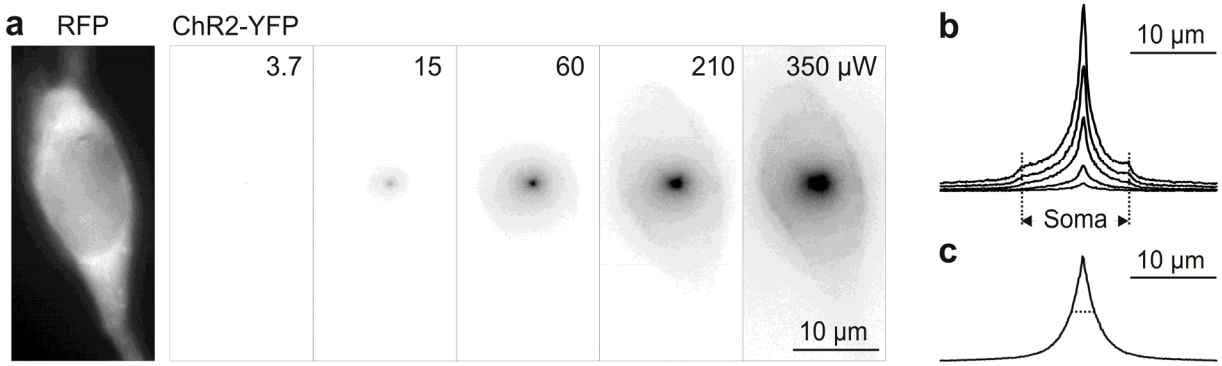

Fig. A.2. High laser power leads to excitation of ChR2-YFP molecules outside the focal spot. *(a) Left: RFP image showing soma of transfected cell. Right: ChR2-YFP signal excited with different laser intensities (0.3 s exposure). (b) YFP fluorescence intensity profiles across the soma through the center of the laser spot. (c) Laser-excited fluorescence intensity profile measured in thin film of fluorescein solution (FWHM = 2.7 µm, laser power = 60 µW).*

Local photocurrents could potentially be used as a tool to investigate electrotonic or active signal propagation in individual dendrites. To explore this possibility, we stimulated voltage-clamped cells in a grid pattern (30 and 10 µm step size) at different laser intensities (Fig. A.3a). We found that current amplitudes were highly reproducible, revealed the location of the soma and the orientation of the main dendrite, but did not resolve higher order dendrites (Fig. A.3b). As an operational definition of spatial resolution, we determined the FWHM of a Gaussian fit in the direction of the steepest drop of the currents from the center of the soma (Fig. A.3c). This strategy minimizes the influence of cell morphology (e.g. apical dendrite) on the resolution measurement. For the cell analyzed in Fig. A.3, resolution was 41 µm at 4 µW, 69 µm at 60 µW, and 114 µm at 260 µW laser power. At the lowest laser power tested, spatial resolution could be further improved by sampling in 10 µm steps (28 µm at 4 µW, Fig. A.3b, small square map). For 60 µW laser power, 10 µm steps did not improve resolution (63 µm FWHM). Similar results were obtained in 5 strongly expressing cells.

At the low laser powers that were best for mapping, somatic photocurrents were very small (< 140 pA, Fig. A.3d). Therefore, one important factor that limits the resolution of current maps is the noise floor of the electrophysiological recordings. Another unfavorable effect is the scattering of blue excitation light in the organotypic cultures. We wanted to test if the spatial resolution of ChR2 activation could be improved in isolated cells. For this purpose, we prepared low-density hippocampal cell cultures co-transfected with ChR2-YFP and RFP. Compared to cells in organotypic cultures, dissociated cells produced smaller photocurrents (Fig. A.3e). The spatial resolution of current mapping was comparable to the resolution in organotypic slices at the same laser power (n = 4), indicating that light scattering was not a limiting factor when mapping cells in organotypic slice cultures.

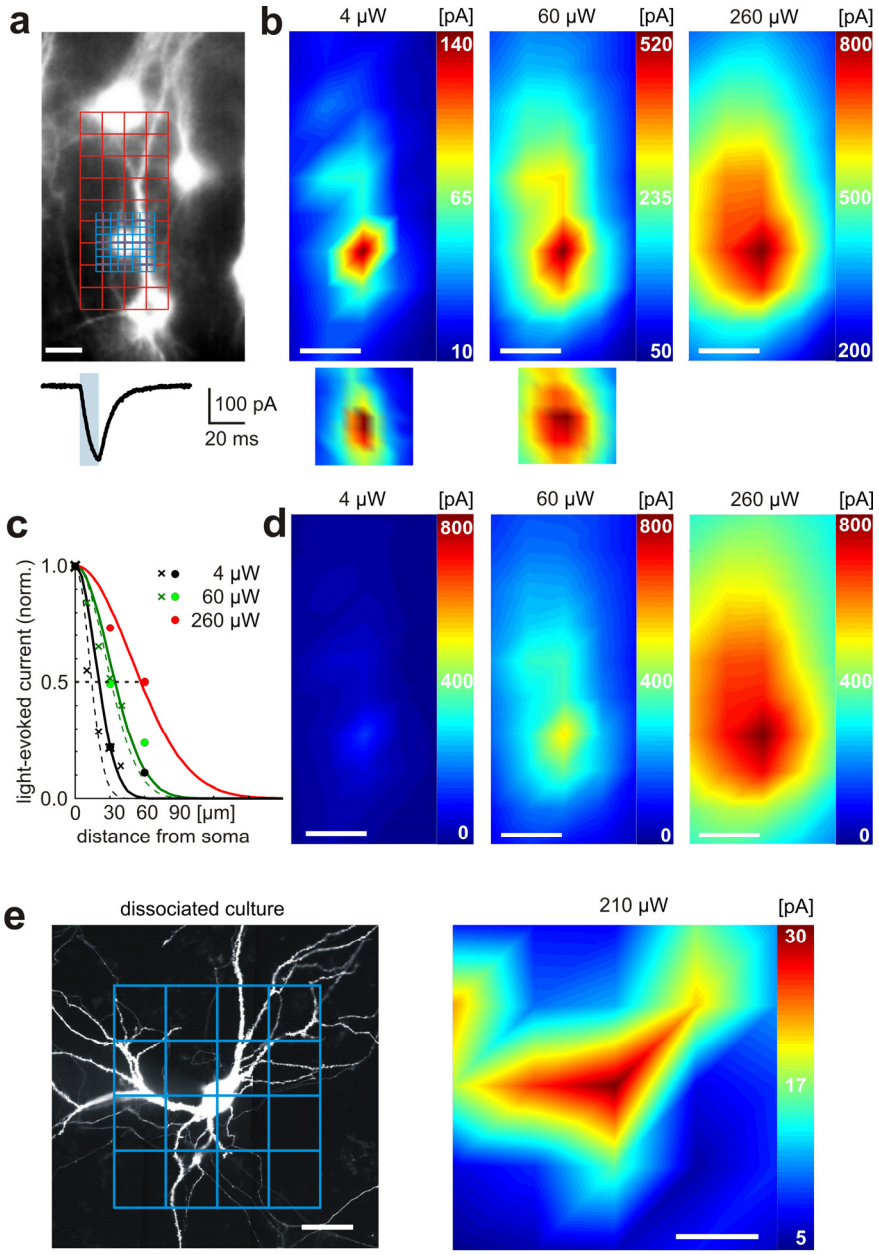

Fig. A.3. Resolution of current maps depends on laser power. *(a) Fluorescence image of ChR2 transfected cells in entorhinal cortex. The stage was moved relative to the laser focus in 30 µm (red grid) and 10 µm (blue grid) steps. Below: Example trace, 10 ms laser pulse. (b) Interpolated current maps for 3 different laser intensities for 30 µm and 10 µm grid (lower maps). Maps are scaled to min/max current, 30 µm and corresponding 10 µm maps have identical scaling. Scale bars: 50 µm. Maps are averages of two repetitions. (c) Gaussian fits to the current drop away from the soma (best direction) show influence of laser power on resolution. 30 µm grid: circles, solid line fit, FWHM = 41 µm, 69 µm, 114 µm. 10 µm grid: crosses, dashed line fit, FWHM = 28 µm, 63 µm. (d) Same data as in b, uniform scaling. (e) Fluorescence image of ChR2-transfected cell in dissociated hippocampal cell culture. Stimulation grid: 50 µm steps, 210 µW laser power. Right: Interpolated current map (average of 3 repetitions). Spatial resolution: 108 µm FWHM.*

Spatial resolution of action potential triggering by local ChR2 activation

The findings above suggested the possibility to spike ChR2-expressing cells with high spatial selectivity using low stimulation intensities. We investigated this possibility using cell-attached recordings and 10 ms laser pulses. At laser intensities just above threshold (typically 70-100 µW), action potentials (APs) were elicited only when the laser was exactly centered on the soma (Fig. A.4a). A modest increase in laser power immediately decreased the spatial selectivity, since now APs were also triggered along the main trunk of the apical dendrite. Similar results were obtained using whole-cell current clamp recordings (Fig. A.4b), confirming the inverse relationship between laser power and spatial resolution. At laser powers > 300 µW, spatial specificity was completely lost within a 100 µm radius in most cells (Supp. fig. A.1). In cells with lower ChR2 expression levels, high laser powers or longer laser pulses were needed to reach spike threshold. Consequently, spatial resolution in these cells was very poor, as action potentials were generated at distances > 100 µm from the soma (*n* = 4, data not shown). Taken together, these results show that ChR2-mediated action potentials can be triggered with high spatial selectivity using low stimulation intensities, and that the expression level of ChR2 limits the spatial resolution.

With increasing laser power, we noticed a pronounced after-depolarization appearing in the wake of the action potential (Fig. A.4c, blue traces). This effect was not seen at laser intensities just above threshold (Fig. A.4c, green traces) or if laser illumination was applied to the axonal arborization distal from the soma, generating an antidromic spike with a delay of 7 -12 ms (Fig. A.4c, black traces). After-depolarization following wide-field illumination leads to increased calcium influx and increases the probability of transmitter release at ChR2-expressing axonal boutons (Zhang & Oertner, 2007). We suggest that these effects could be largely avoided using focal illumination just above threshold.

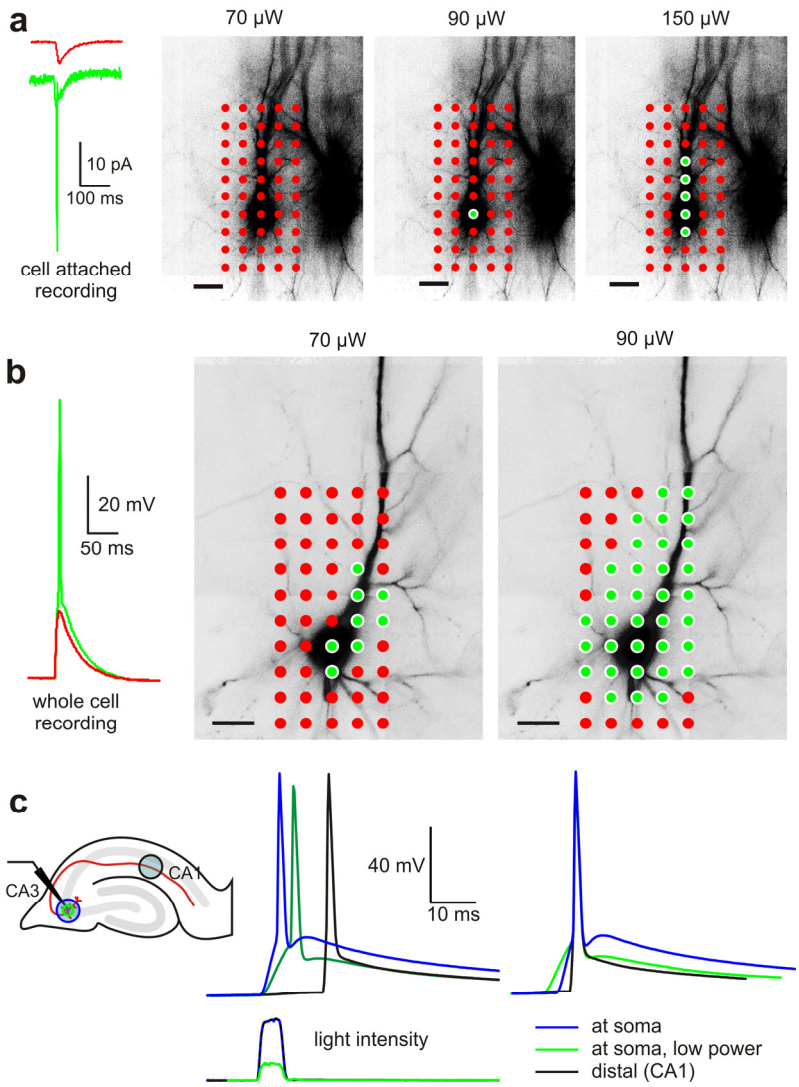

Fig. A.4. Spatial resolution of action potential triggering. *(a) Cell-attached recording of CA1 pyramidal cell. Red trace: subthreshold stimulation. Green trace: suprathreshold stimulation. Stimulation grid: 30 µm step size. Scale bar: 50 µm. At laser powers just above threshold, spatial resolution was very good. Increasing laser power decreased spatial resolution of spike map (right). (b) Whole cell current clamp recording of CA1 pyramidal cell. High ChR2 expression level resulted in spike threshold < 70 µW laser power. (c) After-depolarization in CA3 pyramidal cell is most pronounced if high intensity pulses are applied directly to the soma (blue trace). An identical laser pulse applied distally in CA1 triggers an antidromic spike with no apparent after-*

Discussion

Here we show that the spatial resolution of ChR2 activation depends on the intensity of the laser beam. The soma represents only a small fraction of the total membrane of the cell, most surface area is contained in the extensive dendritic and axonal arborization. For this reason, wide-field illumination evokes 5-10 fold larger photocurrents than focused laser illumination at the soma (Fig. A.1a). Due to the Gaussian intensity profile of a focused laser beam and scattering of excitation light, out-of-focus membrane becomes increasingly illuminated as the focal intensity is increased (Fig. A.2), increasing the total photocurrent. This effect is counteracted by saturation of ChR2 activation in the center of the

beam, resulting in a sublinear increase of total ChR2 current with increasing laser intensity (Fig. A.1b). Since the 3-dimensional geometry of the cell increasingly determines ChR2 current amplitudes at high laser powers, the relationship between laser power and current amplitude can not be predicted from first principles.

Comparing the shape of photocurrents at different laser intensities, we noted increasing inactivation with increasing laser power (Fig. A.1a). To study the photocycle of light-gated channels, light pulses have to be either very brief or of saturating intensity to ensure synchronous activation of the entire channel population (Nagel *et al.*, 2003; Bamann *et al.*, 2008). Focused laser light, on the other hand, provides a spatial gradient of light intensities (Fig. A.2). As a result, only channels in the focus will be activated synchronously, while more distal channels get activated at random time points, obscuring single channel kinetics in the total ChR2 current. At very low laser powers, the pool of channels in the ground state never gets depleted, resulting in an apparently non-inactivating photocurrent (Fig. A.1a). In summary, stimulation with long and focused laser pulses is not a suitable method to analyze channel kinetics.

We used laser stimulation of ChR2 to generate current maps with subcellular resolution in organotypic and dissociated hippocampal cultures (Fig. A.3). The best resolution (28 µm FWHM) was obtained in a strongly expressing cell at very low laser power (Fig. A.3c). Under these conditions, ChR2 currents were very small and a low-noise recording setup was required. Furthermore, resolution was slightly better with 10 µm step size than with 30 µm steps at the lowest laser powers, indicating that 30 µm steps were undersampling the signal bandwidth. Therefore, for optimal (Nyquist) sampling, step size should be scaled to laser intensity.

To further increase spatial resolution, higher ChR2 current densities would help to increase the signal-to-noise ratio at low laser power. This could be achieved by higher expression levels or increased single channel conductance of ChR2. We have not explored the possibility of non-Gaussian beam profiles, which could help to reduce ChR2 saturation and inactivation in the center. Light scattering in the tissue seems to play a minor role for the relatively superficial transfected cells in organotypic slice cultures, but might be a key issue for *in vivo* applications (Aravanis *et al.*, 2007; Arenkiel *et al.*, 2007).

Under current clamp conditions, the sharp threshold of action potential generation leads to binarization of the depolarization map into a suprathreshold center and a subthreshold surround (Wang et al., 2007). We show that at laser intensities just above firing threshold, spatial selectivity can be better than 30 µm (Fig. A.4a). Since we relied on patch-clamp recordings to adjust the laser power, these calibration experiments might seem to be of little practical relevance. However, optical detection of single action potentials has been demonstrated using bulk loading of calcium- or voltage-sensitive dyes (Kasuga *et al.*, 2003; Stosiek *et al.*, 2003), and might also be possible with genetically encoded calcium indicators (Mao et al., 2008). A combination of optical stimulation and optical readout could be used to build a closed-loop stimulation system in which excitation intensity is automatically adjusted to be just above threshold for individual cells. Our experiments suggest that this would be an ideal strategy to optimize the specificity of optical stimulation and to compensate for cell-to-cell variability in ChR2 expression levels.

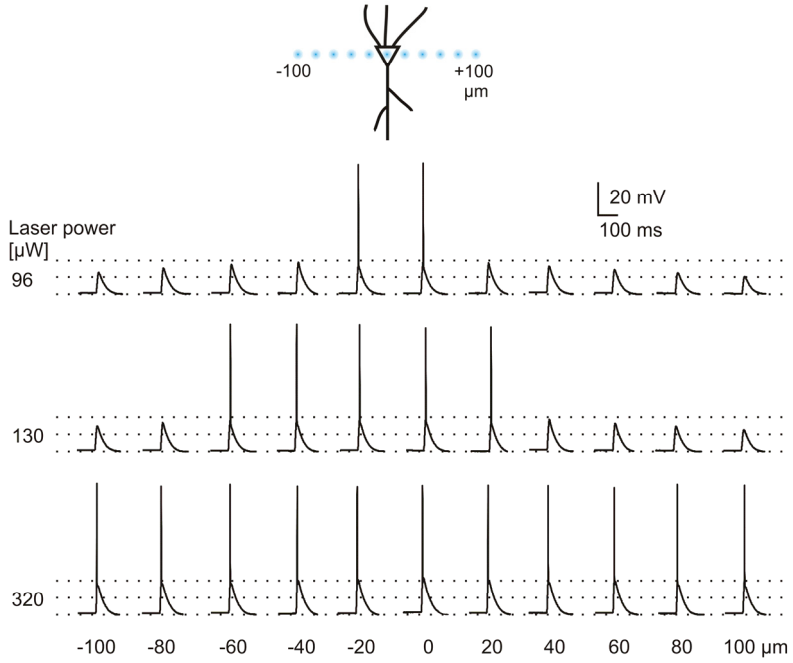

Supplemental fig. A.1. *Spatial selectivity of spike initiation breaks down at laser powers > 300 µW. A ChR2-transfected CA1 pyramidal cell was stimulated in a line pattern perpendicular to the orientation of the apical dendrite with 10 ms laser pulses at 3 different laser intensities. The soma was positioned in the middle.*

Acknowledgements

We thank Daniela Gerosa-Erni for excellent technical assistance, Nunu Mchedlishvili for software development, and Georg Nagel, Karl Deisseroth and Roger Y. Tsien for essential constructs. The work was supported by the Novartis Research Foundation.

Part 4.B

Temporal control of immediate early gene induction by light

Philipp Schoenenberger, Daniela Gerosa, and Thomas G. Oertner

PLoS One. 2009 Dec 4;4(12):e8185.

Abstract

The light-gated cation channel channelrhodopsin-2 (ChR2) is a powerful tool for the optical induction of action potentials in neurons. Mutations of the cysteine 128 (C128) residue have been shown to greatly extend the lifetime of the conducting state of ChR2. However, until now, only subthreshold depolarizations have been reported from C128 mutants. Here we report the induction of long high-frequency spike trains by brief light pulses in ChR2(C128A)-transfected pyramidal cells in hippocampal slice culture. ChR2(C128A)-mediated spike bursts triggered expression of the immediate early gene c-fos in pyramidal neurons. Robust and cell-specific expression of c-Fos protein was detected after a single blue light pulse and depended on action potential firing, but not on synaptic activity. However, photocurrents diminished upon repeated stimulation and limited the number of action potential bursts that could be elicited. We conclude that the C128A mutant is not suitable for chronic stimulation of neurons, but very useful for light-controlled induction of immediate early genes. This property of ChR2(C128A) could be harnessed to control the expression of proteins under control of the c-fos promoter with precise timing and single cell specificity.

Introduction

Optogenetic control of neuronal firing has become a widely used tool to manipulate the activity of single neurons or neuronal ensembles *in vitro* and *in vivo* (Adamantidis *et al.*, 2007; Zhang & Oertner, 2007; Huber *et al.*, 2008; Lagali *et al.*, 2008). Since the advent of the light-gated cation channel channelrhodopsin-2 (ChR2) in the neurosciences (Boyden *et al.*, 2005), the optogenetic toolbox has been steadily extended. For example, ChR2 mutants with greatly extended lifetimes of the open channel state have been generated. These 'bi-stable' channelrhodopsins are based on point mutations at the C128 position and elicit long-lasting photocurrents that can be switched off by a green light pulse (Berndt *et al.*, 2008). Three different point mutations at the C128 position have been shown to give rise to ChR2 variants with slow channel closing kinetics: ChR2(C128T) has a closing time constant of 2 s, whereas ChR2(C128A) and ChR2(C128S) are characterized by even slower channel closure and time constants of 52 s and 106 s, respectively (Berndt *et al.*, 2008). The C128A mutant has very interesting kinetics in that its open state outlast the activation light pulse by many orders of magnitude but it still spontaneously inactivates within an experimentally accessible time window. In their original publication, Berndt and colleagues used the C128A mutant to induce long and reversible subthreshold depolarizations in dissociated neurons and to sensitize cells to synaptic input (Berndt *et al.*, 2008).

In this study, we characterized the effects of ChR2(C128A) activation when the mutant channel is expressed at high levels in pyramidal cells in hippocampal slice culture. Photocurrents were very large initially, leading to high frequency spike trains. However, due to incomplete recovery of photocurrents in the dark, the number of spike trains that could be induced successively was limited. In the second part of the study, we focused on light-triggered expression of c-fos, an immediate early gene that has been used to map neural activity for more than two decades (Hunt *et al.*, 1987; Morgan *et al.*, 1987). Genetic activity reporters based on c-fos have allowed to follow the fate of cells activated during learning (Reijmers *et al.*, 2007) and to investigate the trafficking of newly synthesized AMPA receptors (Matsuo *et al.*, 2008). We show that ChR2(C128A)-triggered spike trains reliably induce c-Fos expression in pyramidal neurons. We propose that co-expression of ChR2 mutants with activity reporters could be used to study activity-related processes *in vitro* and *in vivo*.

Results

Stability of ChR2(C128A) photocurrents in hippocampal pyramidal neurons

We used the human synapsin 1 promoter to drive expression of ChR2(C128A) specifically in neurons. Using particle-mediated gene transfer, individual neurons in rat organotypic hippocampal slice cultures were co-transfected with ChR2(C128A) and the red fluorescent protein tdimer2 as a cytosolic marker (Fig. B.1A). To asses ChR2(C128A)-mediated currents, we recorded from pyramidal cells stimulated with 50 ms blue light pulses from a mercury arc lamp. Photocurrents were isolated by bath application of NBQX and bicuculline to block synaptic input and TTX to block fast Na^+ channels. The average photocurrent in cells voltage-clamped at -65 mV was 1325 ± 110 pA (*n* = 52; Fig. B.1B), considerably larger than reported previously (Berndt *et al.*, 2008). When a cell was repeatedly stimulated, photocurrents were strongly reduced (Fig. B.1C), although inter-stimulus intervals (ISIs) were sufficiently long to allow for full inactivation of the photocurrent (2.5 – 4.0 min). This effect was comparable for high (8.4 mW, 50 ms) and low (0.05 mW, 1000 ms) light intensities despite a reduction of the total light dose by a factor of 8.4. The response to identical light pulses was reduced after each stimulation pulse, dropping to 24.7 ± 3.7% of the initial amplitude after 9 repetitions for bright pulses (*n* = 6; Fig. B.1D) and 15.9 ± 0.8% for low intensity pulses (*n* = 3). Further increasing the light dose by using longer light pulses (200 ms, 8.4 mW) did not lead to a stronger reduction of peak currents (75.3 ± 4.0% reduction after 8 stimulations (*n* = 5), compared to 73.7 ± 3.6% with 50 ms pulses), suggesting that photocurrent reduction was not a light dose-dependent phenomenon such as the bleaching of fluorophores.

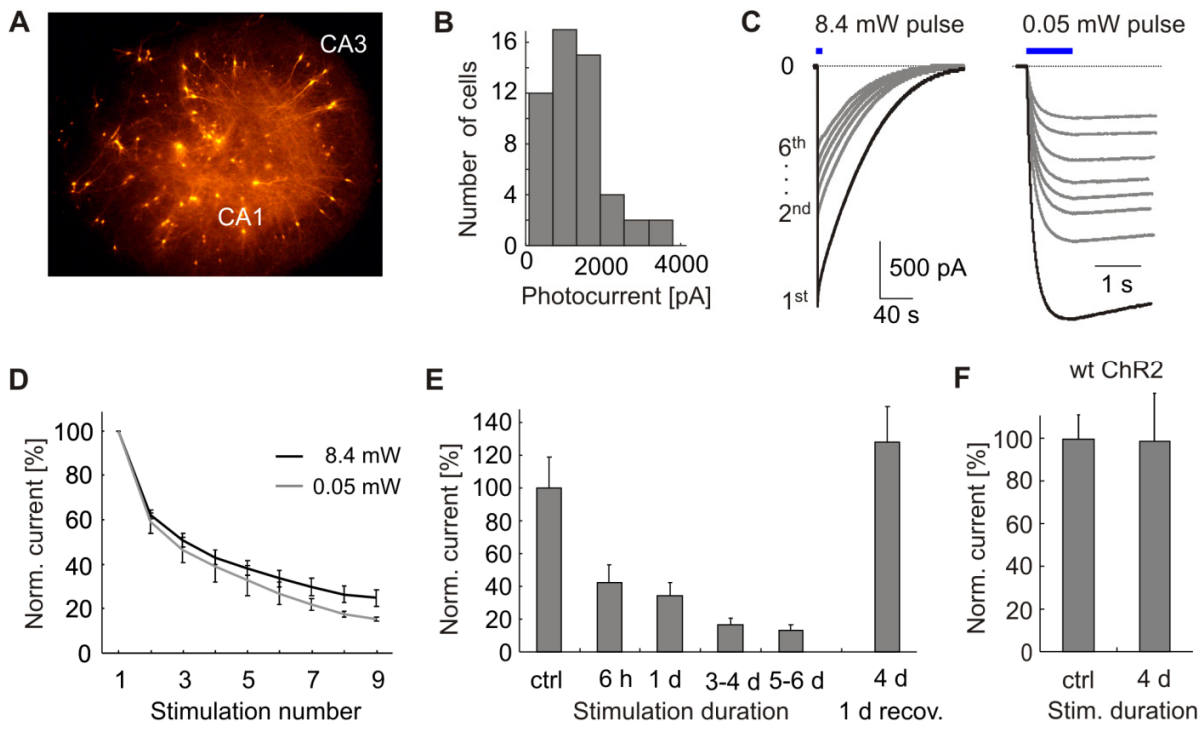

Figure B.1. ChR2(C128A) photocurrents in hippocampal pyramidal neurons. *(A) Rat organotypic slice culture co-transfected with ChR2(C128A) and cytoplasmic RFP. (B) Light-induced currents in voltage-clamped pyramidal cells (n = 52). Cells were stimulated using blue 50 ms light pulses (8.4 mW), current measurements were performed in the presence of 1 µM TTX, 10 µM NBQX, and 10 µM bicuculline. (C) Repeated stimulation of pyramidal neurons with high (8.4 mW for 50 ms; left) or low (0.05 mW for 1000 ms; right) light intensity. Blue bars indicate light stimulation pulses. (D) Photocurrent reduction with repeated stimulation at high or low light intensity (n = 6, 3, resp.). (E) Population comparison of photocurrents in non-stimulated cells (ctrl, n = 10) or cells stimulated in the incubator prior to photocurrent measurement (50 ms blue LED pulses at 90 s intervals, n = 6, 5, 18, 10). Photocurrents in cells stimulated for 4 d fully recovered within 24 h in the dark (n = 9). (F) No photocurrent reduction was observed in 4 d stimulated cells expressing wt ChR2 (n = 8) compared to non-stimulated control cells (n = 11).*

Could the photocurrent reduction be related to cytosolic wash-out during whole-cell recordings? To test this possibility, we stimulated transfected cultures inside the cell culture incubator using blue high-power LEDs (50 ms pulses, 90 s intervals) prior to photocurrent measurements. Light-induced currents were reduced after only a few hours of stimulation, and the reduction was even more pronounced after several days (Fig. B.1E). This indicates that the photocurrent reduction we observed was not caused by whole-cell dialysis. A dark period of 24 h prior to electrophysiological recording was sufficient for full recovery of photocurrents, showing that the decrease in current amplitude was not permanent but slowly reverted in the dark within several hours (Fig. B.1E). Photocurrents in cells expressing wild type ChR2 were not reduced after 4 d stimulation (Fig. B.1F), again indicating that ChR2(C128A) photocurrent run-down was not caused by photodamage to the chromophore but due to the extremely slow kinetics

of the mutant channel. Together, these data show that ChR2(C128A) can generate very large photocurrents, and that repeated activation of the channel rapidly reduces the amplitude of light-triggered currents.

Loss of functional channels occurs during relaxation from the open state

Work on the ChR2 photocycle suggested that activated channels relax to the dark state via one or two relatively long-lived closed intermediate states (Bamann *et al.*, 2008; Ritter *et al.*, 2008). We wanted to determine whether the run-down of photocurrents was caused by a fraction of activated channels entering a non-functional state after each stimulation or by very slow recovery of the dark state after channel closure. In the latter case, we would expect a recovery of photocurrent amplitude that is proportional to the interval between subsequent pulses. To address this issue, we stimulated neurons with three blue light pulses. The first two pulses were spaced 2.5 min apart, sufficient for inactivation of photocurrents between pulses. The 3rd light pulse was applied after a dark period of 2.5 min (n = 10) or 15 min (n = 4). The reduction in peak photocurrent in response to the 3rd light pulse was independent of the length of the preceding dark period (current after 3rd pulse: 48.5 ± 2.1%, 50.7 ± 2.0%, resp., $p > 0.5$; Fig. B.2A), suggesting that a fraction of channels was available for activation directly after channel closure whereas the remaining fraction entered a long-lived closed state that did not recover to the dark state within 15 min. For simplicity, we refer to this non-functional state as 'lost' state (Fig. B.2D).

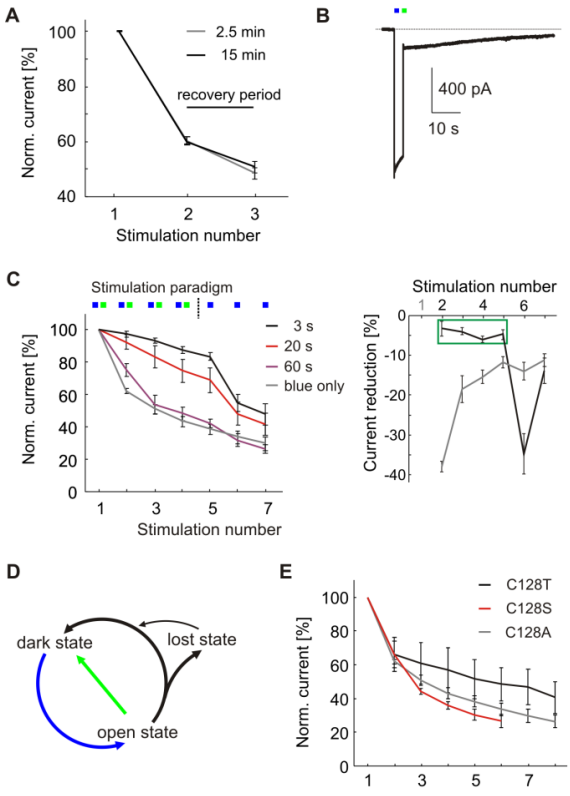

Figure B.2. Photocurrent reduction can be alleviated by green switch-back pulses. *(A) Neurons were stimulated with two blue pulses spaced 2.5 min apart. After a 2.5 min (gray, n = 10) or 15 min (black, n = 4) recovery period photocurrent reduction was comparable (p > 0.5). (B) Following excitation by a blue light pulse, ChR2(C128A) photocurrents could be inactivated by a green switch-back pulse. Inactivation efficiency was 90.6 ± 1.2% (n = 24). (C) Left: Photocurrent reduction was markedly diminished when activated channel was inactivated by a green switch-back pulse after a 3 s interval (black line). Application of a green light pulse after 20 s or 60 s was less effective in preventing current reduction (n = 3, 3). Gray line: Current reduction with single blue pulses for comparison. Right: Quantification of photocurrent reduction relative to the previous stimulation pulse without green switch-back (gray line) or with a green light pulse applied 3 s after blue light stimulation (black line). The green box indicates stimulation trials following a trial terminated with a green pulse (D) Minimal model for the ChR2(C128A) photocycle, modified after Berndt et al., 2008. (E) Photocurrent reduction with repeated stimulation was also observed in ChR2(C128T) and ChR2(C128S) mutants.*

Could the loss of functional channels be alleviated by rapidly switching open channels back to the dark state using a green light pulse (Berndt *et al.*, 2008)? We stimulated pyramidal cells with a blue light pulse followed by a green pulse after 3 s, which reduced the photocurrents to 9.4 ± 1.2% (*n* = 24; Fig. B.2B). Residual current was allowed to fully inactivate before the next stimulation (ISI > 2.5 min). This switch-back procedure markedly reduced the run-down of photocurrents upon repeated stimulation (16.7 ± 2.3% reduction after 5 pulses, *n* = 6, compared to 66.5 ± 3.8% without green switch-back; Fig. B.2C). As expected, a single blue pulse applied after a sequence of blue - green switches led to strong reduction of peak photocurrents at the next pulse (Fig. B.2C). Application of the green light pulse 20 s or 60 s after the blue stimulation pulse was less effective in preventing photocurrent reduction. We conclude that loss of functional ChR2(C128A) channels occurred during relaxation from the open state - either directly from the open state or from a closed intermediate - and could be strongly reduced by rapid optical channel closure (Fig. B.2D).

To determine whether photocurrent reduction after repeated stimulation is a property that is specific for ChR2(C128A) we also generated and tested the other two bi-stable ChR2 mutants reported by

Berndt and colleagues (Berndt *et al.*, 2008). We extended the ISI to 6 min to account for the very slow inactivation of ChR2(C128S) and we maintained an ISI of 2.5 min for ChR2(C128T). Indeed, rapid and pronounced photocurrent loss upon repeated stimulation was also observed for the C128T and the C128S mutants indicating that photocurrent run-down could be a general feature of ChR2 variants (Fig. B.2E).

Properties of light-triggered spike trains in pyramidal neurons

Next, we investigated ChR2(C128A)-triggered spike trains in hippocampal pyramidal cells in current-clamp. To reduce variability between trials, we adjusted the resting potential to -60 mV by injection of a small holding current. To prevent spontaneous network activity, we blocked excitatory transmission by NBQX. In response to a brief blue light pulse (50 ms), transfected cells fired a burst of action potentials (APs) (Fig. B.3A). Subsequent light pulses evoked a steadily decreasing number of APs, indicating a reduction of the underlying photocurrents (Fig. B.3B). We also observed a reduction in depolarization between spikes and a decrease in the initial firing frequency with repeated stimulation, consistent with a run-down of photocurrents. Next, we tested whether the number of spike trains fired by a cell could be increased by interrupting the light-triggered depolarization using a green light pulse applied 20 s after each blue pulse (Fig. B.3C). We found that both the number of stimulations that triggered spikes and the reduction of the maximal depolarization were comparable to stimulation with blue light only (Fig. B.3D), suggesting that the reduction in photocurrent loss was too weak to have a pronounced effect spike train firing. Thus, it appears that the run-down of photocurrents upon repeated stimulation limited the number of light-triggered spike trains in ChR2(C128A)-expressing cells.

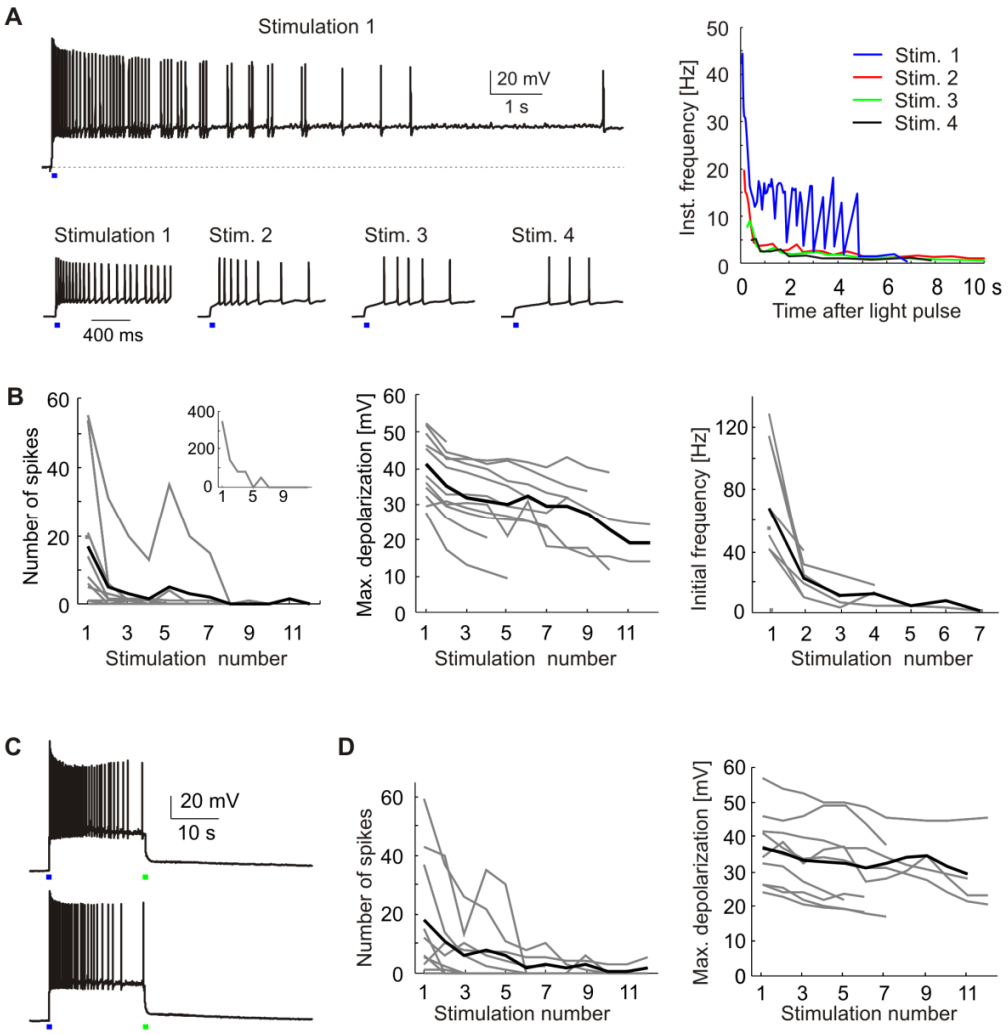

Figure B.3. Light-induced spike trains in pyramidal neurons. *(A) Spike trains triggered by four subsequent blue stimulation pulses. Depolarization was allowed to revert to baseline between stimulations. Right: Instantaneous frequency of spike trains. (B) Analysis of light-triggered spike trains. The number of spikes, maximal depolarization, and initial frequency decreased with repeated stimulation. Insert in first panel shows cell firing 355 APs after first stimulation pulse. Gray lines represent 12 individual cells, average is shown in black. (C) Light-induced depolarizations were interrupted by a green switch-back pulse after 20 s. Traces depict two subsequent spike trains. (D) The reduction in spike numbers and maximal depolarizations was comparable to experiments without green switch-back pulse (n = 10).*

Why did some pyramidal cells fire long spike trains whereas others fired only single spikes or failed to fire APs altogether? We classified cells based on their response to the first stimulation pulse into four categories (Fig. B.4): Cells that did not reach firing threshold (n = 4), sparse firing (1 – 30 APs; n = 5), train firing (> 30 APs, n = 6), and cells entering depolarization block (n = 7). Cells entering depolarization block were defined by strong spike amplitude attenuation due to incomplete repolarization between spikes

(Fig. B.4A). The range of depolarizations leading to train firing was very narrow (38.2 ± 1.8 mV; Fig. B.4B), as was the range of initial firing frequencies in this group (45.8 ± 3.5 Hz; Fig. B.4C). Cells entering depolarization block were characterized by strong depolarization (Fig. B.4B), high initial firing frequencies - in some cases exceeding 100 Hz (Fig. B.4C) - and very short delays to first spike (4.2 ± 0.4 ms; Fig. B.4D). In summary, responses of individual pyramidal cells were quite variable; consistent with the large variability of photocurrents we measured (Fig. B.1B).

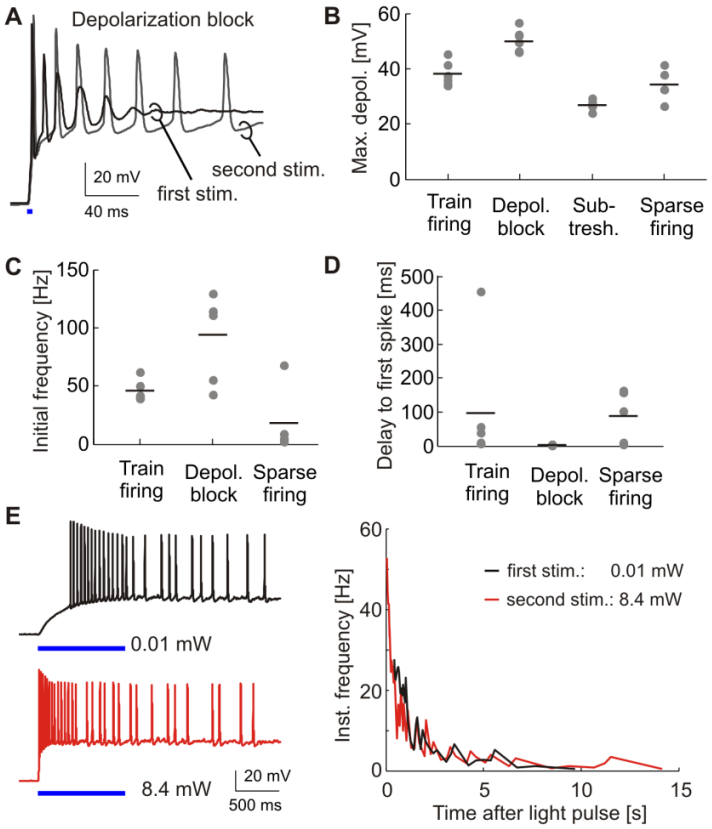

Figure B.4. Analysis of light-triggered activity in current-clamped cells. *(A) Sample traces of cell entering depolarization block after the first stimulation pulse. Note the pronounced spike amplitude attenuation. The second pulse induced a smaller depolarization and a series of APs. (B – D) Spike train parameters. Cells were classified based on their response to the first stimulation pulse. Train firing: > 30 APs, n = 6. Depolarization block, n = 7. Subthreshold depolarization, n = 4. Sparse firing: 1 – 30 APs, n = 5. (E) Spike trains in a pyramidal neuron stimulated with very low or high light intensity. Analysis of the instantaneous firing frequency reveals a similar rapid frequency drop under both conditions.*

An attractive property of the slow ChR2 mutants is their enhanced light sensitivity, which could enable light stimulation *in vivo* without the need to implant fiber optics. We were interested whether extremely low light intensities would induce different firing patterns in ChR2(C128A)-expressing neurons. We first stimulated cells with a long but very dim light pulse (0.01 mW, 1000 ms). A second stimulation pulse with high light intensity (8.4 mW, 1000 ms) was applied after a 2.5 min interval (Fig. B.4E). To minimize current loss between stimulation trials, light-induced depolarization was terminated by applying a green pulse 20 s after stimulation. Bursts of APs were fired in response to stimulation with either low or high

light intensity in 5 cells we recorded from. Interestingly, the number of spikes was very similar under both stimulation conditions (0.01 mW: 22.8 ± 5.1 APs; 8.4 mW: 23.6 ± 7.2 APs). However, due to the slow depolarization with low light intensity, the first spike was fired after a delay of 393 ± 64 ms whereas the delay was only 43 ± 16 ms for high light intensity. The firing pattern of a given cell was similar after low and high intensity light stimulation. The initial firing frequency was higher with a bright stimulation pulse and thus rapid depolarization, but the firing frequency rapidly dropped independently of the stimulation condition (see Fig. B.4E, right). When the stimulation paradigm was repeated the number of APs per stimulation trial rapidly decreased (after 6 repetitions: 0.01 mW: 1.4 ± 1.3 APs; 8.4 mW: 2.8 ± 1.9 APs). These results indicate that ChR2(C128A) can reliably induce AP firing even at very low light intensities, a property that may be useful to activate cells deep within the brain.

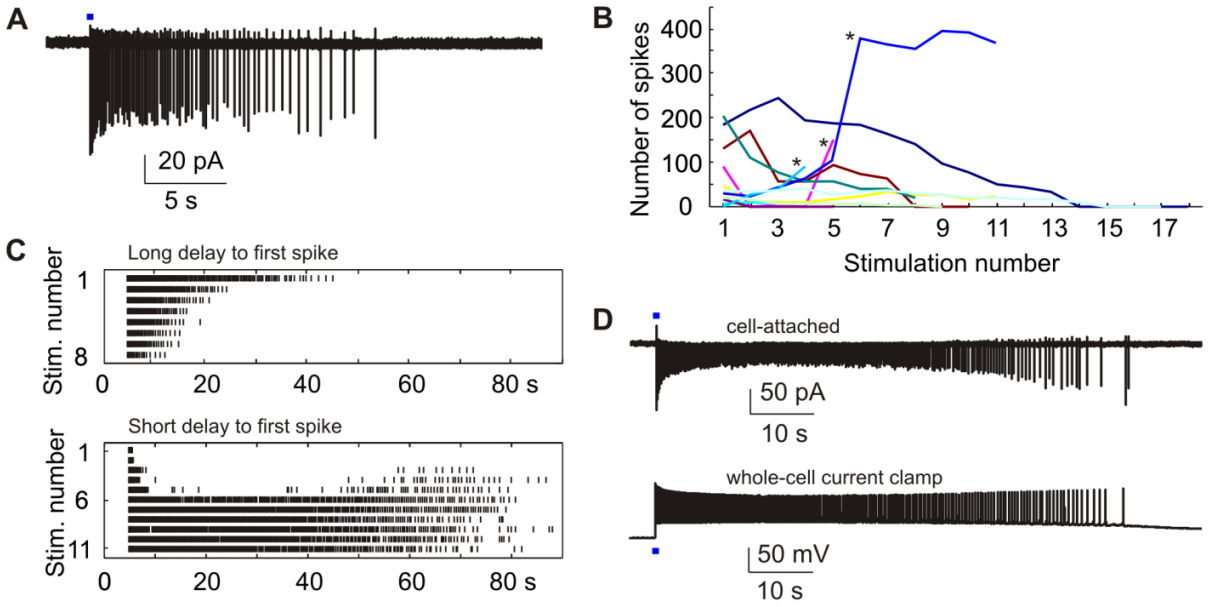

Figure B.5. Cell-attached recordings of light-induced spike trains. *(A) Sample trace. Cell-autonomous activity was isolated by bath-application of NBQX. (B) In the majority of cells the number of spikes decreased with repeated stimulation (8/11 cells). Asterisks indicate cells presumably entering depolarization block after initial stimulation pulses. (C) Top: Spike raster for cell with long delay to first spike (10.75 ms). Bottom: Spike raster for cell with short delay to first spike (4.25 ms) presumably entering depolarization block. (D) Top: Long spike train containing 394 APs. Bottom: Spike train in current-clamped cell (355 APs), for comparison.*

Recording of light-triggered responses in cell-attached mode

To characterize light-triggered activity in unperturbed pyramidal neurons, we performed a series of cell-attached recordings (Fig. B.5A). Similar to whole cell recordings, the number of APs decreased with repeated stimulation in most cells (8/11 cells; Fig. B.5B and C (top)). We also observed cells that fired an

increasing number of spikes upon repeated stimulation (3/11 cells; Fig. B.5B and C (bottom)). During the first stimulations, these cells fired a brief high frequency burst with pronounced spike amplitude attenuation immediately after light onset (average delay: 4.0 ± 0.7 ms), and a few more spikes after a silent period of 20-60 s (Fig. B.5C, bottom). In these cells, run-down of photocurrents paradoxically led to an increase in total spike output in subsequent stimulations, suggesting that during the first stimulations, they entered depolarization block. Qualitatively, our cell-attached recordings thus confirmed the results of light stimulation in whole-cell configuration: Similar response classes were found, and long bursts of APs with decreasing frequency were observed in both recording configurations (Fig. B.5D). Quantitatively, spike trains were often longer in cell-attached recordings, indicating that whole-cell recording slightly impeded AP generation.

Cell-autonomous c-Fos induction by light-triggered action potential firing

To investigate the cellular consequences of ChR2(C128A)-induced spike bursts, we stained stimulated and non-stimulated rat hippocampal slice cultures for endogenous c-Fos protein. Under basal conditions, c-Fos expression was very low (Fig. B.6A). Exposing the cultures to 50 mM K^+ (3 x 2 min, 10 min intervals) led to strong c-Fos induction 2 h after stimulation (Fig. B.6A). To test for light-induced expression of c-Fos, we stimulated transfected cultures in the cell culture incubator with LED-generated light pulses (300 ms pulse length, ISI = 90 s). In a first set of experiments, we fixed cultures at different time points after stimulation with 10 light pulses and stained for c-Fos (Fig. B.6B). Interestingly, c-Fos levels were already significantly increased after 30 min ($p < 0.01$; Fig. B.6C). After 1 h, c-Fos expression reached a plateau that was maintained for about 2 h.

Next, we stimulated cultures with different numbers of stimulation pulses. We found that a single blue light pulse was sufficient to induce c-Fos expression in transfected pyramidal cells ($p < 0.03$ compared to non-stimulated control; Fig. B.6D). After a single light pulse, c-Fos levels were heterogeneous: Significant c-Fos upregulation (signal larger than mean + 2 SD of control) was detected in 7/15 cells. After 10 light pulses, maximal optical c-Fos induction was reached. High K^+ stimulation induced even stronger c-Fos signals (Fig. B.6D, dotted line). We conclude that the lack of further c-Fos upregulation by additional light pulses was most likely due to run-down of photocurrents, limiting the number of spike trains

triggered in individual neurons. Importantly, induction of c-Fos after light stimulation was restricted to ChR2-transfected cells (see Fig. B.6B).

Light-triggered depolarizations were typically very large (Fig. B.4B), raising the possibility that action potentials were not required to induce immediate early gene expression. We tested the possibility that calcium influx through ChR2 itself and through low-voltage-activated calcium channels was sufficient for c-Fos induction. Application of the Na^+ channel blocker TTX during stimulation blocked c-Fos induction, indicating that spiking activity was necessary to trigger the signaling cascade leading to c-Fos expression (Fig. B.6E). On the other hand, glutamate receptor antagonists (NBQX, CPP) did not impair light-induced c-Fos expression, indicating that synaptic activity was not required to induce c-Fos. These results validate the use of c-Fos expression as an indicator for cellular activity (Morgan *et al.*, 1987; Smeyne *et al.*, 1992). Moreover, these data show that calcium influx through the ChR2 pore itself (see Zhang & Oertner, 2007) is not sufficient to induce c-Fos expression.

In order to investigate if ChR2(C128A) could be used to control c-fos promoter-driven transgene expression, we prepared hippocampal slice cultures from fosGFP transgenic mice (Barth *et al.*, 2004). These mice express a fosGFP fusion protein and have been used to identify and characterize recently activated neurons in live brain tissue (Barth *et al.*, 2004). Under basal conditions, virtually no fosGFP signal was detectable. Brief stimulation with 50 mM K^+ (3 x 2 min, 10 min intervals) induced strong fosGFP expression in pyramidal neurons (Fig. B.6F). Light stimulation of cultures transfected with ChR2(C128A) and RFP (300 ms pulse length, 10 pulses, ISI = 90 s) led to strong and significant expression of the fosGFP reporter protein specifically in transfected neurons (Fig. B.6G,H; $p < 0.05$). As a control, we verified that transfected but not light-stimulated cells did not express GFP above background. Taken together, our data show that light-triggered spike bursts reliably induced c-Fos expression in a cell-specific and cell-autonomous manner. Moreover, light-induced spike trains can be exploited to control the expression of custom transgenes driven by the c-fos promoter.

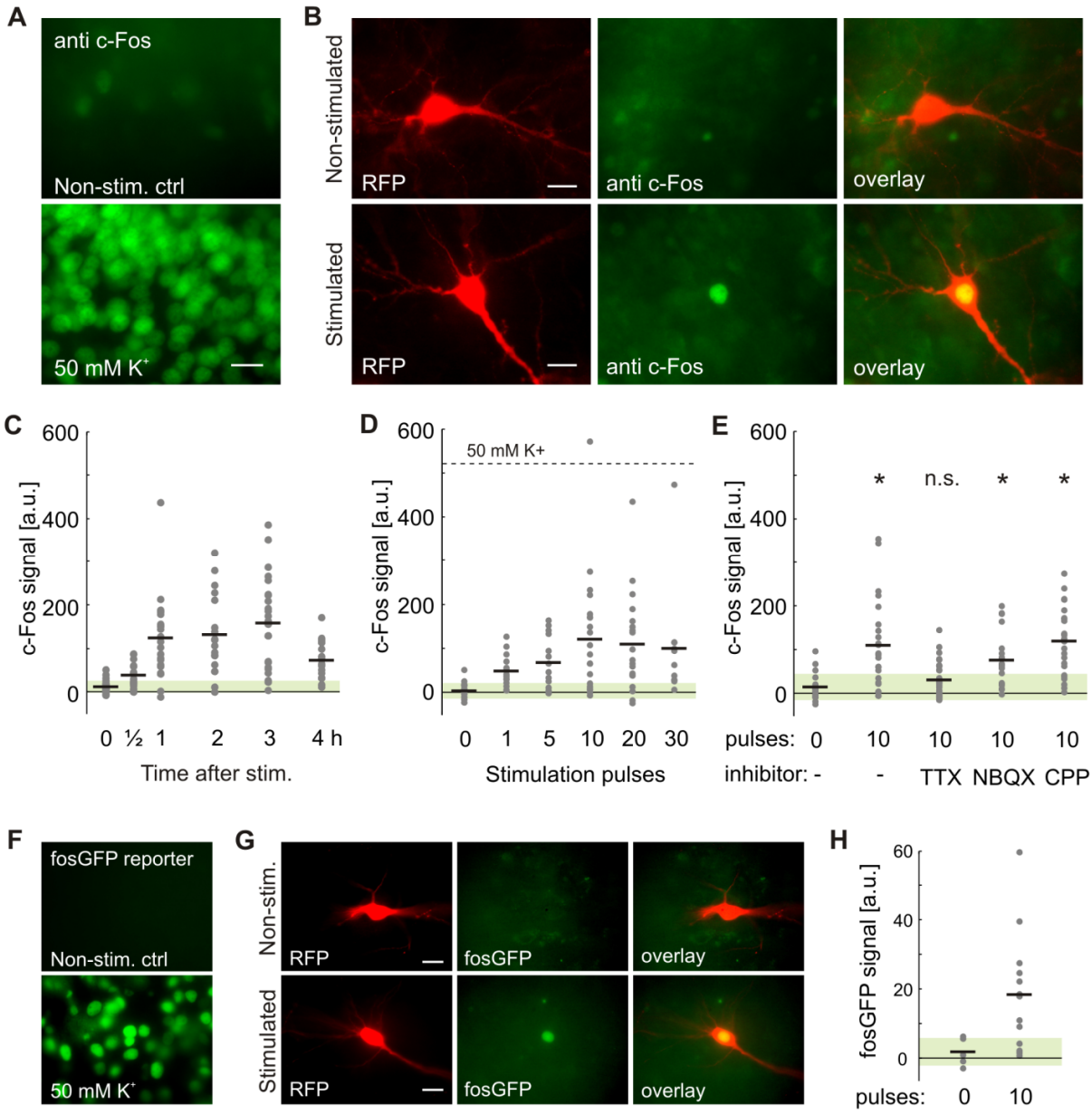

Figure B.6. Cell-specific c-Fos induction by light-triggered spike trains. *(A) Immunostaining for endogenous c-Fos in CA1 area of rat hippocampal slice cultures under basal conditions (top) and 2 h after stimulation by extracellular application of 50 mM K^+ (bottom). (B) c-Fos induction in a pyramidal neuron expressing ChR2(C128A) and cytosolic RFP after 10 stimulation pulses. Cultures were fixed 2 h after stimulation and stained for c-Fos. (C) c-Fos signal in non-stimulated cells (n = 27) and at different time points after light stimulation (n = 18, 24, 18, 25, 21). Green shaded bar indicates mean ± SD of non-stimulated control cells. c-Fos induction was significant at all time points ($p < 0.01$). (D) Significant c-Fos induction was observed after a single blue light pulse (n = 17, 15, 14, 21, 19, 11). Dashed line indicates average c-Fos signal after 50 mM K^+ stimulation. (E) Light-triggered c-Fos induction was blocked by TTX, but not by NBQX or CPP. *: $p < 0.01$ compared to control. (F) Green fluorescence in live organotypic slice cultures (CA3) from fosGFP transgenic mice under basal conditions (top) and 4 h after brief stimulation with 50 mM K^+ (bottom). (G) Light-induced GFP expression in fosGFP reporter mouse neurons expressing ChR2(C128A) and RFP. (H) Light-induced GFP expression was quantified 4 h after light stimulation (10 pulses). Scale bars in (A,B,F,G): 10 μm.*

Discussion

Here we report that hippocampal pyramidal neurons expressing the bi-stable channelrhodopsin mutant ChR2(C128A) fire long spike trains in response to brief flashes of blue light. During repeated activation, pronounced reduction of photocurrent amplitudes limited the number of spike trains that could be triggered in individual cells. Downstream of spiking activity, we found that a single blue light pulse was sufficient to induce expression of the immediate early gene c-fos in about half of the transfected cells. We propose that the specific properties of ChR2(C128A) could be exploited for temporally controlled cell-specific induction of transgenes under the control of the c-fos promoter.

An unexpected property of ChR2(C128A) was the rapid decrease of peak photocurrent amplitude and bursting activity during repeated light stimulations. In fact, our first set of photostimulation experiments were not successful (data not shown), because a diffuse white LED we used to position the slice culture under the microscope already induced permanent inactivation of most of the photocurrent. This cautionary tale provides a potential explanation why a previous study of the very light-sensitive ChR2(C128A) reported only subshreshold depolarization and illustrates the practical importance of our findings (Berndt *et al.*, 2008). In this context, it is important to note that we used RFP instead of YFP as a fluorescent marker and thus avoided blue light exposure while searching for transfected cells, thereby preventing loss of photocurrent.

The loss of photocurrent with repeated stimulations was not observed in cells expressing wt ChR2. Moreover, photocurrent run-down did not depend on the blue light dose applied in each stimulation trial. Therefore, we can exclude bleaching processes such as destruction of the chromophore (*all-trans* retinal) as a cause for run-down of light-induced currents. For inter-stimulus intervals up to 15 min, there was no recovery of photocurrents. Loss of photocurrent could be largely prevented by rapidly closing the channels with green light, confirming that the light-gated channel was not degraded by the blue light used for stimulation (Fig. B.2C). We conclude that the time spent in the open state is the critical parameter that determines the fraction of channels lost in every trial. For wt ChR2, relatively long-lived closed channel intermediates have been described (Bamann *et al.*, 2008; Ritter *et al.*, 2008), raising the possibility that we stimulated the cells at too short ISIs, preventing full recovery of the dark

state between trials. However, prolonging the ISI from 2.5 to 15 min resulted in very similar reduction of peak photocurrent, arguing against a single rate-limiting step in a linear photocycle (Fig. B.2A). More likely, the photocycle of ChR2(C128A) branches during relaxation from the open state, causing accumulation of more and more channels in a non-functional 'lost' state (Fig. B.2D). Indeed, after 24 h in the dark, photocurrents did recover, indicating that spontaneous transitions from the lost to the dark state were very rare. Branched photocycles are not a novel concept, but have been proposed for various rhodopsins (Nagel *et al.*, 1998; Hegemann *et al.*, 2005; Nikolic *et al.*, 2009). Future spectroscopic studies of the ChR2(C128A) photocycle may help to understand the nature of the lost state and to develop strategies to minimize photocurrent reduction upon repeated stimulation. Photocurrent run-down was not restricted to ChR2(C128A), but was also observed after repeated stimulation of ChR2(C128T) and ChR2(C128S) mutants, indicating that this phenomenon might be a general feature of ChR2 variants (Fig. B.2E).

Our findings suggest that ChR2(C128A) is best suited for the temporally controlled induction of a limited number of strong activity bursts. The potential for chronic stimulation is limited at present, but might improve in the future as more information becomes available about the channel photocycle. A very interesting application would be light-triggered protein expression in selected cells. Genetic activity reporters based on the activity-dependent activation of the c-fos promoter have been used for in vivo activity mapping (Smeyne *et al.*, 1992; Reijmers *et al.*, 2007) or for activity-induced transgene expression (Matsuo *et al.*, 2008). Combining selective ChR2(C128A) expression using suitable promoters with the spatial precision of light activation (Schoenenberger *et al.*, 2008) will allow to use light pulses for precisely timed induction of c-fos promoter-controlled transgenes in specific cells. In contrast to methods for conditional gene expression relying on caged molecules (Cambridge *et al.*, 1997; Ando *et al.*, 2001; Cambridge *et al.*, 2009), no addition of chemicals would be needed for optogenetic induction, an important advantage for *in vivo* applications. Indeed, we observed reliable light-triggered induction of a c-fos promoter-driven reporter protein in ChR2(C128A)-transfected neurons in cultures from transgenic mice, demonstrating the successful implementation of this approach (Fig. B.6G,H). In summary, ChR2(C128A) seems ideally suited to trigger gene expression in single cells with high temporal precision.

Although c-Fos has been used in many studies as an activity reporter (Morgan *et al.*, 1987; Smeyne *et al.*, 1992; Barth *et al.*, 2004; Tronson *et al.*, 2009), it is unclear what the minimal trigger for c-Fos induction is. Here we show that a single light pulse induced c-Fos in 47% of transfected pyramidal neurons (Fig. B.6D). The fraction of c-Fos expressing cells rose to 57% for 5 stimulation pulses and to 65% for 10 or more pulses. c-Fos induction was blocked by TTX but not by AMPA or NMDA receptor antagonists, suggesting that c-Fos upregulation requires action potential firing, but not excitatory synaptic input. This is consistent with studies showing that Ca^{2+} influx through voltage-gated calcium channels can trigger c-Fos expression (Murphy *et al.*, 1991; Bading *et al.*, 1993). In our cell-attached recordings, 54% of cells fired a spike train in response to the first light stimulation, a success rate that fits well to 47% of cells expressing c-Fos after a single light pulse. Our data thus suggests that a single train of 30 or more APs is sufficient for c-Fos induction in hippocampal pyramidal cells. Average c-Fos expression levels increased with the number of light pulses, but reached a plateau after 10 pulses. Again, this observation can be readily explained by the failure of most cells to produce more than 10 spike trains in succession. Stimulation by 50 mM K^+ induced c-Fos at levels ~5-fold higher than after light stimulation (Fig. B.6A, D), indicating that the dynamic range of the c-Fos-system is very large and might only become saturated under pathophysiological conditions (i.e. persistent depolarization). In conclusion, we show that ChR2(C128A)-mediated firing induces c-Fos expression in a graded and cell-specific manner. This property could be exploited to drive transgene expression in selected cells with a high degree of temporal control.

Methods

Cell culture and transfection

Hippocampal slice cultures from rats (Sprague Dawley) or fosGFP transgenic mice (C57BL/6) were prepared at postnatal day 4-5 as described (Stoppini *et al.*, 1991), according to the rules of the Federal Veterinary Office of Basel-Stadt. After 6-8 days in culture, we used a Helios gene gun (Bio-Rad) to co-transfect individual cells with DNA encoding ChR2(C128A) and tdimer2 (dimeric RFP), each subcloned into a neuron-specific (synapsin 1) expression vector. The C128X point mutations were introduced into wt ChR2 by site-directed mutagenesis. To achieve high expression levels, 5 mg colloidal gold (1.6 µm, Bio-Rad) was coated with 4 µg of each co-transfected construct.

Electrophysiology

The recording setup was based on a BX-51 microscope equipped with a LUMPlan 60x 0.9NA water immersion objective (Olympus) and a cooled CCD camera (Sensicam QE). For patch-clamp recordings, we used a MultiClamp 700B amplifier (Axon Instruments) controlled by ScanImage (Pologruto *et al.*, 2003) and MP-225 manipulators (Sutter Instrument). Experiments were conducted at 29 - 31°C 1 - 4 weeks after transfection under low ambient light conditions. To ensure that all experiments started with a uniform dark-adapted channel population, we recorded only from one cell per culture. Artificial cerebrospinal fluid (ACSF) contained (in mM) 119 NaCl, 26.2 $NaHCO_3$, 11 D-glucose, 2.5 KCl, 4 $MgCl_2$, 4 $CaCl_2$, 1 NaH_2PO_4. ACSF was complemented with 1 µM TTX, 10 µM NBQX, 10 µM bicuculline for photocurrent measurements in voltage-clamp; 10 µM NBQX for current-clamp or cell-attached recordings. Pipettes for cell-attached experiments contained 150 mM NaCl. Glass pipettes for patch-clamp recordings were filled with intracellular solutions containing (in mM): 135 potassium gluconate, 10 HEPES, 4 $MgCl_2$, 4 Na_2-ATP, 0.4 Na-GTP, 10 Na_2-phosphocreatine, and 3 ascorbate.

Photostimulation

EGFP (Chroma # 41017; 470/40 exciter) and rhodamine filter sets (Zeiss # 43; 545/25 exciter) were used for arc lamp stimulation. Light pulses (50 ms if not indicated otherwise) were controlled by a mechanical shutter (Uniblitz). Light pulse power (measured in the back focal plane of the objective) was 8.4 mW for blue and 44 mW for green pulses, if not indicated otherwise. In electrophysiological experiments, a minimal interval of 2.5 min was maintained between stimulation pulses. For stimulation in the cell culture incubator, culture inserts in 35 mm cell culture dishes were illuminated from below with blue LEDs (Luxeon V Star blue, Philips; 0.2 mW/mm^2 at 15 mm from the emitter).

Immunohistochemistry

For c-Fos immunolabeling cultures were fixed at the indicated intervals after onset of stimulation using Formal-Fixx (Shandon). The primary antibody (Anti-c-Fos rabbit pAb, Calbiochem) was applied over-night in permeabilization buffer (PBS containing 1% BSA, 0.3% Triton X-100). After extensive washing the secondary antibody (Alexa Fluor 488 goat anti-rabbit IgG, Invitrogen) was applied for 2 h in 1:3 diluted

permeabilization buffer. After extensive washing cultures were mounted on glass slides and stored at 4°C.

Data analysis

For analysis of c-Fos expression, transfected cells were selected based on the RFP signal. For unbiased analysis of c-Fos expression levels, the nuclear c-Fos signal (green fluorescence) was measured and background subtracted using ImageJ. The experimenter was blind to the experimental conditions. Electrophysiological recordings were analyzed with custom software written in MATLAB. For characterization of spike trains, the initial frequency is the frequency of the first two spikes fired in a burst and the instantaneous frequency is the frequency between two subsequent spikes. Numerical values are given as mean ± s.e.m. Statistics were performed using two-tailed t tests (Bonferroni-corrected for multiple comparisons).

Acknowledgements

We are very grateful to Alison L. Barth, Andreas Lüthi and Christian Müller for providing fosGFP transgenic mice. We thank Verena Senn for advice on the c-Fos induction experiments, and Georg Nagel, Karl Deisseroth and Roger Y. Tsien for essential constructs. The work was supported by the Novartis Research Foundation and SystemsX.ch.

Part 4.C

Designer-Channelrhodopsins enable fast neuronal stimulation at low light levels

André Berndt[1*], Philipp Schoenenberger[2*], Joanna Mattis[3], Kay M. Tye[3], Karl Deisseroth[3], Peter Hegemann[1] and Thomas G. Oertner[2]

Submitted

[1] Humboldt-Universität zu Berlin, Experimental Biophysics, Invalidenstr. 42, D-10115 Berlin, Germany

[2] Friedrich Miescher Institute for Biomedical Research, Maulbeerstr. 66, CH-4058 Basel, Switzerland

[3] Department of Bioengineering, Stanford University, Stanford, CA 94305, USA

* These authors contributed equally to this work

Summary

Channelrhodopsin-2 (ChR2) has become an indispensable tool in neuroscience, allowing precise induction of action potentials with short light pulses. A limiting factor for many optophysiological experiments is the relatively small photocurrent induced by ChR2. We screened a large number of ChR2 point mutants and discovered a dramatic increase in photocurrent amplitude after threonine-to-cysteine substitution at position 159. When we tested the T159C mutant in hippocampal pyramidal neurons, action potentials could be induced at very low light intensities, where currently available channelrhodopsins were unable to drive spiking. In addition, we combined T159C with the recently published E123T substitution to speed up channel kinetics. The resulting ET/TC double mutant delivered fast photocurrents with large amplitudes and increased the precision of single action potential induction over a broad range of frequencies. Furthermore, the kinetics of ET/TC did not slow down at depolarized membrane potentials, suggesting it as a new standard for light-controlled activation of neurons.

Introduction

Optogenetic stimulation of neurons using Channelrhodopsin-2 (ChR2) has become a widely used tool in neuroscience. ChR2, a directly light-gated cation channel of the green algae *Chlamydomonas reinhardtii*, allows depolarizing and firing neurons with brief blue light pulses (Nagel *et al.*, 2003; Boyden *et al.*, 2005). Because the single channel conductance of ChR2 is very small, high expression levels are required to fire neurons reliably. Over the last few years, techniques for ChR2 expression in neurons have been improved substantially. High expression levels can be obtained by expressing ChR2 under the control of strong promoters, for example in virally transduced neurons. In mice, the combination of Cre-dependent viruses with specific Cre-expressing driver lines has enabled strong ChR2 expression in cell types where no specific strong promoters are known (Cardin et al., 2009; Sohal et al., 2009). In spite of these advanced expression strategies, reliable and well-timed action potential (AP) induction can still be difficult, especially at high stimulation frequencies, or for *in vivo* experiments where local light intensities are low. Several engineered channelrhodopsins that address some of the current limitations have been reported. ChR2(H134R) carrying a single point mutation at position H134 generates larger photocurrents than wild-type (wt) ChR2, but slows down channel kinetics, which can interfere with the precision of single AP induction (Nagel et al., 2005). The recently reported E123T ('ChETA') mutation speeds up channel kinetics, but reduces photocurrent amplitudes (Gunaydin et al., 2010). Combined with the H134R mutation, E123T produced photocurrents that nearly reached the amplitude of wt ChR2 currents while preserving favorable accelerated kinetics, enabling stimulation of fast spiking interneurons at up to 200 Hz (Gunaydin et al., 2010). Pyramidal cells, due to their different K^+ channel complement, resist such high spike frequencies (Martina et al., 1998). Finally, the bi-stable C128 variants have very long-lived open channel states and therefore induce neuronal depolarization at very low light intensities (Berndt et al., 2009). Due to their slow kinetics and strong light-dependent inactivation, however, bi-stable ChR2 variants are not suitable for long-term control of AP induction (Schoenenberger et al., 2009). To control AP firing in large neurons such as cortical pyramidal cells with high reliability and temporal precision even at high frequencies, mutants that can generate large photocurrents with rapid channel kinetics are required. Ideally, if such mutants would also work at low light intensities, transcranial or intra-uterine optogenetic stimulation could become possible, obviating the need to implant optical fibers into the brain. Here we present two novel ChR2 variants that improve the reliability and versatility of optogenetic neuronal stimulation. ChR2(T159C), which we refer to as ChR2-TC or simply TC, generates very large photocurrents and sensitizes neurons to very low light intensities.

The E123T/ T159C double mutant (ET/TC) enables reliable and sustained optical stimulation of hippocampal pyramidal neurons up to 60 Hz. Our biophysical analysis suggests that the fast and voltage-independent kinetics of ET/TC is responsible for the excellent performance at high frequencies.

Results

Biophysical characterization of ChR2 mutants

The retinal binding pocket of ChR2 is conserved from other microbial opsins such as bacteriorhodopsin, of which high resolution 3D structures are available (Luecke et al., 1999). Using this structural homology as a guideline, we were able to target mutations specifically to the retinal binding pocket of ChR2, affecting channel properties such as ion selectivity, kinetics and absorbed wavelengths. Point mutants were characterized in *Xenopus* oocytes, a well established test system for the kinetic analysis of photocurrents. We screened >50 ChR2 mutants and found quite dramatic changes after amino acid substitutions at position T159, in close vicinity of the previously characterized C128 and D156 residues (Fig. C.1A). Mutation of Thr 159 to Cys (TC) resulted in a dramatic increase of photocurrent amplitudes, but, in contrast to mutations at the C128 and D156 positions, did not result in bi-stable behavior (Fig. C.1B). Since ChR2(H134R) (Nagel et al., 2005) has become a popular choice for neuronal stimulation, we included this mutant for comparison (green trace). We confirmed that the stationary current of H134R in oocytes increased about 3 times compared to wild-type (wt) ChR2 (Fig. C.1C). In the new TC mutant, however, current amplitudes were more than 10 times larger compared to wt ChR2.

Large photocurrents are very desirable, but often accompanied by slower channel kinetics. We measured the time constant of channel closure (τ_{off}) after 0.5 s of illumination, which was indeed slowed down in H143R and in the TC mutant (Fig. C.1D). In an attempt to accelerate the kinetics of TC, we mutated the counter ion at E123, a position that has been reported to accelerate channel kinetics (Gunaydin et al., 2010).The double mutants E123T/T159C (ET/TC) and E123A/T159C (EA/TC) showed current amplitudes of 2.5 and 1.5 times wt level, and the closing process, which was significantly decelerated in TC (19 ms), was almost back to wt levels (10 ms) in ET/TC and EA/TC (12 and 14 ms). One drawback of wt ChR2 is its strong inactivation during continuous light stimulation, which can be quantified by the ratio of stationary ($I_{stationary}$) to peak current (I_{peak}) (Fig. C.1E). Inactivation of TC and

ET/TC was similar to wt, while H134R and EA/TC showed less inactivation. We also tested the double mutant H134R/TC, but the improvements of the single mutations were not combined, and the current increased relative to wt by only 3.5 times. In addition, this mutant had very slow *off*-kinetics (Fig. C.1D).

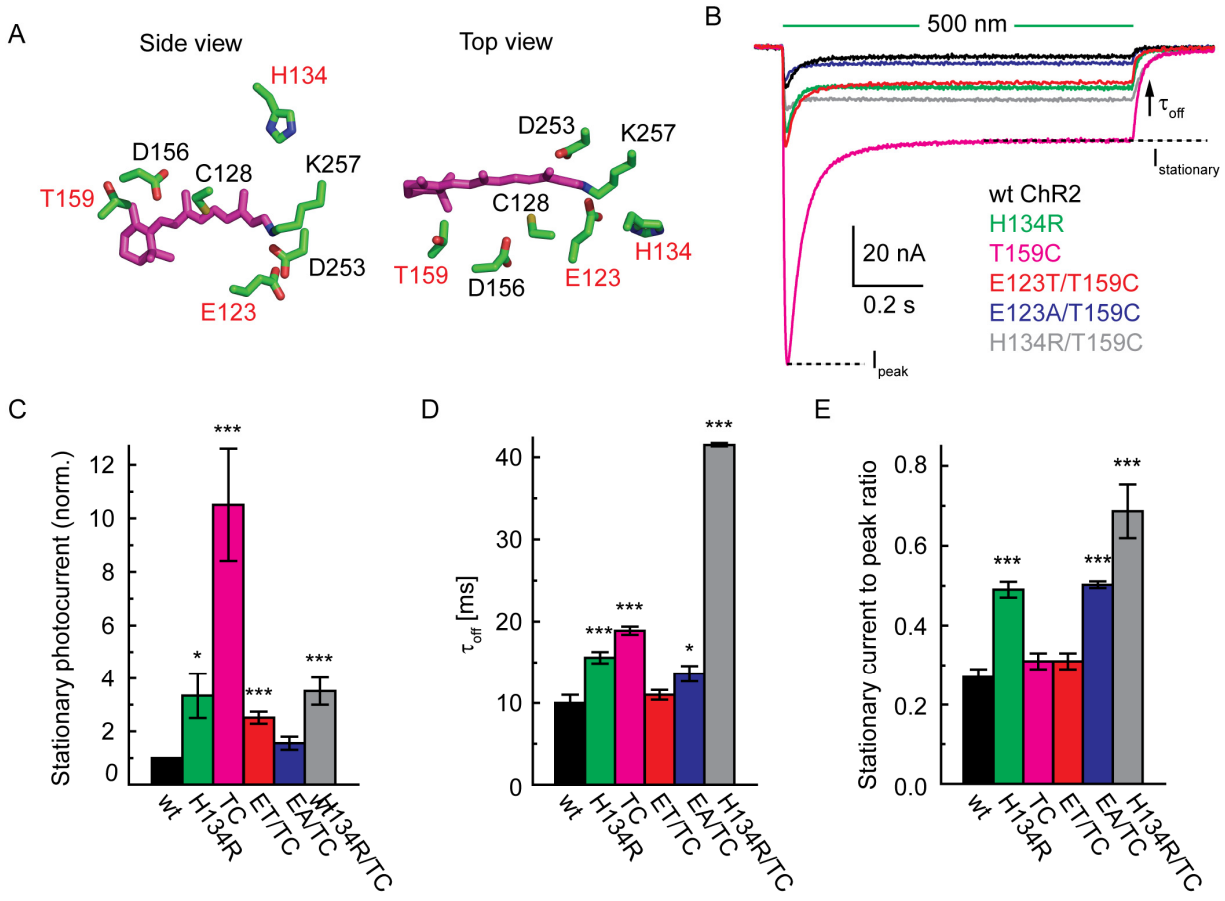

Figure C.1. Biophysical characterization of photocurrents in Xenopus oocytes.

(A) Homology model of the ChR2 retinal binding pocket based on bacteriorhodopsin x-ray data (pdb database No. 1C3W). The chromophore is shown in magenta; residues that have been replaced in this study are labeled in red. (B) Typical photocurrents in oocytes excited by continuous light (500 nm, green bar) measured at -100 mV. During light stimulation, the peak current (I_{peak}) decays to a lower stationary level ($I_{stationary}$). The off-kinetics (τ_{off}) were extracted from tail currents. (C) Stationary photocurrents of single and double mutants ($I_{stationary}$), normalized to the reference values of wt ChR2 (I_{wt}, black, n = 15). H134R (green, n = 9), TC (magenta, n = 9), ET/TC (red, n = 13), EA/TC (blue, n = 9), and HR/TC (gray, n = 8). (D) Channel closure (τ_{off}) of ET/TC (red) was as fast as wt ChR2 (black), all other tested mutants were significantly slower. (E) Inactivation under continuous light conditions (ratio of $I_{stationary}$ to I_{peak}) of TC and ET/TC was similar to wt ChR2. In H134R, EA/TC and HR/TC, inactivation was significantly reduced. Significance levels: P < 0.005 (***), P < 0.05 (*).

Since fast channel kinetics and large current amplitudes are essential for most neurobiological applications, we focused our characterization on TC and the ET/TC double mutant. For more precise measurements of channel kinetics, we excited the mutants by 10 ns laser flashes and measured the time

to peak photocurrent (flash to peak, FtP). Time constants of channel closure (τ_{off}) were determined by mono-exponential fit to the decay phase of the flash-induced currents. Consistent with our measurements during continuous light (Fig. C.1), TC was slower than wt (both FtP and τ_{off}), while ET/TC was faster (Fig. C.2A). Interestingly, the kinetics of H134R, TC, and wt ChR2 were strongly dependent on membrane potential: At +50 mV, channel closure was about 3 times slower compared to -100 mV (Fig. C.2B). In contrast, ET/TC had very fast kinetics (τ_{off} = 8 ms) at all tested membrane potentials. For neuronal stimulation, fast channel closure is critical to enable rapid repolarization after action potentials (APs).

A further design goal was fast recovery of the peak current during repetitive stimulation (Fig. C.2D, inset). The recovery time constant in the dark ($\tau_{recovery}$) was slightly accelerated for H134R ($\tau_{recovery}$ = 8.5 s vs. 10 s for wt), and slower for TC ($\tau_{recovery}$ = 16 s). In ET/TC, recovery of the peak current was remarkably fast ($\tau_{recovery}$ = 2.6 s), making it most suitable for repetitive stimulation. All tested ChR2 variants maintained the typical inward rectification of wt ChR2 with reversal potentials close to zero, suggesting that ion selectivity was not dramatically altered (Fig. C.2E). The reversal potential of TC was slightly but significantly shifted from -6.7 mV (wt) to -0.8 mV (Fig. C.2E, insert), pointing to enhanced Na^+ permeability.

Action spectra in hippocampal neurons

The spectral properties of H134R, TC and ET/TC were characterized in patch-clamp recordings from cultured hippocampal neurons. Photocurrents were induced by low-intensity light pulses of different wavelengths (Fig. C.2F). Action spectra of H134R and TC were similar to wt ChR2, with the largest currents induced at 470 nm (blue). In ET/TC, however, the optimal wavelength was red-shifted to 505 nm (green). Red-shifted excitation is desirable for *in vivo* applications since short wavelengths are strongly scattered in brain tissue.

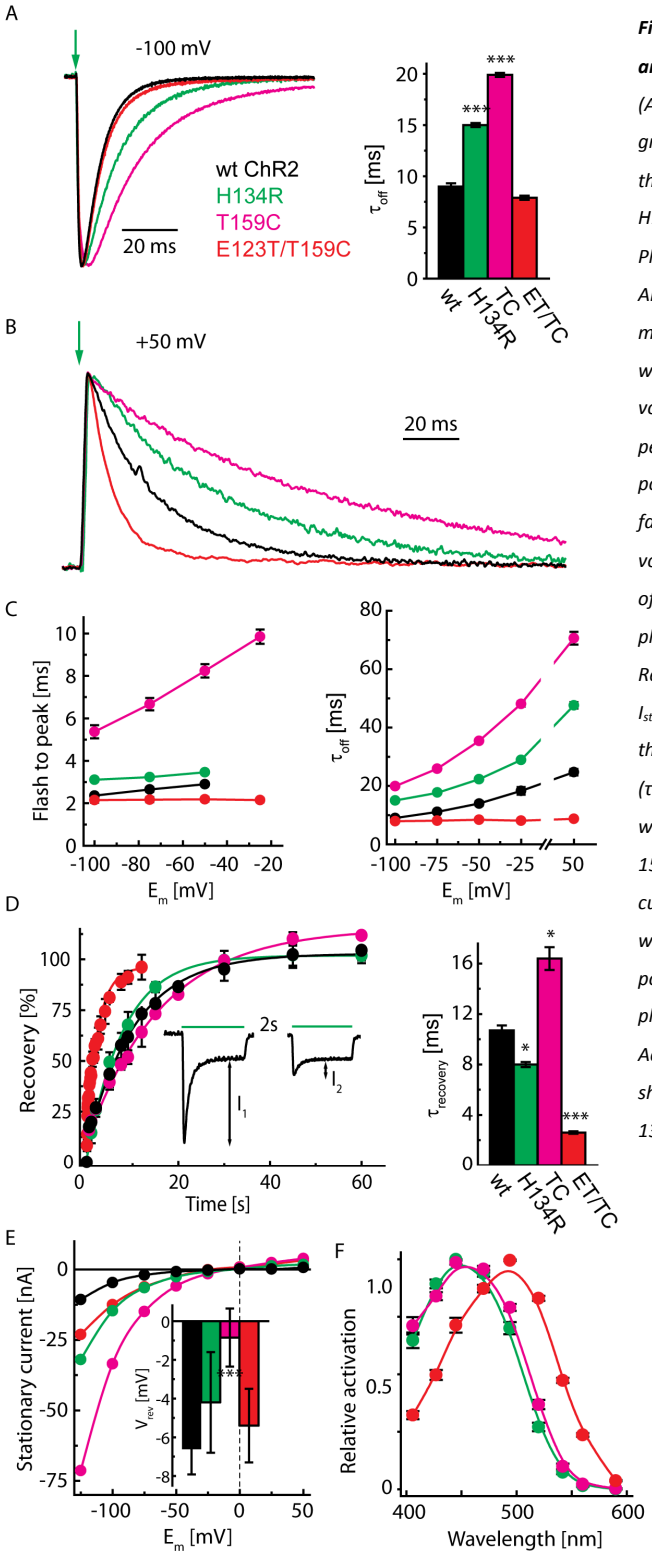

Figure C.2. Voltage-dependence of channel kinetics and spectral properties of ChR2 mutants.

(A) Photocurrents after laser flash activation (10 ns, green arrow) measured at -100 mV, normalized to the peak. ET/TC was as fast as wt ChR2, while H134R and ET/TC were significantly slower. (B) Photocurrents after laser flash activation at +50 mV. All mutants slowed down considerably at this membrane potential, except ET/TC (red trace), which retained its fast kinetics. (C) To quantify the voltage-dependence of channel kinetics, flash-to-peak and τ_{off} were analyzed at different membrane potentials (n = 10 cells for each mutant). ET/TC was fastest at all tested potentials and had no apparent voltage-dependence. (D) Time-dependent recovery of peak currents (I_{peak}) was measured under physiological conditions at -75 mV in oocytes. Recovery was defined as the ratio of ΔI_2 ($I_{peak2} - I_{stationary2}$) to ΔI_1 ($I_{peak1} - I_{stationary1}$) and plotted against the inter-pulse interval. Recovery time constants (τ_{rec}) of H134R (green, n = 3) and ET/TC (red, n = 3) were significantly faster than wt ChR2 (black, n = 15), while TC (magenta, n = 3) was slower. (E) IV-curves show that the typical inward rectification of wt ChR2 (black) is retained in all mutants. Reversal potentials ($V_{reversal}$) were close to zero under physiological conditions (inset, n = 10, 10, 12, 8). (F) Action spectra measured in hippocampal neurons show red-shifted wavelength optimum of ET/TC (n = 13) relative to H134R (n = 10) and TC (n = 11).

Photocurrents in hippocampal slice culture

To test the performance of TC and ET/TC in pyramidal cells, we co-expressed them with cytoplasmic RFP in rat hippocampal slice cultures. Wild-type ChR2 and the H134R variant served as references. The sparse expression pattern we obtained with particle-mediated gene transfer allowed us to identify transfected hippocampal pyramidal neurons and to target them for whole-cell recordings (Fig. C.3A). Neurons transfected with the ChR2 variants appeared to be healthy and did not display any obvious morphological abnormalities (Fig. C.3B). We first quantified stationary photocurrent amplitudes in response to 500 ms pulses of bright blue light (42 mW/mm^2, Fig. C.3C). To isolate light-evoked currents, we blocked AMPA and NMDA receptor mediated excitatory synaptic input by NBQX and CPP, respectively. Compared to photocurrents in wt ChR2 cells (967 ± 114 pA), currents in TC cells were significantly increased (1762 ± 182, $p < 0.005$). Photocurrents in ChR2(H134R) (1312 ± 154 pA, $p = 0.102$) or ET/TC expressing cells (1420 ± 180 pA, $p = 0.071$) were also larger than in cells expressing wt ChR2.

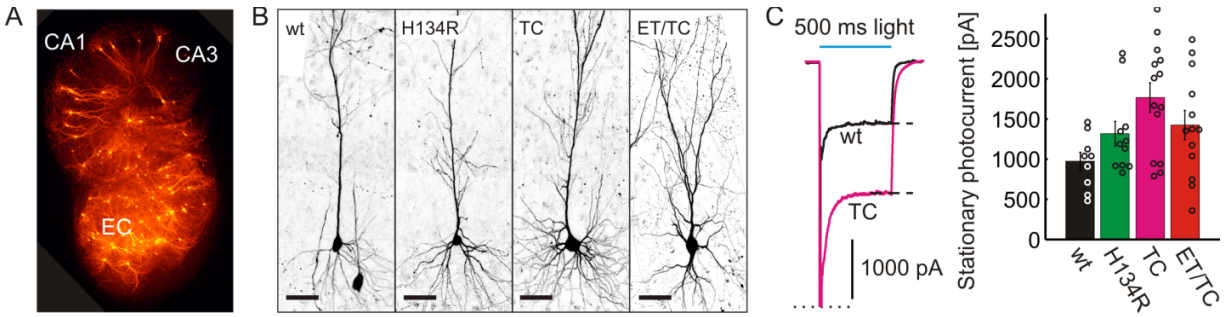

Figure C.3. Photocurrents of novel ChR2-TC variants in hippocampal pyramidal neurons.

(A) Neurons in a sparsely transfected rat organotypic slice culture expressing TC and dimeric RFP. (B) Contrast-inverted two-photon images of individual transfected pyramidal neurons. Scale bar: 50 µm. (C) Left: Photocurrents evoked by 500 ms blue laser illumination (42 mW/mm^2). Stationary photocurrents were quantified at the end of the stimulation pulse (dashed line) in neurons that were electrically isolated by blocking excitatory synaptic input with NBQX and dCPP. Escape action potentials (APs) were cropped for clarity (dotted line). Right: Quantification of stationary photocurrents (n = 9, 11, 14, 13 for wt, H134R, TC, ET/TC, resp.). Circles depict measurements from individual cells.

Action potential induction at 1 – 100 Hz

The large photocurrent amplitudes showed that all channelrhodopsin variants we tested were well expressed in neurons and confirmed the photocurrent enhancement with TC we observed in oocytes. The most common and important application of ChR2 in neurons, however, is the induction of APs with high temporal precision using brief light pulses. Hippocampal pyramidal cells transfected with wt ChR2 or H134R were able to reliably follow a train of 60 bright light pulses at 40 Hz only for the first 4-7 pulses

(Fig. C.4A, left). Later during the train, they fired action potentials only sporadically, reflecting the transition from high peak currents to substantially lower stationary currents that is characteristic for ChR2. In contrast, neurons transfected with TC and ET/TC typically sustained firing during the entire train of 60 light pulses. Some TC-transfected neurons did produce APs of reduced amplitude *early* in the train, indicating depolarization block due to overly large photocurrents. At very low light levels, on the other hand, TC-transfected neurons were the only ones still responsive to the stimulus (Fig. C.4A, right). This example might illustrate that there is no 'ideal' channelrhodopsin for all applications, but experimental conditions have to be considered when choosing the 'right' optogenetic tool.

To evaluate the performance of different ChR2 variants more systematically under a broad range of stimulus conditions, we stimulated transfected pyramidal cells with 2 ms light pulses at seven different frequencies (1 - 100 Hz). Each light pulse train was presented at four different intensities (1.9 mW/mm^2, 6.7 mW/mm^2, 23 mW/mm^2, 42 mW/mm^2), resulting in a total of 28 different stimulus patterns for each neuron. At low stimulation frequencies (1 Hz) and high light intensities, the firing success rate (defined as the percentage of light pulses triggering at least one AP) was close to 100% for all ChR2 variants. For wt ChR2 and H134R, the success rate decreased rapidly with increasing stimulation frequency (Fig. C.4B). In contrast, most cells expressing TC or ET/TC fired reliably throughout the stimulation train up to 40 Hz. As expected, the faster double mutant outperformed TC at very high frequencies (60-100 Hz), but only under bright light conditions. When lower light intensities were used for stimulation (1.9 – 6.7 mW/mm^2), TC had the advantage over all other mutants at all tested frequencies, recommending it for low-light applications.

For some optogenetic experiments, the average spiking performance across all transfected cells might be less important than the fraction of cells that follow the light stimulus reliably. Therefore, we also analyzed firing reliability in individual neurons. Using a success rate of 80% as an arbitrary threshold for 'good' performance, 45% of ET/TC neurons still performed well at 60 Hz stimulation, but only 18% of TC neurons, 11% of H134R neurons, and no neuron expressing wt ChR2 (Fig. C.S1). Thus, for high frequency spiking under bright light conditions, channel kinetics trumps photocurrent amplitude. At lower frequencies, both TC and ET/TC neurons could be stimulated reliably with only few neurons dropping below the 80% level. Together, these data show that TC and ET/TC outperform the commonly used

H124R variant across the entire stimulus space. Specifically, the TC mutant makes it possible to spike large pyramidal cells with very dim and short light pulses whereas all other ChR2 variants failed to induce spikes in this regime.

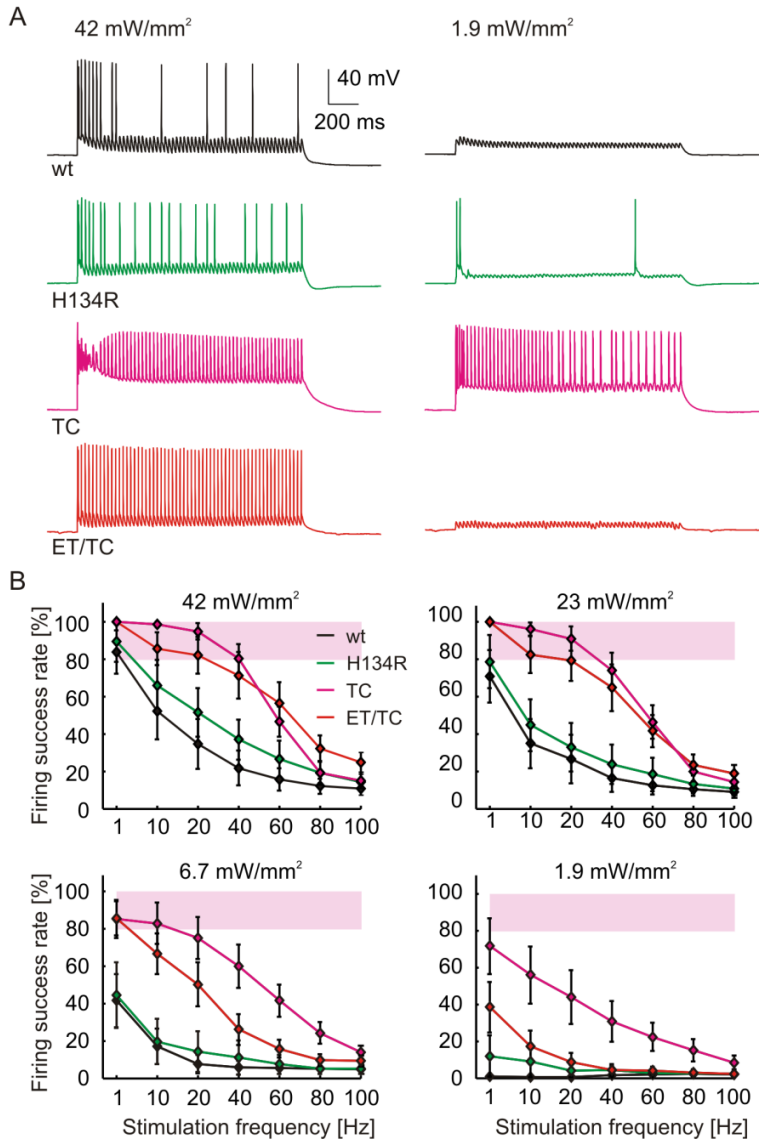

Figure C.4. Stimulation performance of TC variants at 1 – 100 Hz. *(A) Left: Whole-cell current-clamp recordings from pyramidal neurons stimulated with 60 brief (2 ms) light pulses at 40 Hz at high laser intensity (42 mW/mm²). Light-evoked activity was isolated by blocking excitatory synaptic input. Right: Stimulation of the same cells with very low (1.9 mW/mm²) light power. (B) Summary of the firing success rates from 1 to 100 Hz at different stimulation intensities (n = 9, 9, 12, 13 for wt, H134R, TC, ET/TC, resp.). Note the high stimulation efficacy of TC and ET/TC even at low light intensities (see also Figure S1 and S2).*

Precision of action potential induction

Compared to the fast Na^+ and K^+ channels activated during the AP, the *on*- and *off*-kinetics of ChR2 are relatively slow. Channelrhodopsin photocurrents can therefore outlast the AP, resulting in an after-depolarization that affects release probability at axonal boutons of ChR2-expressing neurons (Zhang & Oertner, 2007). In addition, at high expression levels, ChR2 can evoke several APs in response to a single

light pulse. Spurious extra spikes compromise the precision of optogenetic AP induction, and the enhanced photocurrents combined with slightly slower *off*-kinetic we measured in TC-expressing cells suggested potential multiplet firing. Not surprisingly, in many strongly expressing TC neurons, we observed induction of doublets or triplets in response to high intensity 2 ms light pulses (Fig. C.5A). In general, multiplet firing was much reduced at lower light intensities (Fig. C.5A, right), and largely absent at frequencies of 10 Hz or higher (Fig. C.5B). Even in TC-expressing neurons, only the first light pulses in a long train could trigger sufficiently large currents to induce more than one spike, due to the transition from peak to stationary photocurrents (Fig. C.1B).

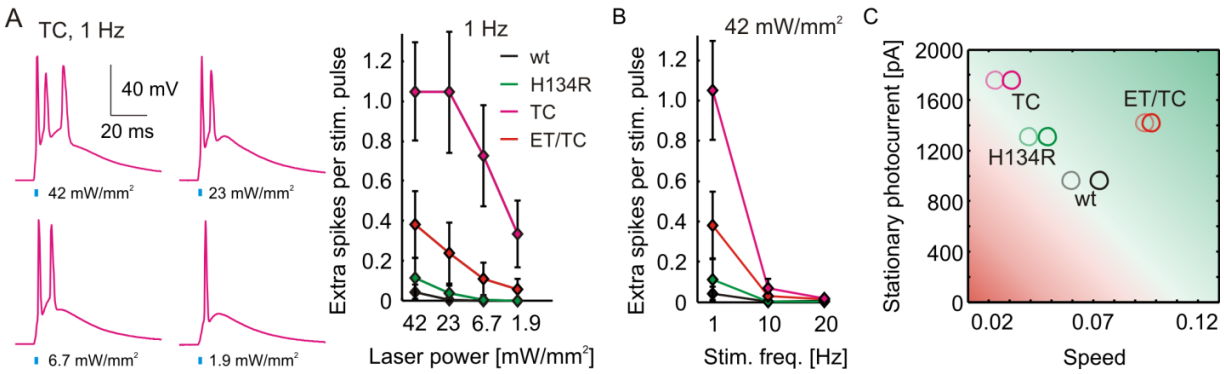

Figure C.5. Precision of single AP induction. *(A) Left: With high stimulation light intensity, TC often evoked several spikes in response to a single 2 ms light pulse during 1 Hz stimulation. Right: Multiplet firing is observed mostly with TC and is reduced at lower stimulation intensity. (B) Multiplet firing is largely restricted to 1 Hz stimulation and rarely occurs at higher stimulation frequencies. (C) Comparison of photocurrent amplitude (same data as Fig. 3C) and channel speed (defined as: (flash to peak + τ_{off})$^{-1}$, same data as Fig. 2C) for wt ChR2, H134R, TC, and ET/TC. Bright circles: Kinetics at -75 mV; pale circles: at -50 mV. The ideal ChR should gate large currents with rapid kinetics (green shaded corner).*

A second consequence of large photocurrents with slow off-rates is build-up of plateau depolarizations at high stimulation frequencies since cells cannot repolarize sufficiently between individual stimulation pulses. Plateau potentials were largest in neurons expressing ChR2-TC, reaching a maximum of 23.7 ± 2.4 mV at 80 Hz stimulation with 42 mW/mm^2 laser power (Fig. C.S2). Similar to multiplet firing, plateau potentials were reduced at lower light intensities and at lower stimulation frequencies. Interestingly, large plateau potentials were also observed in neurons transfected with H134R (17.5 mV ± 1.2 mV at 100 Hz), whereas wt ChR2 and ET/TC-transfected cells had only small plateaus (12.8 mV ± 1.8 mV, 10.7 mV ± 2.3 mV at 100 Hz, respectively), despite similar photocurrent amplitudes with the H134R variant and ET/TC. This suggests that the amplitude of plateau depolarizations is dominated by channel kinetics, with faster channels enabling stronger membrane repolarization between stimulation pulses. Taken

together, these data suggest that TC is best suited for optical stimulation at very low stimulation intensities, whereas at moderate and high light intensities, ET/TC allows single AP induction with high accuracy due to its accelerated kinetics at all membrane potentials (see Fig. C.2C).

Discussion

Previous attempts to improve ChR2 have yielded faster mutants that produced smaller currents, and mutants with large currents that were slower than wt ChR2. The anti-correlation between photocurrent amplitude and kinetics (Fig. C.5C) is not surprising, since thermodynamic stabilization of the open state increases the charge transfer through single channels but also slows down channel closure. Here we introduce two new ChR2 mutants that are particularly suitable for optogenetic stimulation of neurons. The ET/TC double mutant has an accelerated photocycle, which is apparent from the fast rise and decay of the photocurrent, and, once in the dark, the rapid recovery to the ground state (Fig. C.2D). In addition, ET/TC produces larger stationary photocurrents while maintaining the ion selectivity of wt ChR2, as indicated by the scaled-up IV curve (Fig. C.2E). The action spectrum is red-shifted by about 35 nm, which should be helpful for *in vivo* applications where the strong scattering of blue light can be a problem. Furthermore, the red-shifted absorption makes it possible to activate ET/TC at 530 nm, where the recently discovered photoactivated adenylyl cyclases (Schroder-Lang et al., 2007; Stierl et al., 2010) do not absorb. Both membrane potential and intracellular cAMP levels can therefore be controlled independently by blue and green light, respectively. When ET/TC was expressed in pyramidal cells, spikes were induced with higher fidelity across a wide range of light intensities and stimulation frequencies, despite the relatively small increase in photocurrent amplitude compared to wt ChR2 and H134R. We attribute the greatly improved performance of ET/TC in neurons largely to its accelerated kinetics, allowing rapid membrane repolarization following each AP. In contrast, during high frequency stimulation of wt ChR2 and H134R a plateau depolarization develops (Fig. C.S2), leading to Na^+ channel inactivation. In summary, ET/TC breaks the amplitude vs. speed relationship of previous ChR2 variants (Fig. C.5C) and will outperform wt ChR2 and H134R for all experimental conditions.

The second mutant we present in this paper is the TC single mutant, which generated extremely large stationary photocurrents of up to 3 nA in pyramidal cells. When driven by the synapsin 1 promoter, the

currents were large enough to trigger multiple spikes in response to bright 2 ms light pulses, and could even lead to depolarization block. We also demonstrated that TC could still induce spikes at very low light intensities where all other ChR2 variants produced only subthreshold depolarizations. The low light levels needed to stimulate TC-expressing neurons greatly reduce the risk of phototoxicity, especially in chronic stimulation experiments (Godley et al., 2005). In the future, we will also explore the possibility to stimulate TC-expressing cortical neurons transcranially, without inserting optical fibers or windows into the skull. Large photocurrents may also be helpful when weaker and more specific promoters have to be used, for example to activate specific subsets of interneurons.

Of note was the different magnitude of current enhancement by TC in oocytes (10 fold over wt) and neurons (2 fold over wt). Very likely, the TC mutation improved protein expression, folding, or targeting to the plasma membrane, as well as single channel properties. We do not fully understand the mechanism of the current enhancement, but noted the slightly positively shifted reversal potential of TC, pointing to enhanced Na^+ conductance (Berndt et al., 2010). Despite the very large currents they generated, the expression and activation of TC and ET/TC did not seem to cause any toxic effects in oocytes or in neurons.

With respect to rational molecule design, it was interesting to see that the kinetics and the current amplitude produced by the ET/TC double mutant were somewhere between the properties of the individual ET and TC mutations, but, by fortunate coincidence, the spectral properties of ET were fully retained (Gunaydin et al., 2010). We conclude that individual beneficial mutations of ChR2 can be combined to some extent in a module-like fashion, but careful assessment of the properties of multiple mutants will always be necessary. What would be important design goals for the future? Our data suggest that we are now in a situation where photocurrent amplitudes are no longer limiting stimulation performance. To further improve the reliability of optogenetic stimulation at high frequencies, light-gated channels with even faster kinetics would be required that completely eliminate plateau potentials while still gating very large photocurrents. As we have shown previously, APs triggered by wt ChR2 are associated with an increased transmitter release probability, most likely due to the relatively long duration of the light-induced current (Zhang & Oertner, 2007). Ideally, photocurrent amplitude would also be constant during continuous or repeated illumination, such that reliability and precision of AP

induction does not depend any more on the history of light stimulation. Lastly, a further red-shift of the absorption spectrum would be welcome, too.

In conclusion, for stimulation with minimal light intensities or deep within neuronal tissue, we recommend the TC single variant since it greatly increases the light sensitivity of transfected neurons. For all other experimental conditions, ET/TC is the most powerful tool since it combines rapid kinetics with large photocurrents and thereby dramatically improves the reliability of high frequency stimulation.

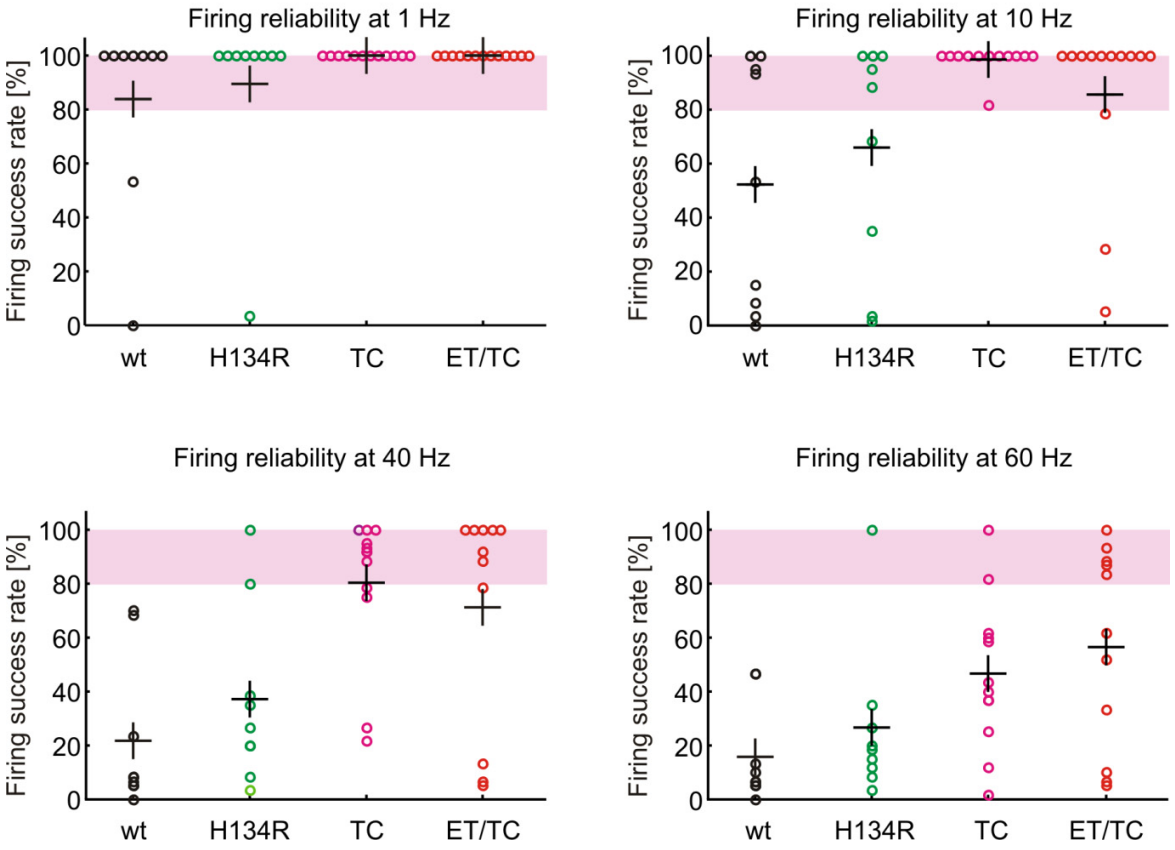

Figure C.S1. Firing reliability in individual pyramidal neurons. *Pyramidal neurons were stimulated with 60 light pulses of 2 ms duration at 42 mW/mm^2 laser power. Crosses indicate averages. Note that with 40 Hz stimulation, TC and ET/TC drive firing with high reliability between 80 – 100% in more than half of the neurons. At a stimulation frequency of 60 Hz, 5/11 cells expressing ET/TC still enable sustained firing with >80% reliability.*

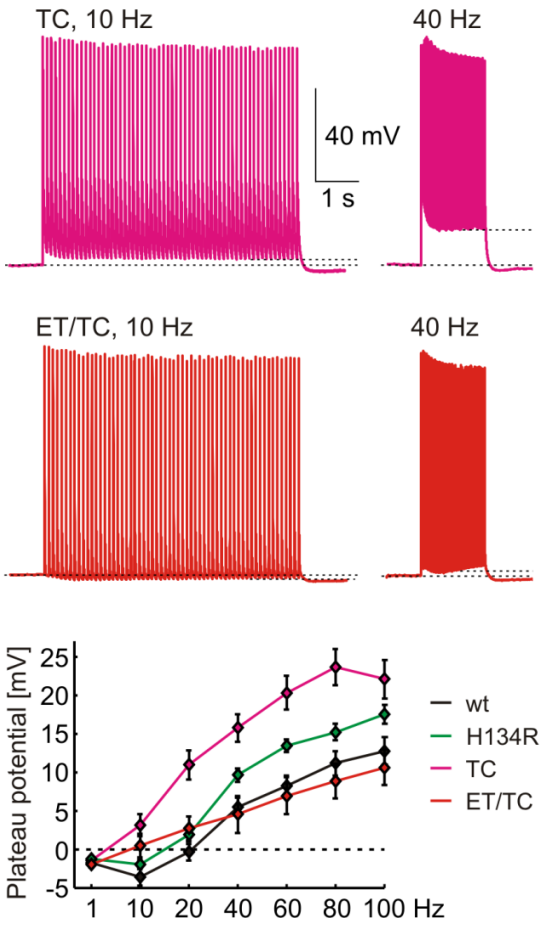

Figure C.S2. Plateau potentials at high stimulation light intensity. *Top: Example spike trains from neurons expressing TC or ET/TC stimulated with 60 2 ms pulses at 42 mW/mm^2. Plateau potentials were measured between baseline and the minimal membrane depolarization during the last 500 ms of the stimulation train (dashed lines). Bottom: Summary of plateau potentials for 1 – 100 Hz stimulation (n = 9, 11, 14, 13 for wt, H134R, TC, ET/TC, respectively).*

Experimental Procedures

Homology model

ChR2 sequence AF 461397 was aligned to the dark state structure of bacteriorhodopsin (1C3W) (Luecke et al., 1999) with the Swiss-PdbViewer and the ChR2 homology model was generated by the automated protein modelling server SWISS-MODEL (Guex & Peitsch, 1997).

Oocyte preparation

Amino acid replacement was realized by site directed mutagenesis (QuickChange, Agilent Technologies) of the pGEMHE-ChR2 plasmid. We used a shortened ChR2 sequence (residues 1-315) as template for

mRNA synthesis by T7 RNA polymerase (mMessage mMachine, Ambion). 20 ng mRNA were injected into oocytes from *Xenopus laevis* (Ecocyte). They were stored for 3–7 d in the dark at 18 °C in Ringer solution (96 mM NaCl, 5 mM KCl, 1.8 mM $CaCl_2$, 1 mM $MgCl_2$ and 5 mM MOPS-NaOH, pH 7.5) in the presence of 1 mg/ml penicillin, 1 mg/ml streptomycin.

Two Electrode Voltage Clamp and Data analysis

TEVC data were recorded with a Turbo Tec-05X (NPI Electronic) or a GeneClamp 500 (Molecular Devices) amplifier. The data acquisition was controlled by Clampex 10 software via DigiData 1322A or 1440A interfaces (Molecular Devices) and was performed at sampling rates between 10 and 250 kHz. Continuous light was provided by a 75 W Xenon lamp (Jena Instruments) and delivered to the oocytes via a 3 mm light guide. The light passed through a 500 ± 25 nm broadband filter (Balzers) and provided 46 mW/cm^2 light intensity. We applied 10 ns laser flashes at 470 and 500 nm with an adjustable Rainbow OPO (Opotek) pumped by Brilliant b Nd:YAG-Laser (Quantel) for fast kinetics measurements. All measurements were performed in an extracellular solution with 100 mM NaCl, 1 mM $MgCl_2$, 0.1 mM $CaCl_2$, and 5 mM MOPS buffer adjusted to pH_o 7.5. Mutants and wild-type ChR2 (wt ChR2) were always measured on the same day since protein expression and photocurrent amplitudes increased over time. Data were analyzed with Clampfit 10 (Molecular Devices) and OriginPro 8G (OriginLab Corporation) and displayed as mean ± SEM. We used Student's t-test (two-tailed) to assign statistical significance.

Action spectra measurements

Mammalian codon-optimized ChR2(H134R), ChR2(T159C), and ChR2(E123T/T159C) was cloned into a lentiviral backbone with CaMKIIα promoter (FCK), and fused in-frame with YFP at the C-terminus to enable visualization of expressing neurons. Primary hippocampal cultures were prepared from P0 Sprague-Dawley rat pups, transfected at 4 days in vitro with 2 μg of DNA per coverslip, and recorded 4 to 6 days later. For whole-cell patch clamp recordings, the intracellular solution contained (in mM) 130 K-gluconate, 10 KCl, 10 HEPES, 10 EGTA, 2 MgCl2, titrated to pH 7.0 with KOH. Tyrode was used as the extracellular solution, containing 125 NaCl, 2 KCl, 3 CaCl2, 1 MgCl2, 30 glucose, and 25 HEPES, titrated to pH 7.3 with NaOH. Recordings were performed at room temperature in the presence of bath-applied TTX (1 μM; Sigma-Aldrich) and intracellular QX-314 chloride (1 mM; Tocris Bioscience) to prevent

escaped spikes. Light pulses were delivered through a 40x water-immersion objective. Light was emitted from a 300 W DG-4 lamp (Sutter Instruments, Novato, CA) and passed through bandpass and neutral densitiy filters to generate closely-matched power densities. Action spectra were determined by measuring the peak photocurrent in response to 3 ms sub-saturating light pulses (range: 4.4-6.3 mW/mm^2). Measured photocurrents were scaled to correct for the small power density differences at different wavelengths, then normalized to action spectrum peak within cells followed by averaging across cells. Data are presented as mean ± SEM.

Slice culture and transfection

Hippocampal slice cultures from Wistar rats were prepared at postnatal day 4-5 as described (Stoppini et al., 1991). After 7 days in culture, we used a Helios gene gun (Bio-Rad) to co-transfect individual cells with DNA encoding a specific ChR2 variant and soluble tdimer2 (Campbell et al., 2002), each subcloned into a neuron-specific expression vector where expression was controlled by the human synapsin-1 promoter. For gene-gun transfection, 5 mg 1.6 µm gold bullets (Bio-Rad) were coated with a total of 8 mg DNA at a ChR2:tdimer2 molar ratio of 6:1. Point mutations (H134R, T159C, E123T) were introduced into wt ChR2 by site-directed mutagenesis (QuickChange, Agilent Technologies).

Electrophysiology and photostimulation of slice cultures

The recording setup was based on a BX-51 microscope equipped with a LUMPlan 60x 0.9NA water immersion objective (Olympus) and a cooled CCD camera (Sensicam QE). A secondary camera port was used to couple in 473 nm light (Oxxius SLIM-473 laser) via a single-mode optical fiber (MFD = 3.2 µm). An acousto-optic modulator (AA Opto-Electronic) was used to control laser pulse duration and amplitude. For patch-clamp recordings, we used a MultiClamp 700B amplifier (Axon Instruments) and MP-225 manipulators (Sutter Instrument). The acousto-optic modulator and patch-clamp amplifier were controlled by the open-source Matlab-based Ephus software package (Suter et al., 2010). Experiments were conducted at 29 - 31°C 1-3 weeks after transfection. Artificial cerebrospinal fluid (ACSF) contained (in mM) 127 NaCl, 25 $NaHCO_3$, 25 D-glucose, 2.5 KCl, 1 $MgCl_2$, 2 $CaCl_2$, 1.25 NaH_2PO_4. ACSF was complemented with 10 µM NBQX and 10 µM dCPP to block excitatory glutamatergic synaptic input. In current-clamp experiments, a small holding current was injected to hold the cells at -60 mV. Voltage-

clamp experiments were performed with -65 mV holding potential. Glass pipettes for patch-clamp recordings were filled with intracellular solutions containing (in mM): 135 potassium gluconate, 10 HEPES, 4 $MgCl_2$, 4 Na_2-ATP, 0.4 Na-GTP, 10 Na_2-phosphocreatine, and 3 ascorbate.

Data analysis

Electrophysiological recordings from neurons were analyzed with custom software written in MATLAB. APs were detected as brief membrane potential excursions with minimal amplitude of 40 mV. Firing success rate was defined as the percentage of light pulses evoking at least one AP. Extra spikes fired in response to a single light pulse were summed up for each pulse train and divided by the number of light pulses that successfully induced AP firing. This measurement thus quantifies the precision of single AP induction, whereas the firing success rate quantifies the reliability of spike induction. Plateau potentials were defined as the difference between baseline membrane potential and the most negative potential during the last 500 ms of the stimulation train. Numerical values are given as mean ± SEM.

Acknowledgments

A.B. is supported by the Leibniz Graduate School for Molecular Biophysics and an EMBO short term fellowship. P.S. and T.G.O would like to thank Daniela Gerosa Erni for excellent technical support and the Novartis Research Foundation and the Gebert Rüf Foundation for generous funding.

Part 4.D

Channelrhodopsin as a tool to investigate synaptic transmission and plasticity

Philipp Schoenenberger*, Yan-Ping Zhang Schärer, and Thomas G. Oertner

Exp Physiol. 2010 June 18. [Epub ahead of print]

* Corresponding author

Abstract

The light-gated cation channel channelrhodopsin-2 (ChR2) has been used in a variety of model systems to investigate the function of complex neuronal networks by stimulation of genetically targeted neurons. In slice physiology, ChR2 opens the door to novel types of experiments and greatly extends the technical possibilities offered by traditional electrophysiology. In this short review, we first consider several technical aspects concerning the use of ChR2 in slice physiology, providing examples from our own work. More specifically, we discuss differences between light-evoked action potentials (APs) and spontaneous or electrically induced APs. Our work implies that light-evoked APs are associated with increased calcium influx and a very high probability of neurotransmitter release. Furthermore, we point out the factors limiting the spatial resolution of ChR2 activation. In the second part, we discuss how synaptic transmission and plasticity can be studied using ChR2. Postsynaptic depolarization induced by ChR2 can be combined with two-photon glutamate uncaging to potentiate visually identified dendritic spines. ChR2-mediated stimulation of presynaptic axons induces neurotransmitter release and reliably activates postsynaptic spines. In conclusion, ChR2 is a powerful tool to investigate activity-dependent changes in structure and function of synapses.

Introduction

Within only a few years after its first introduction into neurons (Boyden *et al.*, 2005), the algal cation channel channelrhodopsin-2 (ChR2) has become a very important tool in neuroscience. ChR2 can be expressed in virtually any cell type in vertebrates and invertebrates and allows depolarizing and firing neurons with blue light. The light-gated channel has found prominent application both *in vivo* and *in vitro,* where it enables stimulation of genetically defined cells in complex neuronal networks (Lagali *et al.*, 2008; Claridge-Chang *et al.*, 2009; Gradinaru *et al.*, 2009; Varga *et al.*, 2009; Adesnik & Scanziani, 2010; Cruikshank *et al.*, 2010; Hagglund *et al.*, 2010). A number of studies have provided important insights into the function of neural circuits without the need to control the precise firing patterns in ChR2-expressing neurons because many circuit functions do not depend on the timing of individual action potentials (APs; see e.g. Gradinaru *et al.*, 2009; Hagglund *et al.*, 2010). In such experiments, the effectiveness of stimulation can be controlled by extracellular recordings to obtain a population response to the light stimulus.

In slice physiology, the experimenter often tries to control firing of individual action potentials with high temporal precision to investigate processes that typically operate on millisecond timescales. ChR2-based stimulation opens the possibility to stimulate distributed populations of genetically defined neurons using light. However, due to expression level differences, reliability and timing of AP induction varies from cell to cell. Electrophysiological control recordings from individual neurons are possible, but cannot provide information about the entire population of ChR2-positve cells. Furthermore, for certain experiments - such as chronic stimulation over several days – combining photostimulation with electrophysiology may not possible because of deleterious effects on cell viability. In fact, the possibility to stimulate cells *without* inserting glass or metal electrodes into the tissue is one of the main advantages of optogenetic approaches over traditional electrical stimulation methods. Optimization of ChR2 expression and stimulation as well as careful electrophysiological calibration measurements are therefore key to ensure reliable firing of ChR2-expressing neurons, in particular in the absence of simultaneous control recordings.

ChR2 expression and stimulation

If ChR2 is used to elicit APs in neurons, light-induced depolarization has to reach the firing threshold. Because of the small single channel conductance of ChR2 (Bamann *et al.*, 2008), expression levels required for reliable AP induction are quite high. Moreover, due to variable expression levels in individual transfected cells, there will often be a subpopulation of ChR2-expressing neurons that experience only subthreshold depolarization during blue light stimulation.

We have obtained very good results using gene gun transfection and the human synapsin 1 promoter (Kugler *et al.*, 2001) for neuron-specific expression in hippocampal slice culture. High expression levels are reached within about 10 days after transfection. Importantly, we did not observe any signs of cytotoxicity even in most strongly expressing cells. This may seem surprising given that overexpression of transmembrane proteins can cause ER stress if the ER protein folding machinery is overstrained (Zhang & Kaufman, 2006). The *rate* of heterologous protein synthesis, rather than absolute protein levels, may therefore determine safe ChR2 levels.

Light-induced action potentials

Large photocurrents lead to rapid cell depolarization, triggering APs with short delay and minimal jitter. Conversely, cells with small photocurrents depolarize more slowly and reach firing threshold with delays of several milliseconds and less precise timing – if the firing threshold is reached at all. Large photocurrents are therefore essential for temporally precise AP induction. However, compared to the very brief AP, ChR2 kinetics are slow (Bamann *et al.*, 2008; Ritter *et al.*, 2008) and the maximal depolarization is reached several milliseconds after the onset of the light pulse. If the light-evoked AP (AP_L) is fired with a very short delay, the ChR2 photocurrent therefore outlasts the repolarising K^+ current of the AP_L, resulting in an after-depolarization (Figure D.1A).

In two-photon calcium imaging experiments, we have found that the calcium transients in dendrites and spines evoked by AP_L were significantly larger than calcium transients associated with APs triggered by brief somatic current injection (AP_C). Application of TTX completely blocked AP_C and the concomitant

calcium influx, whereas light pulses still evoked calcium transients. However, calcium influx was completely abolished when the cell membrane was clamped to -65 mV, indicating that the additional calcium influx during AP_L was mainly due to increased activation of voltage-gated calcium channels (VGCCs) without any measurable contribution from calcium flux through the ChR2 pore (Zhang & Oertner, 2007).

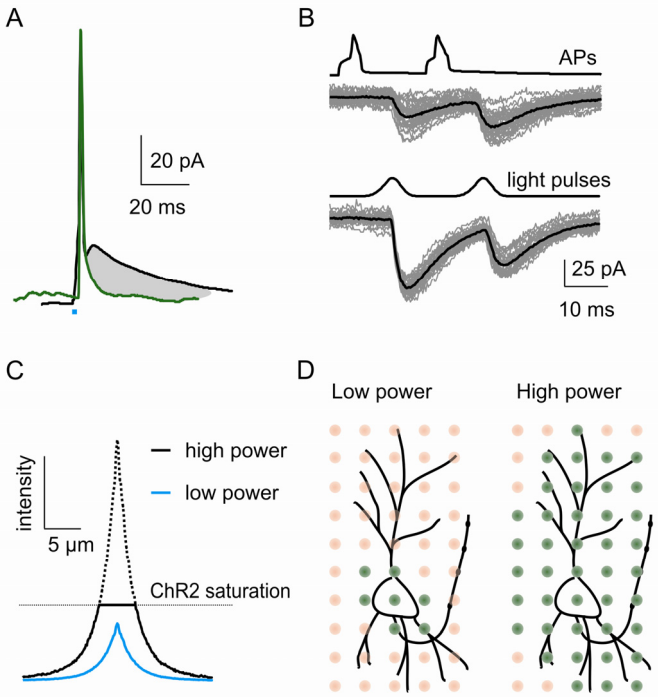

Figure D.1. ChR2-mediated photostimulation *(A) Peak-aligned spontaneous AP (green) and light-induced AP (black; 2 ms light pulse indicated by blue square) in a pyramidal CA1 neuron. The gray area indicates the after-depolarization associated with ChR2 activation. (B) Comparison of electrically triggered EPSCs (top) with light-triggered EPSCs in a CA1 neuron (bottom). Neurotransmitter release from ChR2-expressing CA3 neurons was induced by somatic current injection or by photostimulation of axons in CA1 area, respectively (modified from Zhang & Oertner, 2007). (C) Light intensity profile in the focal plane for high and low laser power. High light intensities lead to saturation of ChR2 activation in the laser focus. (D) Schematic illustration of action potentials (green dots) and subthreshold depolarizations (red dots) induced in a neuron with focal laser stimulation in a grid pattern (C, D based on Schoenenberger et al., 2008).*

Light-induced neurotransmitter release

The increased calcium influx during AP_L has important functional consequences. We performed patch-clamp recordings from untransfected hippocampal CA1 cells to compare EPSCs resulting from light-activation of ChR2-expressing CA3 cells ($EPSC_L$) with electrically induced EPSCs ($EPSC_C$). $EPSC_L$ induced by application of blue light in CA1 area had very short latencies compared to light-stimulation in CA3 area or electrical stimulation of individual CA3 neurons by somatic current injection, indicating that AP_L were induced locally in the axon (Figure D.1B). Furthermore, the amplitudes of $EPSC_L$ evoked by stimulation in CA1 area were very uniform, suggesting a high release probability (p_r). Indeed, by direct two-photon imaging of calcium transients in individual postsynaptic spines, we measured release probabilities of approximately 0.9 after light-stimulation of presynaptic axons (compared to ~0.3 at electrically

stimulated Schaffer collateral synapses (Oertner *et al.*, 2002). Most probably the increase in p_r is caused by the additional calcium influx during AP_L (Zhang & Oertner, 2007).

The recently reported accelerated ChR2 variants exhibit reduced after-depolarizations and might therefore allow firing neurons without enhancing transmitter release at their output synapses (Gunaydin *et al.*, 2010). These novel variants should thus enable the investigator to choose between wild-type ChR2 for experiments profiting from high p_r and the accelerated ChR2 variants for experiments attempting to mimic natural spiking. Since accelerated ChR2 variants typically produce smaller photocurrents, special care has to be taken to achieve high expression levels for reliable AP induction (Gunaydin *et al.*, 2010).

Chronic ChR2 stimulation

A general concern associated with the use of light in live tissue is phototoxicity and bleaching of fluorescent reporters or light-controlled effectors. However, $EPSC_L$ recorded in untransfected cells receiving input from ChR2-expressing cells are very stable, and we have not observed any use-dependent run-down of presynaptic release reliability or $EPSC_L$ amplitude in whole-cell recordings of up to 60 min.

To test for potential light-dependent ChR2 degradation or phototoxic effects of chronic light stimulation, we stimulated ChR2-transfected slice cultures in the cell culture incubator for up to 4 days with bright light pulses emitted by high-power LEDs. We did not observe any signs of cytotoxicity, neither in ChR2-expressing cells nor in untransfected neighbours. The photocurrents quantified in ChR2-expressing pyramidal cells after 4 days of stimulation were not different from currents in non-stimulated control cells. From these stimulation experiments employing a total of ~35’000 light pulses amounting to 17 min of intense blue light illumination we concluded that ChR2 exhibits no light-dependent degeneration and repeated blue light exposure is not detrimental to culture viability (Schoenenberger *et al.*, 2009).

ChR2 variants

As already mentioned, several engineered ChR2 variants have been reported. Still, we have performed the large majority of experiments with the original wild-type ChR2 first introduced into neurons by the group of Karl Deisseroth (Boyden *et al.*, 2005) because it is well tolerated by transfected neurons and under optimal conditions allows induction of single APs at frequencies up to about 40 Hz in pyramidal neurons. If stimulation light intensities or expression levels are low, the H134R mutant may enable more robust firing than wild-type ChR2 because of its enhanced photocurrents (Nagel *et al.*, 2005).

Of the engineered ChR2 variants, the so-called bi-stable channelrhodopsins containing amino acid substitutions at the C128 position exhibit most remarkable properties (Berndt *et al.*, 2009). In extensive experiments with ChR2(C128A), we have found that this channel can induce long spike trains after a brief stimulation pulse even with minimal light intensities. However, photocurrent amplitudes were dramatically reduced after repeated stimulation, which limited the number of spike trains that could be elicited. Most likely, this was due to accumulation of desensitised channel in a non-conducting state (Schoenenberger *et al.*, 2009; Stehfest *et al.*, 2010). Despite use-dependent inactivation, the bi-stable ChR2 variants will be valuable tools if a limited number of spike trains or long-lasting subthreshold depolarizations are sufficient for a certain application.

In our experiments, the vigorous firing evoked by ChR2(C128A) induced expression of the immediate early gene c-fos in a graded and cell-specific manner (Schoenenberger *et al.*, 2009). Potential induction of immediate early genes and other activity-dependent factors may seem an unwanted side effect of stimulated neuronal activity because it may alter functional and structural properties of cells. However, it opens the door to study activity-related processes on the level of individual neurons (Matsuo *et al.*, 2008) and allows identification of stimulated cells without the need to monitor electrical activity during stimulation.

Local ChR2 activation

Most studies employing ChR2 have used wide-field illumination for channel activation. However, spatially restricting the excitation light can be exploited to probe connectivity between neurons (Petreanu *et al.*, 2007; Petreanu *et al.*, 2009) or to avoid direct activation of presynaptic axons and increased calcium influx at presynaptic terminals. Moreover, local ChR2 activation might allow depolarization of subcellular structures down to the level of single dendritic spines, which is not possible with electrophysiological approaches and therefore constitutes one of the most interesting applications of optogenetics in slice physiology. We therefore investigated the factors determining the spatial resolution of ChR2 activation (Schoenenberger *et al.*, 2008).

When we stimulated ChR2-YFP expressing neurons with a blue laser beam directed at the soma with increasing light intensities, we found that ChR2 activation rapidly saturated in the laser focus. High laser intensities did not only increase the photocurrents, but also lead to a loss of spatial selectivity of photocurrent induction. Large currents were induced even when the laser was directed at positions farther than 100 µm laterally from the soma. How can the loss of spatial resolution with high light intensity be explained? Because of focal saturation of ChR2 excitation, the photocurrent amplitude can only be increased by illuminating a larger membrane area for a given pulse duration. Increasing the laser intensity results in stimulation of a larger membrane area by the spatial tails of the laser beam (see Figure D.1C) and by scattered light. The additional photons in the laser focus do not enhance photocurrents, but contribute light scattering and thereby increase activation of out-of-focus membrane.

In contrast to photocurrent induction, where resolution can be gradually improved by using lower laser power, APs are only fired if the spike threshold is reached. As a consequence, neurons with high ChR2 expression levels can be fired with low light intensities and therefore high spatial selectivity (Figure D.1D). Weakly expressing cells, however, may only fire APs if the entire cell membrane is illuminated.

We have restricted our local stimulation experiments to the soma and main dendrites of neurons, but the principles established here also apply to stimulation of any subcellular structure and should apply to one-photon excitation of any optogenetic agent. Because of unavoidable stimulation of ChR2 in out-of-focus membrane, one-photon activation is not ideal for local stimulation of small subcellular structures. Two-photon excitation, in contrast, can restrict ChR2 activation to a very small volume and should enable stimulation of subcellular structures with very high spatial selectivity (Rickgauer & Tank, 2009; Zhu *et al.*, 2009).

Investigating synaptic transmission and plasticity with channelrhodopsin-2

Long-term potentiation (LTP), the most extensively studied form of synaptic plasticity, is triggered when presynaptic activity coincides with postsynaptic depolarization. To investigate the sequence of molecular events and morphological changes that occur during potentiation, it would be desirable to directly visualize the synapses where LTP is induced. In classical electrophysiological LTP protocols, however, it is difficult to isolate responses of individual synapses and to identify their location. In addition, wash-out of second messengers and soluble proteins (Tanaka *et al.*, 2008) associated with whole-cell patch-clamp recordings limit the time window for effective LTP induction after break-in to the postsynaptic cell. These limitations of purely electrophysiological approaches can be overcome using optogenetics: ChR2-mediated stimulation of fluorescently labelled axons helps to identify active synapses, whereas optogenetic depolarization of the postsynaptic cell eliminates wash-out problems.

Postsynaptic activation by ChR2

ChR2 allowed us to induce brief bursts of action potentials in individual postsynaptic neurons in a non-invasive fashion. Since the intracellular milieu of the postsynaptic cell was not affected, we had no time limitations to find synapses and follow plasticity-induced changes. One of our goals was to measure volume changes of dendritic spines after potentiation. Frequently used fluorescently tagged ChR2 would have resulted in staining of the cell membrane, which is not optimal for volume measurements. Therefore, we combined unlabelled ChR2 and the soluble red fluorescent protein tdimer2 (Campbell *et al.*, 2002) in a single plasmid, which lead to reliable co-expression and enabled us to assess ChR2 expression levels in individual neurons. Whole cell recordings showed that in response to blue light

illumination, 19 out of 21 cells reliably produced spikes. Knowing that the postsynaptic cells could be activated by light, we stimulated single synapses on identified spines by two-photon uncaging of MNI-glutamate (Figure D.2A). Repeated pairing of single uncaging pulses with photostimulation of the postsynaptic cell induced LTP and an increase in volume of the stimulated spines.

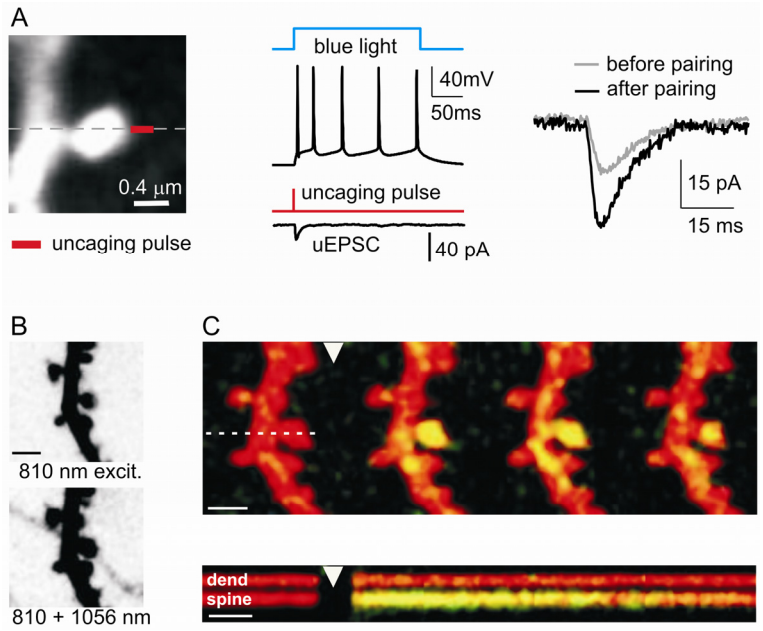

Figure D.2. Investigation of single synapses using ChR2 *(A) Left: Simultaneous two-photon imaging and two-photon MNI-glutamate uncaging on a dendritic spine. Middle: Optical pairing protocol: single uncaging-evoked EPSCs (uEPSC) were paired with blue light pulses that evoked 5 – 6 APs in the postsynaptic neuron. Right: Average uEPSCs before and after optical pairing (reproduced from Zhang et al., 2008). (B) Visualization of potential synaptic contacts between a ChR2-tdimer2-expressing axon and Alexa 594-filled spines. Scale bar: 2 µm. (C) Top: overlay of green (Fluo-5F) and red fluorescence (Alexa 594) from the dendrite shown in (B). Calcium transient after light stimulation (arrowhead) is restricted to a single spine (yellow). Scale bar: 2 µm. Dashed line indicates position of line scan. Bottom: line scan across dendrite and spine head. Scale bar: 50 ms (B, C modified from Zhang & Oertner, 2007).*

We successfully applied this optical pairing protocol to visualize translocation of αCaMKII, a key component in the LTP signalling cascade, at individual dendritic spines and revealed input-specific accumulation of αCaMKII after potentiation (Zhang *et al.*, 2008b). An alternative method to induce LTP at individual synapses is glutamate uncaging in the absence of extracellular magnesium. Since removal of magnesium can induce seizure-like activity in brain slices, it is typically combined with TTX to block fast sodium channels and prevent action potential firing (Matsuzaki *et al.*, 2004). This protocol strongly enhances calcium influx at stimulated spines, since in the absence of extracellular magnesium, NMDA

receptors are fully conductive as long as they are bound to glutamate (> 100 ms after the uncaging pulse). We prefer optogenetic induction of APs in the postsynaptic cell because it allows to mimic spike-timing-dependent plasticity, arguably the most physiological of all plasticity induction protocols.

Presynaptic activation by ChR2

Although two-photon glutamate uncaging allows for excellent spatial resolution, this technique completely bypasses the presynaptic terminal and is therefore restricted to investigation of postsynaptic mechanisms. An interesting application of ChR2 is the selective activation of visually identified axons in intact tissue. To stimulate and image axons in brain slices, we tagged ChR2 with tdimer2 (Campbell *et al.*, 2002) based on the following considerations: First, the optical properties of tdimer2 make it ideal for simultaneous imaging with synthetic dyes such as Alexa 594 and Fluo-5F in the postsynaptic spines. The emission spectrum of Alexa 594 overlaps with that of tdimer2. However, these two fluorophores can be easily separated by two-photon excitation at different wavelengths (Figure D.2B). Secondly, inspection of red labelling with green excitation light allowed us to select cultures with a favourable expression pattern without fully activating ChR2-positive cells. Finally, tdimer2 does not form aggregates even at high expression levels.

Using two-photon microscopy, we identified potential points of contact between the dendrite of a dye-filled CA1 pyramidal cell and ChR2-positive axons. In response to blue light, ChR2-expressing axonal terminals provided a reliable and precisely timed source of glutamate, which was clearly revealed by two-photon calcium imaging at postsynaptic spines (Figure D.2C). As a result, pairing of light-evoked synaptic release with postsynaptic depolarization lead to lasting potentiation of synaptic connections (Zhang & Oertner, 2007). In these experiments, postsynaptic depolarization was still provided by a somatic patch electrode, but presynaptic terminals were not perturbed. This approach is therefore suitable for optical analysis of proteins involved in vesicular release and presynaptic plasticity.

Future directions

To tap the full potential of optogenetics in slice physiology – remote control of neuronal activity without the need for electrical access to cells or tissue – ChR2-based stimulation has to be combined with optical measurements of the structure or function under investigation, as we have demonstrated for αCaMKII translocation. Rapidly improving fluorescent reporters of electrical activity, ion influx, and enzyme activity (Dimitrov *et al.*, 2007; Lee *et al.*, 2009; Tian *et al.*, 2009) extend the potential of such all-optical experiments. ChR2-based stimulation will also benefit from the combination with genetically encoded calcium indicators (GECIs) to provide a direct and rapid stimulation feedback (Mank *et al.*, 2008; Tian *et al.*, 2009). Since currently available GECIs are based on GFP or CFP/YFP FRET pairs and thus have excitation spectra overlapping with the ChR2 action spectrum, optical read-out is always associated with some degree of ChR2 activation. Genetically encoded calcium sensors based on RFP would therefore be advantageous for all-optical experiments.

A second important focus of current efforts is the engineering or identification of spectrally shifted channelrhodopsins (Zhang *et al.*, 2008a). Dual- or even multicolour control of different optogenetic agents will allow probing the contributions of distinct neuronal population to phenomena ranging from dendritic integration to behaviour. The challenge for protein engineers will be to alter the action spectra without compromising channel conductance, kinetics, or expression levels. A third largely unexplored territory is targeting of ChR2 to specific regions of the cell (Lewis *et al.*, 2009) or to intracellular organelles. Given the range of possibilities, the optogenetic revolution might have only just begun.

Acknowledgements

We thank Åsa Grunditz, Tobias Rose, Simon Wiegert, and Daniel Udwari for helpful comments on the manuscripts. This work was supported by the Novartis Research Foundation.

5. OPTOGENETIC LTD INDUCTION

5.1 Introduction

The aim of this thesis project was to develop strategies for the optogenetic control of synaptic plasticity. Different forms of Hebbian and non-Hebbian synaptic plasticity have been described at Schaffer collateral synapses, each with its own induction protocols. Homeostatic plasticity is expressed after prolonged silencing of firing or prolonged strong hyperexcitation, whereas LTP induction requires high frequency bursts or correlated activity in pre- and postsynaptic neurons to trigger spike-timing dependent plasticity (STDP). For technical reasons, LTD should be most easily induced, since it is reliably expressed after 15 min low-frequency stimulation (LFS) at 1 Hz. The large cell-to-cell variability in firing thresholds and firing reliability has been the largest roadblock on the way to optogenetic control of synaptic plasticity. However, in cultures containing CA3 neurons that reliably follow 1 Hz LFS, strong and stable LTD can be induced, suggesting that non-invasive optogenetic LTD induction is feasible in principle, but hinges on the firing reliability of light-stimulated presynaptic neurons.

5.2 Methods

Slice culture and transfection

Hippocampal slice cultures from Wistar rats were transfected using a Helios gene gun to express wt ChR2 and tdimer2 in individual neurons. Transgene expression was controlled by the CaMKII promoter.

Electrophysiology

Experiments were conducted at 29 - 31°C 1 - 2 weeks after transfection. Artificial cerebrospinal fluid (ACSF) contained (in mM) 119 NaCl, 26.2 $NaHCO_3$, 11 D-glucose, 2.5 KCl, 4 $MgCl_2$, 4 $CaCl_2$, 1 NaH_2PO_4. ACSF was complemented with 30 µM serine. Voltage-clamp experiments were performed at -65 mV holding potential. Glass pipettes for patch-clamp recordings were filled with intracellular solutions containing (in mM): 135 potassium gluconate, 10 HEPES, 4 $MgCl_2$, 4 Na_2-ATP, 0.4 Na-GTP, 10 Na_2-phosphocreatine, and 3 ascorbate. EPSCs were quantified using custom-written Matlab software.

Photostimulation

A blue LED (Luxeon V Star blue, lambertian radiation pattern) positioned approximately 5 mm above the cultures were used for whole-field stimulation. 10 ms light pulses were controlled by a Luxdrive 3021 BuckPuck providing 700 mA constant current output.

5.3 Results

Wild-type (wt) ChR2 was coexpressed with fluorescent tdimer2 in hippocampal slice culture using gene gun transfection. Transgenes were controlled by the CaMKII promoter, ensuring expression exclusively in excitatory neurons. To identify cultures with strong and reliable input to CA1 neurons from ChR2-expressing CA3 cells, I performed whole-cell recordings from non-transfected CA1 neurons and stimulated light-responsive neurons by whole-field LED illumination. Cultures with stable EPSC amplitudes over 10 min test pulse stimulation at 0.1 Hz were chosen for LTD experiments. In 3/3 cultures with stable CA3 stimulation, EPSC amplitudes in CA1 neurons were depressed after 15 min LFS. However, in 2 of these cultures, EPSC amplitudes were small (17 pA, 20 pA, respectively) and spontaneous activity was strong, making it difficult to quantitatively assess LTD magnitude and stability. In only one culture, light-induced EPSCs in CA1 neurons during 10 min baseline stimulation were large and stable (Fig. 4A). The average EPSC amplitude during 0.1 Hz baseline stimulation was 172 ± 3 pA (Fig. 4A). Trial-to-trial variability was very small, suggesting a high release probability (P_r) with light-stimulation (see Zhang & Oertner, 2007). After 15 min LFS in current-clamp (CC), EPSCs were reduced to about 53% of baseline (Fig. 4A, B). Importantly, depression of synaptic transmission was stable throughout the experiment, i.e. for about 90 min after LFS. Furthermore, depression of EPSC amplitudes was accompanied by a strong increase in variability, indicating that P_r was reduced after LFS. This observation suggests that LTD overrides the increase in P_r after ChR2 stimulation our lab reported previously (Zhang & Oertner, 2007), which may be due to a strong presynaptic component in LTD expression.

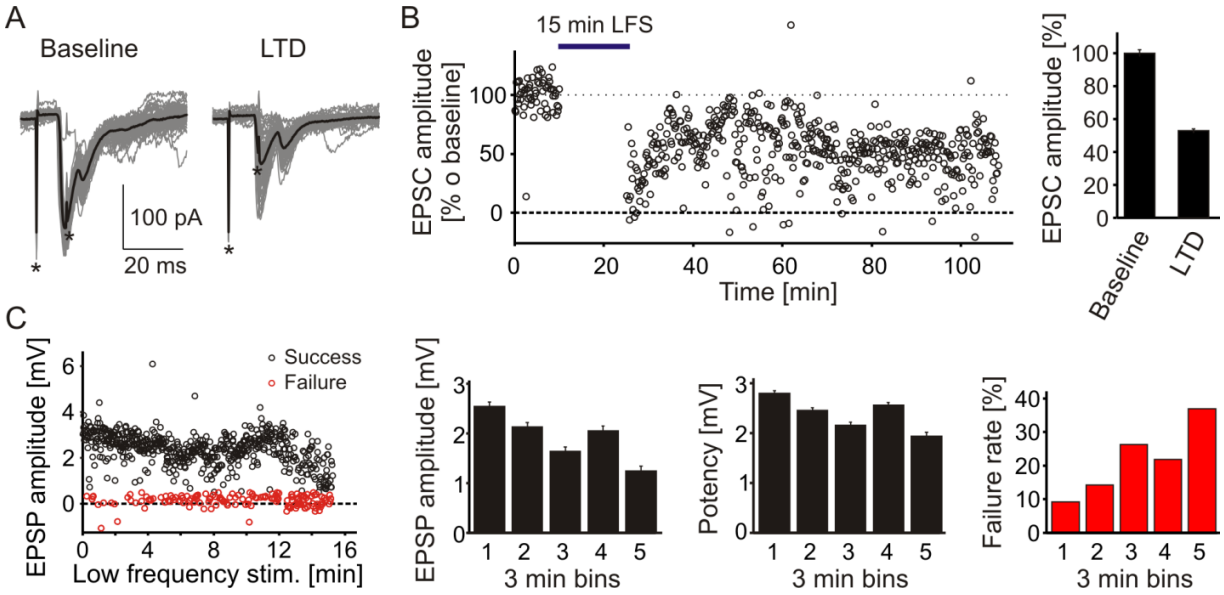

Figure 4. Optogenetic LTD induction. *(A) Voltage-clamp recordings from a wild-type CA1 neuron receiving input from excitatory neurons expressing ChR2 under the CaMKII promoter. Presynaptic neurons were stimulated with 10 ms LED pulses at 0.1 Hz. Baseline: Before 1 Hz low frequency stimulation (LFS; mean = -172 ± 3 pA). LTD: First 10 min after 15 min LFS (mean = -71 ± 5 pA). Gray lines depict individual trials, average is shown in black. Asterisks mark LED switch artifacts. (B) EPSC amplitudes during the entire experiment. LFS induced a stable depression of synaptic transmission to about 53% of baseline. (C) Left: EPSP amplitudes during LFS in current-clamp can be separated into failures and responses. The threshold for responses was 0.5 mV. Right: Quantification of average EPSP amplitudes (including failures), synaptic potency and failure rates in 3 min bins during LFS. Bars indicated mean ± SEM.*

I next analyzed synaptic transmission during 1 Hz LFS. EPSPs could be separated into successes and transmission failures using a threshold of 0.5 mV (Fig. 4C). Average EPSP amplitudes during LFS were steadily decreased during LFS, dropping from 2.5 ± 0.1 mV in the first 3 min bin to 1.2 ± 0.1 mV in the last bin (Fig. 4C). Interestingly, this effect was conferred mainly by to a strong increase in failure rate from 9% to 37%, with a weaker contribution from a reduction in synaptic potency (Fig. 4C). Together, these observations suggest that optogenetic LTD at Schaffer collateral synapses is expressed by a combination of pre- and postsynaptic effects. Moreover, LTD was stable for 90 min after induction, emphasizing the need for non-invasive plasticity induction protocols to assess the stability of changes in synaptic strength over prolonged periods of time.

5.4 Discussion

The data presented here demonstrates that optogenetic induction of LTD by 15 min LFS is possible. This should not come as a surprise given that LFS has been used routinely to induced LTD at CA3 to CA1 synapses by electrical stimulation (Dudek & Bear, 1992; Debanne *et al.*, 1996; Oliet *et al.*, 1997) or even by two-photon uncaging in a recent study on mGluR-dependent LTD at single spines (Holbro *et al.*, 2009). The limiting factor in our experiments was not the neurons' ability to undergo changes in synaptic strength in response to LFS, but rather the limited availability of slice cultures with transfected CA3 neurons reliably firing with 0.1 Hz as well as 1 Hz stimulation. Very similar firing characteristics in response to both stimulation frequencies were crucial in this experimental design to ensure that all the neurons probed during 0.1 Hz test stimulation were following the 1 Hz LTD protocol. In the example discussed here, the initial EPSC amplitude was -172 pA. As the average synaptic potency between connected CA3 and CA1 neurons is about 44 pA (see appendix on gene gun transfection), we estimate that about 3 - 4 presynaptic neurons provided light-controlled input to the CA1 neurons that was recorded. A large initial light-evoked response facilitates the quantification of changes in synaptic strength, especially if spontaneous activity is high. In principle, however, connection-specific LTD should be induced even if a single CA3 neuron is stimulated by LFS.

Our goal is to eventually stimulate cultures in the cell cultures incubator with light flashes to induce LTD between synaptically connected pairs of CA3 and CA1 cells. This goal can be achieved if two requirements are fulfilled. First, cultures with transfected and light-responsive CA3 neurons have to be available in sufficiently large numbers. With gene gun transfection, about 1 or 2 cultures per membrane insert (each insert containing 3 cultures) have a favorable expression pattern. Single-cell electroporation might increase the fraction of cultures that are suitable for experiments and allows to selectively transfect CA3 neurons, thus defining presynaptic cell identity very precisely. Since single-cell electroporation is much more time-consuming that gene gun transfection, it is unclear which transfection approach will ultimately be more efficient. The second requirement is that transfected CA3 neurons respond reliably to LFS. After gene gun transfection, only about 50% of CA3 neurons expressing wt ChR2 follow 1 Hz stimulation with the light intensities achieved by LED stimulation in the cell culture incubator. Thus, only in about half of the connected pairs of a transfected CA3 cell and a randomly

selected non-transfected CA1 neuron the synaptic connection can be assumed to undergo LTD after light-controlled LFS, which limits experimental throughput and complicates the interpretation of results.

The stimulation reliability of hippocampal pyramidal neurons is dramatically increased with the novel TC channelrhodopsin variants, which sensitize neurons to reduced light intensities and largely eliminate stimulation failures. I am therefore very confident that optogenetic control of synaptic plasticity can now be achieved routinely, allowing to study the stability of depressed synaptic connections over extended periods of time.

6. GENERAL CONCLUSIONS AND OUTLOOK

6.1 Subcellular channelrhodopsin-2 activation

Local activation of light-gated channels and enzymes holds great promise to investigate electrical and biochemical signaling with subcellular resolution. Common pharmacological manipulation has yielded very important insight into the control of many aspects of cell biology from uptake of nutrients and cell division to migration and pathogen infection. However, in living organisms many cell types such as neurons and epithelial cells are polarized and can have elaborate three-dimensional morphologies with subcellular structures that may constitute isolated or locally interacting compartments for the integration of chemical and electrical signals (Grunditz *et al.*, 2008; Harvey *et al.*, 2008; Losonczy *et al.*, 2008; Zhang *et al.*, 2008b; Larkum *et al.*, 2009). Together with the discovery of compartmentalized signaling in submicron domains such as lipid rafts and signaling endosomes this underlines the importance of local and temporally precise signaling (Ye *et al.*, 2003; Korade & Kenworthy, 2008). Local activation of light-controlled enzymes will therefore provide much more accurate control over diverse cellular processes than pharmacological manipulation and will be important not only for neuroscience but also to areas where optogenetic approaches currently plays a minor role (Levskaya *et al.*, 2009).

We have found that the spatial resolution of one-photon ChR2 activation depends on the stimulation light intensity and is inherently limited by the optics of focused laser beams. Furthermore, spatial selectivity is degraded by scattering of visible light in biological tissue. The same principles will apply to activation of any other molecular tool with single photon activation. Recent work has reported successful activation of ChR2 by two-photon excitation eliminating channel activation by scattered light (Rickgauer & Tank, 2009; Zhu *et al.*, 2009). Furthermore, the very high photon density required for efficient two-photon absorption restricts ChR2 excitation to the center of the focused laser beam and provides 3D sectioning of optical stimulation. The latest development in innovative stimulation approaches, so-called temporal focusing of ultrashort infrared laser pulses, even allows exciting arbitrary tissues volumes in three dimensions to stimulate subcellular structures, individual neurons, or entire groups of cells individually or simultaneously (Papagiakoumou *et al.*, 2010).

6.2 Bi-stable channelrhodopsins and c-Fos induction

We have shown that the bi-stable ChR2(C128X) mutants strongly inactivate after repeated stimulation due to accumulation of channel in a long-lived desensitized state. This limits the usefulness of these variants to very specialized applications such as weak depolarization over up to several days or induction of a small number of AP bursts. The branched photocycle of the C128 variants involving a slow side reaction was unexpected, but has recently been confirmed by a spectroscopy study from the Hegemann group that originally generated the bi-stable mutants (Stehfest *et al.*, 2010). ChR2 variants carrying mutations at position D156 also have long-lived open states that can depolarize neurons for several seconds (Bamann *et al.*, 2010). Their behavior in response to repeated stimulation, however, has not been investigated.

We demonstrate that the vigorous firing evoked by ChR2(C128A) reliably induces c-Fos expression in hippocampal pyramidal cells. Furthermore, burst firing induced expression of GFP controlled by the c-fos promoter. Light-induced expression of transgenes may be used to study the trafficking and turnover of proteins synthesized after strong electrical activity (Matsuo *et al.*, 2008). The c-fos promoter can be induced by various external stimuli and even culture feeding and handling (see e.g. (Buckmaster *et al.*, 1991), and data not shown). Activity-dependent activation of the c-fos promoter therefore might have to be combined with pharmacological suppression of c-fos promoter activity to specifically allow ChR2-controlled expression of foreign genes in a defined time window and to avoid non-specific c-fos promoter activation by other stimuli (Reijmers *et al.*, 2007).

Immediate early gene (IEG) expression can also provide a feedback on optogenetic stimulation efficacy and allows to specifically target light-responsive neurons for experiments. This is important as depending on expression levels, stimulation light intensity and pulse duration, cell type and ChR2 variant, a considerable fraction of transfected neurons does not fire APs in response to optical stimulation (see (Huber *et al.*, 2008), and data presented in previous sections). IEGs are expressed in response to certain activity patterns that trigger specific signaling pathways. Therefore, IEGs can only provide feedback about a limited range of firing pattern. The c-fos promoter for example is induced by high frequency firing, but not by 1 Hz LFS for up to 30 min (data not shown). Successful c-Fos induction

thus provides feedback on burst firing using ChR2(C128A), but cannot confirm that a light-stimulated neurons has followed an LTD protocol (see below).

6.3 High efficiency ChR2 variants and next steps for improved optogenetic stimulation tools

We have characterized the novel ChR2 TC variants and have found that they are superior to currently used channelrhodopsins over a very large range of experimental conditions. Although ChR2 has become an indispensable tool in neuroscience and has opened new areas for experimental investigation, there is still room for improvement. One of the main factors limiting ChR2 performance is the very low single channel conductance that necessitates high expression levels for AP induction. The TC variants generate very large photocurrents and thereby can sensitize neurons to reduced light intensities, which will be an important advantage for in vivo applications. More research is needed to explain the mechanism of enhanced photocurrents.

We have investigated a number of limitations of currently available channelrhodopsin variants, such as the inactivation of C128 variants or the buildup of plateau potentials even with the rapid ET/TC variant. The knowledge of current limitations together with a detailed understanding of biophysical properties and the photocurrent gating mechanism of ChR2 will allow bioengineers to further improve ChR2 properties and to adapt it even more to the needs of neuroscientists. Alternatively, light-activated ion channels with favorable properties and larger single channel conductances as well as entirely new classes of light-controlled enzymes may eventually be isolated from natural sources. The cloning and expression of a red-shifted channelrhodopsin from Volvox cateri and the systematic comparison of a large number of ion pumps from a diverse collection of microorganisms have demonstrated the potential of this approach (Zhang *et al.*, 2008a; Chow *et al.*, 2010). In the future, mutagenesis and the generation of protein chimeras will steadily enlarge the optogenetic toolbox (Berndt *et al.*, 2008; Lin *et al.*, 2009; Wen *et al.*, 2010). Apart from larger conductances, we expect important progress with more rapid kinetics and a larger number of spectral variants of light-gated channels. Furthermore, localization of optogenetic agents to specific cellular domains will enable manipulation of ion and second messenger concentrations with subcellular resolution, thereby reducing undesired effects of cell-wide activation of light controlled proteins and also allowing manipulation of electrical and chemical signaling with high spatial accuracy.

6.4 Optogenetic control of synaptic plasticity

We show that optogenetic induction of LTD in hippocampal slice culture is possible. However, LTD induction in neurons transfected with wt ChR2 was severely hampered by the large fraction of transfected cells that are not reliably fired in response to photostimulation because of insufficient photocurrent amplitudes. Therefore, LTD induction had to be monitored by electrophysiological measurements of synaptic strength before and after LFS, precluding long-term experiments as for standard approaches studying LTD with traditional electrophysiology.

The novel TC channelrhodopsin variants widely eliminate stimulation failures, even under conditions of limited stimulation light intensities that can easily be achieved using unfocused LEDs, for example in the cull culture incubator. Since stimulation failures can be largely excluded, we can assume that all neurons expressing TC or ET/TC will follow optical 1 HZ LFS and thus all synapses with postsynaptic partners will be depressed. The TC variants will therefore allow us to study synaptic strength at any time point after LTD induction to assess the long-term stability of LTD and to investigate potential factors that modulate LTD over prolonged periods of time. This will finally add the ‘long-term’ aspects to long-term synaptic plasticity.

6.5 Concluding remarks

In the present dissertation we have characterized the properties of a number of ChR2 variants with a focus on their potential to control synaptic plasticity by light. To reach this goal, several factors are of crucial importance, and presently no single variant combines all of the favorable properties. The work presented here has paved the way to optogenetic control of synaptic plasticity by pointing out prerequisites for successful plasticity experiments and by tracking current limitations. Non-invasive control of synaptic plasticity has turned out technically very demanding, but has become possible now, thus opening important aspects of synaptic plasticity and its putative contribution to memory formation to experimental investigation.

7. APPENDIX: Reduction of excitatory synaptic input to gene gun-transfected CA1 cells

7.1 Introduction

Particle-mediated gene transfer is a rapid and effective method that allows to transfect a small set of single neurons in organotypic slice culture. Because of the sparse expression pattern with high expression levels that is routinely obtained, gene gun transfection has been used in our lab to study the structure and function of individual neurons. In previous studies we have found that CA1 cells transfected with gene gun are viable and display normal morphology. Furthermore, spines of transfected neurons can readily undergo changes in synaptic strength as we have demonstrated for both LTP and LTD (Zhang *et al.*, 2008; Holbro *et al.*, 2009). However, we have not systematically compared the strength of Schaffer collateral input to transfected or non-transfected CA1 cells to quantify potential effect of gene transfection on synaptic connectivity.

7.2 Methods

Slice culture and transfection

Hippocampal slice cultures from Wistar rats were prepared at postnatal day 4-5 as described (Stoppini et al., 1991), according to the rules of the Federal Veterinary Office of Basel-Stadt. After 6 - 7 days in culture, we used a Helios gene gun (Bio-Rad) to co-transfect individual cells with DNA encoding ChR2 and soluble tdimer2 (Campbell *et al.*, 2002) or tdimer2 alone. cDNAs were subcloned into a neuron-specific expression vector based on a modified pCI backbone (Promega), where expression was controlled by the human synapsin-1 promoter. For gene-gun transfection, 5 mg 1.6 µm gold bullets (Bio-Rad) were coated with a total of 8 µg DNA at a ChR2:tdimer2 molar ratio of 6:1 or with 8 µg tdimer2 alone. Nupherin (Enzo Life Sciences) was used to enhance plasmid transfer and expression (10 µg Nupherin per 1 µg of plasmid). Adeno-associated viruses expressing CR2 and tdimer 2 (Tang *et al.*, 2009) were kindly provided by Drs. Ingrid Ehrlich and Andreas Lüthi . Viruses were injected in CA1 area of slice cultures at DIV 7 and electrophysiological recordings were performed after 2 weeks of expression.

Electrophysiology

Experiments were conducted at 29 - 31°C 1 - 3 weeks after transfection. Artificial cerebrospinal fluid (ACSF) contained (in mM) 119 NaCl, 26.2 $NaHCO_3$, 11 D-glucose, 2.5 KCl, 4 $MgCl_2$, 4 $CaCl_2$, 1 NaH_2PO_4. ACSF was complemented with 30 µM serine. In current-clamp experiments, a small holding current was injected to hold the cells at -60 mV and action potentials were induced by 2 ms current injections. Voltage-clamp experiments were performed at -65 mV holding potential. Glass pipettes for patch-clamp recordings were filled with intracellular solutions containing (in mM): 135 potassium gluconate, 10 HEPES, 4 $MgCl_2$, 4 Na_2-ATP, 0.4 Na-GTP, 10 Na_2-phosphocreatine, and 3 ascorbate.

Data analysis

EPSC peak amplitudes were quantified using custom-written Matlab software. When multi-component EPSCs were generated, the peak of the first component was quantified. When the delay between current injection and EPSC onset was > 15 ms, the connection was considered multisynaptic and the EPSC amplitude was quantified as 0 pA. After paired-pulse stimulation, only the first EPSC was quantified. Medians were compared using Wilcoxon rank sum tests.

7.3 Results

Random sets of neurons in hippocampal slice cultures were transfected using particle-mediated gene transfer to express ChR2 together with tdimer2 (Fig. 5A, top). In control experiments, tdimer2 alone was expressed. I then performed dual recordings to quantify connectivity between non-transfected CA3 cells and transfected or non-transfected CA1 cells (Fig 5A). Action potentials (APs) induced in CA3 cells by brief current injections evoked postsynaptic EPSCs in about 75% of non-transfected CA1 neurons (n = 29; Fig 5B). The median EPSC amplitude (including non-connected pairs) was 20.0 pA and the average synaptic potency was 44 pA. When the postsynaptic neuron was gene gun-transfected with ChR2 and tdimer2, median EPSCs were strongly reduced to 3.5 pA (n = 11, p = 0.16). The reduction of connection strength was even more pronounced when tdimer2 alone was expressed (2.0 pA, n = 15, p = 0.04), indicating that the depression of EPSC amplitudes was not due to ChR2 expression but rather a general

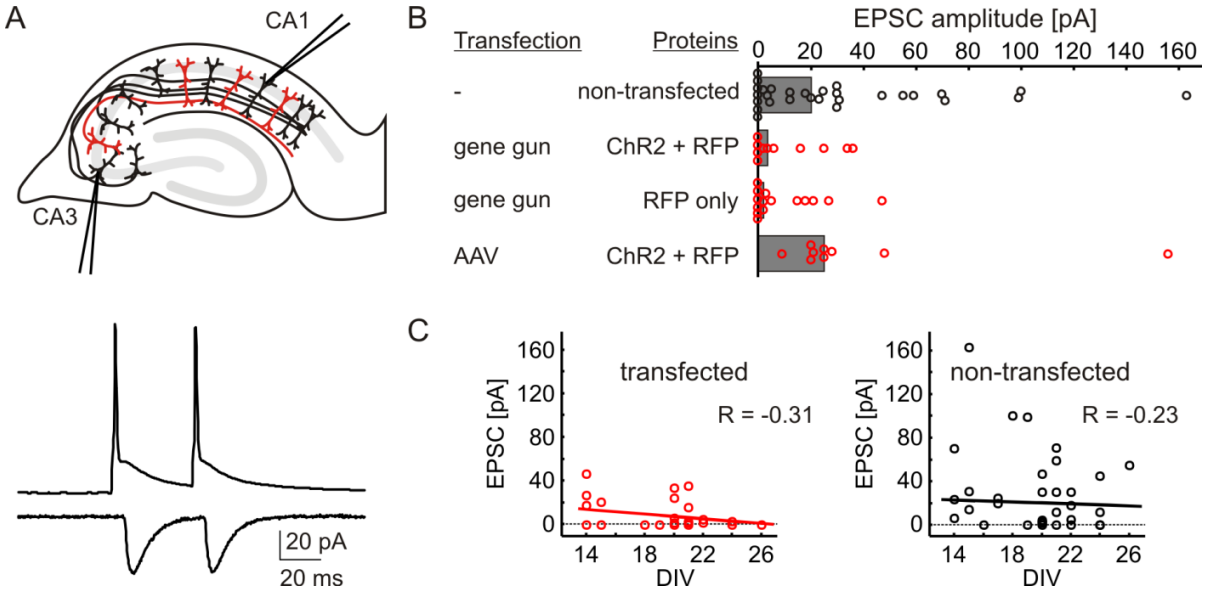

Figure 5. Reduction of excitatory synaptic input by gene gun transfection. *(A) Top: Schematic of recording configuration. Organotypic hippocampal slice cultures were transfected on DIV 6 or 7 using particle-mediated gene transfer to express ChR2 and RFP in a random set of neurons. A non-transfected CA3 neuron was patched and held in current clamp to induce action potentials (APs) by brief current injections. EPSCs in postsynaptic CA1 neurons were recorded in voltage clamp at -65 mV. Bottom: Example traces of two APs in a CA3 neuron (inter-pulse interval = 40 ms) and the corresponding EPSCs in a non-transfected CA1 cell. (B) Summary of EPSC amplitudes in transfected or non-transfected CA1 neurons. Gray bars indicate medians, circles depict individual neurons. Note that gene gun transfection resulted in a strong reduction of synaptic input. (C) In transfected neurons (pooled data from cells expressing ChR2 and RFP or RFP alone) we found a weak and statistically not significant effect of culture age on connection strength (R = -0.31, p = 0.14). EPSC amplitudes in non-transfected neurons were not correlated with culture age (R = -0.23, p = 0.20).*

transfection effect. In transfected neurons, EPSC amplitude trended even lower after prolonged expression (R = -0.31, p = 0.14), whereas EPSC amplitudes in non-transfected neurons were not correlated with culture age (R = -0.23, p = 0.20; Fig. 5C). Culture ages in these experiments were precisely matched (average DIV = 19.2 and 19.6 for transfected and non-transfected neurons, respectively). To investigate whether reduction of synaptic input is generally caused by expression of foreign proteins, I performed control recordings from CA1 neurons transduced with adeno-associated viruses (AAVs) to express ChR2 and tdimer2 (Tang *et al.*, 2009). Injections were done together with Dr. Ingrid Ehrlich at DIV 7. After 2 weeks of expression, photocurrents in virus-transduced neurons were comparable to gene gun-transfected neurons (data not shown). Paired recordings revealed that EPSCs in transduced cells were not reduced compared to non-transfected neurons (25.0 pA; n = 9, p = 0.4), suggesting that the expression of ChR2 and tdimer2 does not result in reduced Schaffer collateral input when CA1 neurons are transduced with AAVs. Together, these data indicate that gene gun transfection can result in reduced synaptic input to CA1 neurons. Expression of transmembrane proteins can induce

cytotoxic effects, but apart from reduced EPSC amplitudes we did not observe any indication that cell viability was impaired after transfection. Furthermore, reduced EPSCs were also observed after transfection with tdimer2 alone. This suggests that the reduction in synaptic input is not due to ChR2 expression but rather a consequence gene gun-transfection, which is further supported by the observation that excitatory input to AAV-transduced CA1 neurons is not altered. Why gene gun transfection reduces synaptic connectivity has remained unclear. A possible explanation is that the mechanical damage caused by the gold particles used for transfection delays the formation of synapses. Since transfection was performed at DIV 7 during synapse formation (De Simoni *et al.*, 2003), transfected neurons may be disadvantaged in the competition for presynaptic partners compared to non-transfected neurons in the same culture, resulting in a developmental deficit in synapse formation. In line with this, EPSC amplitudes were negatively correlated with culture age in transfected neurons. This scenario would thus explain why transfected neurons receive less input from Schaffer collaterals, while the synapses that are present seem fully normal. In conclusion, these findings show that the method of transfection can have strong effects on the synaptic input to transfected neurons. The effect of transfection on the synapses a transfected neuron forms with its postsynaptic partners remains to be tested.

7.4 Alternative transfection methods

A number of viruses have been used to introduce genes into postmitotic neurons. Replication-deficient AAVs have become especially popular because of their low cytotoxicity and their ability to infect a large diversity of neuronal cell types (reviewed in van den Pol *et al.*, 2009). High transgene expression levels can be obtained by injection of large numbers of AAV particles, so that in the injection focus each neuron is infected by many infectious particles. A possible limitation of this approach is that a large fraction of cells is infected near the infection site. Therefore, if fluorescent proteins are expressed, the subcellular structure if individual neurons cannot be investigated because of the high density of fluorescence-labeled structures.

Self-amplifying RNA viruses at very high dilution allow infecting individual neurons and can express proteins at high levels with rapid onset, such that single transduced neurons embedded in non-infected tissue can be studied (Jeromin *et al.*, 2003; van den Pol *et al.*, 2009). Self-amplifying viruses, however, compete with host-cell processes for resources and can confer cytopathic effects after prolonged expression.

Finally, single-cell electroporation can be used to deliver plasmid DNA into single identified neurons (Judkewitz *et al.*, 2009). Because cells can be visually targeted for electroporation and different plasmids can be mixed , this method is very versatile and does not rely on cell-type specific promoters. On the downside, single-cell electroporation is time-consuming and technically challenging.

8. REFERENCES

Adamantidis AR, Zhang F, Aravanis AM, Deisseroth K & de Lecea L (2007). Neural substrates of awakening probed with optogenetic control of hypocretin neurons. *Nature* **450,** 420-424.

Ando H, Furuta T, Tsien RY & Okamoto H (2001). Photo-mediated gene activation using caged RNA/DNA in zebrafish embryos. *Nat Genet* **28,** 317-325.

Aravanis AM, Wang LP, Zhang F, Meltzer LA, Mogri MZ, Schneider MB & Deisseroth K (2007). An optical neural interface: in vivo control of rodent motor cortex with integrated fiberoptic and optogenetic technology. *J Neural Eng* **4,** S143-156.

Arenkiel BR, Peca J, Davison IG, Feliciano C, Deisseroth K, Augustine GJ, Ehlers MD & Feng G (2007). In vivo light-induced activation of neural circuitry in transgenic mice expressing channelrhodopsin-2. *Neuron* **54,** 205-218.

Bading H, Ginty DD & Greenberg ME (1993). Regulation of gene expression in hippocampal neurons by distinct calcium signaling pathways. *Science* **260,** 181-186.

Bamann C, Gueta R, Kleinlogel S, Nagel G & Bamberg E (2010). Structural guidance of the photocycle of channelrhodopsin-2 by an interhelical hydrogen bond. *Biochemistry* **49,** 267-278.

Bamann C, Kirsch T, Nagel G & Bamberg E (2008). Spectral characteristics of the photocycle of channelrhodopsin-2 and its implication for channel function. *J Mol Biol* **375,** 686-694.

Banke TG, Bowie D, Lee H, Huganir RL, Schousboe A & Traynelis SF (2000). Control of GluR1 AMPA receptor function by cAMP-dependent protein kinase. *J Neurosci* **20,** 89-102.

Barria A, Muller D, Derkach V, Griffith LC & Soderling TR (1997). Regulatory phosphorylation of AMPA-type glutamate receptors by CaM-KII during long-term potentiation. *Science* **276,** 2042-2045.

Barth AL, Gerkin RC & Dean KL (2004). Alteration of neuronal firing properties after in vivo experience in a FosGFP transgenic mouse. *J Neurosci* **24,** 6466-6475.

Bastrikova N, Gardner GA, Reece JM, Jeromin A & Dudek SM (2008). Synapse elimination accompanies functional plasticity in hippocampal neurons. *Proc Natl Acad Sci U S A* **105,** 3123-3127.

Becker N, Wierenga CJ, Fonseca R, Bonhoeffer T & Nagerl UV (2008). LTD induction causes morphological changes of presynaptic boutons and reduces their contacts with spines. *Neuron* **60,** 590-597.

Bellone C, Luscher C & Mameli M (2008). Mechanisms of synaptic depression triggered by metabotropic glutamate receptors. *Cell Mol Life Sci* **65,** 2913-2923.

Berndt A, Yizhar O, Gunaydin LA, Hegemann P & Deisseroth K (2009). Bi-stable neural state switches. *Nat Neurosci* **12,** 229-234.

Berndt A, Prigge M, Gradmann D & Hegemann P (2010). Two open states with progressive proton selectivities in the branched channelrhodopsin-2 photocycle. *Biophys J* **98,** 753-761.

Bi GQ & Poo MM (1998). Synaptic modifications in cultured hippocampal neurons: dependence on spike timing, synaptic strength, and postsynaptic cell type. *J Neurosci* **18,** 10464-10472.

Boyden ES, Zhang F, Bamberg E, Nagel G & Deisseroth K (2005). Millisecond-timescale, genetically targeted optical control of neural activity. *Nat Neurosci* **8,** 1263-1268.

Buckmaster A, Nobes CD, Edwards SN & Tolkovsky AM (1991). Nerve Growth Factor is Required for Induction of c-Fos Immunoreactivity by Serum, Depolarization, Cyclic AMP or Trauma in Cultured Rat Sympathetic Neurons. *Eur J Neurosci* **3,** 698-707.

Burrone J, O'Byrne M & Murthy VN (2002). Multiple forms of synaptic plasticity triggered by selective suppression of activity in individual neurons. *Nature* **420,** 414-418.

Busskamp V, Duebel J, Balya D, Fradot M, Viney TJ, Siegert S, Groner AC, Cabuy E, Forster V, Seeliger M, Biel M, Humphries P, Paques M, Mohand-Said S, Trono D, Deisseroth K, Sahel JA, Picaud S & Roska B (2010). Genetic reactivation of cone photoreceptors restores visual responses in retinitis pigmentosa. *Science* **329,** 413-417.

Cambridge SB, Davis RL & Minden JS (1997). Drosophila mitotic domain boundaries as cell fate boundaries. *Science* **277,** 825-828.

Cambridge SB, Geissler D, Calegari F, Anastassiadis K, Hasan MT, Stewart AF, Huttner WB, Hagen V & Bonhoeffer T (2009). Doxycycline-dependent photoactivated gene expression in eukaryotic systems. *Nat Methods* **6,** 527-531.

Campbell RE, Tour O, Palmer AE, Steinbach PA, Baird GS, Zacharias DA & Tsien RY (2002). A monomeric red fluorescent protein. *Proc Natl Acad Sci U S A* **99,** 7877-7882.

Cardin JA, Carlen M, Meletis K, Knoblich U, Zhang F, Deisseroth K, Tsai LH & Moore CI (2009). Driving fast-spiking cells induces gamma rhythm and controls sensory responses. *Nature* **459,** 663-667.

Chow BY, Han X, Dobry AS, Qian X, Chuong AS, Li M, Henninger MA, Belfort GM, Lin Y, Monahan PE & Boyden ES (2010). High-performance genetically targetable optical neural silencing by light-driven proton pumps. *Nature* **463,** 98-102.

De Roo M, Klauser P & Muller D (2008). LTP promotes a selective long-term stabilization and clustering of dendritic spines. *PLoS Biol* **6,** e219.

De Simoni A, Griesinger CB & Edwards FA (2003). Development of rat CA1 neurones in acute versus organotypic slices: role of experience in synaptic morphology and activity. *J Physiol* **550,** 135-147.

Debanne D, Gahwiler BH & Thompson SM (1996). Cooperative interactions in the induction of long-term potentiation and depression of synaptic excitation between hippocampal CA3-CA1 cell pairs in vitro. *Proc Natl Acad Sci U S A* **93,** 11225-11230.

Desai NS, Rutherford LC & Turrigiano GG (1999). Plasticity in the intrinsic excitability of cortical pyramidal neurons. *Nat Neurosci* **2,** 515-520.

Dimitrov D, He Y, Mutoh H, Baker BJ, Cohen L, Akemann W & Knopfel T (2007). Engineering and characterization of an enhanced fluorescent protein voltage sensor. *PLoS ONE* **2,** e440.

Dudek SM & Bear MF (1992). Homosynaptic long-term depression in area CA1 of hippocampus and effects of N-methyl-D-aspartate receptor blockade. *Proc Natl Acad Sci U S A* **89,** 4363-4367.

Engblom D, Bilbao A, Sanchis-Segura C, Dahan L, Perreau-Lenz S, Balland B, Parkitna JR, Lujan R, Halbout B, Mameli M, Parlato R, Sprengel R, Luscher C, Schutz G & Spanagel R (2008). Glutamate receptors on dopamine neurons control the persistence of cocaine seeking. *Neuron* **59,** 497-508.

Engert F & Bonhoeffer T (1999). Dendritic spine changes associated with hippocampal long-term synaptic plasticity. *Nature* **399,** 66-70.

Fischer M, Kaech S, Knutti D & Matus A (1998). Rapid actin-based plasticity in dendritic spines. *Neuron* **20,** 847-854.

Fonseca R, Nagerl UV & Bonhoeffer T (2006a). Neuronal activity determines the protein synthesis dependence of long-term potentiation. *Nat Neurosci* **9,** 478-480.

Fonseca R, Vabulas RM, Hartl FU, Bonhoeffer T & Nagerl UV (2006b). A balance of protein synthesis and proteasome-dependent degradation determines the maintenance of LTP. *Neuron* **52,** 239-245.

Fukazawa Y, Saitoh Y, Ozawa F, Ohta Y, Mizuno K & Inokuchi K (2003). Hippocampal LTP is accompanied by enhanced F-actin content within the dendritic spine that is essential for late LTP maintenance in vivo. *Neuron* **38,** 447-460.

Ge Y, Dong Z, Bagot RC, Howland JG, Phillips AG, Wong TP & Wang YT (2010). Hippocampal long-term depression is required for the consolidation of spatial memory. *Proc Natl Acad Sci U S A* **107,** 16697-16702.

Godley BF, Shamsi FA, Liang FQ, Jarrett SG, Davies S & Boulton M (2005). Blue light induces mitochondrial DNA damage and free radical production in epithelial cells. *J Biol Chem* **280,** 21061-21066.

Gourine AV, Kasymov V, Marina N, Tang F, Figueiredo MF, Lane S, Teschemacher AG, Spyer KM, Deisseroth K & Kasparov S (2010). Astrocytes control breathing through pH-dependent release of ATP. *Science* **329,** 571-575.

Gradinaru V, Mogri M, Thompson KR, Henderson JM & Deisseroth K (2009). Optical deconstruction of parkinsonian neural circuitry. *Science* **324,** 354-359.

Grunditz A, Holbro N, Tian L, Zuo Y & Oertner TG (2008). Spine neck plasticity controls postsynaptic calcium signals through electrical compartmentalization. *J Neurosci* **28,** 13457-13466.

Grutzendler J, Kasthuri N & Gan WB (2002). Long-term dendritic spine stability in the adult cortex. *Nature* **420,** 812-816.

Guex N & Peitsch MC (1997). SWISS-MODEL and the Swiss-PdbViewer: an environment for comparative protein modeling. *Electrophoresis* **18,** 2714-2723.

Gunaydin LA, Yizhar O, Berndt A, Sohal VS, Deisseroth K & Hegemann P (2010). Ultrafast optogenetic control. *Nat Neurosci* **13,** 387-392.

Hagglund M, Borgius L, Dougherty KJ & Kiehn O (2010). Activation of groups of excitatory neurons in the mammalian spinal cord or hindbrain evokes locomotion. *Nat Neurosci* **13,** 246-252.

Harvey CD & Svoboda K (2007). Locally dynamic synaptic learning rules in pyramidal neuron dendrites. *Nature* **450,** 1195-1200.

Harvey CD, Yasuda R, Zhong H & Svoboda K (2008). The Spread of Ras Activity Triggered by Activation of a Single Dendritic Spine. *Science* **321,** 136-140.

Hebb DO (1949). The organization of behavior. *Wiley*.

Hegemann P, Ehlenbeck S & Gradmann D (2005). Multiple photocycles of channelrhodopsin. *Biophys J* **89,** 3911-3918.

Hille B (1992). Ionic channels of excitable membranes. *Sinauer Associates*.

Hofer SB, Mrsic-Flogel TD, Bonhoeffer T & Hubener M (2009). Experience leaves a lasting structural trace in cortical circuits. *Nature* **457,** 313-317.

Holbro N, Grunditz A & Oertner TG (2009). Differential distribution of endoplasmic reticulum controls metabotropic signaling and plasticity at hippocampal synapses. *Proc Natl Acad Sci U S A* **106,** 15055-15060.

Holtmaat A, Wilbrecht L, Knott GW, Welker E & Svoboda K (2006). Experience-dependent and cell-type-specific spine growth in the neocortex. *Nature* **441,** 979-983.

Huber D, Petreanu L, Ghitani N, Ranade S, Hromadka T, Mainen Z & Svoboda K (2008). Sparse optical microstimulation in barrel cortex drives learned behaviour in freely moving mice. *Nature* **451,** 61-64.

Hunt SP, Pini A & Evan G (1987). Induction of c-fos-like protein in spinal cord neurons following sensory stimulation. *Nature* **328,** 632-634.

Ibata K, Sun Q & Turrigiano GG (2008). Rapid synaptic scaling induced by changes in postsynaptic firing. *Neuron* **57,** 819-826.

Kasuga A, Enoki R, Hashimoto Y, Akiyama H, Kawamura Y, Inoue M, Kudo Y & Miyakawa H (2003). Optical detection of dendritic spike initiation in hippocampal CA1 pyramidal neurons. *Neuroscience* **118,** 899-907.

Kubitscheck U, Kuckmann O, Kues T & Peters R (2000). Imaging and tracking of single GFP molecules in solution. *Biophys J* **78,** 2170-2179.

Jeromin A, Yuan LL, Frick A, Pfaffinger P & Johnston D (2003). A modified Sindbis vector for prolonged gene expression in neurons. *J Neurophysiol* **90,** 2741-2745.

Jones EG (1994). Santiago Ramon y Cajal and the Croonian Lecture, March 1894. *Trends Neurosci* **17,** 190-192.
Judkewitz B, Rizzi M, Kitamura K & Hausser M (2009). Targeted single-cell electroporation of mammalian neurons in vivo. *Nat Protoc* **4,** 862-869.
Kamsler A, McHugh TJ, Gerber D, Huang SY & Tonegawa S (2010). Presynaptic m1 muscarinic receptors are necessary for mGluR long-term depression in the hippocampus. *Proc Natl Acad Sci U S* A **107,** 1618-23.
Kane JM & Correll CU Past and present progress in the pharmacologic treatment of schizophrenia. *J Clin Psychiatry* **71,** 1115-1124.
Kauer JA & Malenka RC (2007). Synaptic plasticity and addiction. *Nat Rev Neurosci* **8,** 844-858.
Kelleher RJ, 3rd, Govindarajan A & Tonegawa S (2004). Translational regulatory mechanisms in persistent forms of synaptic plasticity. *Neuron* **44,** 59-73.
Kim J & Tsien RW (2008). Synapse-specific adaptations to inactivity in hippocampal circuits achieve homeostatic gain control while dampening network reverberation. *Neuron* **58,** 925-937.
Kim SH & Ryan TA (2010). CDK5 Serves as a Major Control Point in Neurotransmitter Release. *Neuron* **67,** 797-809.
Knott GW, Holtmaat A, Wilbrecht L, Welker E & Svoboda K (2006). Spine growth precedes synapse formation in the adult neocortex in vivo. *Nat Neurosci* **9,** 1117-1124.
Korade Z & Kenworthy AK (2008). Lipid rafts, cholesterol, and the brain. *Neuropharmacology* **55,** 1265-1273.
Kravitz AV, Freeze BS, Parker PR, Kay K, Thwin MT, Deisseroth K & Kreitzer AC (2010). Regulation of parkinsonian motor behaviours by optogenetic control of basal ganglia circuitry. *Nature* **466,** 622-626.
Kringelbach ML, Jenkinson N, Owen SL & Aziz TZ (2007). Translational principles of deep brain stimulation. *Nat Rev Neurosci* **8,** 623-635.
Kugler S, Meyn L, Holzmuller H, Gerhardt E, Isenmann S, Schulz JB & Bahr M (2001). Neuron-specific expression of therapeutic proteins: evaluation of different cellular promoters in recombinant adenoviral vectors. *Mol Cell Neurosci* **17,** 78-96.
Lagali PS, Balya D, Awatramani GB, Munch TA, Kim DS, Busskamp V, Cepko CL & Roska B (2008). Light-activated channels targeted to ON bipolar cells restore visual function in retinal degeneration. *Nat Neurosci* **11,** 667-675.
Larkum ME, Nevian T, Sandler M, Polsky A & Schiller J (2009). Synaptic integration in tuft dendrites of layer 5 pyramidal neurons: a new unifying principle. *Science* **325,** 756-760.
Lee SJ, Escobedo-Lozoya Y, Szatmari EM & Yasuda R (2009). Activation of CaMKII in single dendritic spines during long-term potentiation. *Nature* **458,** 299-304.
Levskaya A, Weiner OD, Lim WA & Voigt CA (2009). Spatiotemporal control of cell signalling using a light-switchable protein interaction. *Nature* **461,** 997-1001.
Lewis TL, Jr., Mao T, Svoboda K & Arnold DB (2009). Myosin-dependent targeting of transmembrane proteins to neuronal dendrites. *Nat Neurosci* **12,** 568-576.
Lin JY (2010). A User's Guide to Channelrhodopsin Variants: Features, Limitations and Future Developments. *Exp Physiol* **96,** 1803-14.
Lin JY, Lin MZ, Steinbach P & Tsien RY (2009). Characterization of engineered channelrhodopsin variants with improved properties and kinetics. *Biophys J* **96,** 1803-1814.
Losonczy A, Makara JK & Magee JC (2008). Compartmentalized dendritic plasticity and input feature storage in neurons. *Nature* **452,** 436-441.
Luecke H, Schobert B, Richter HT, Cartailler JP & Lanyi JK (1999). Structure of bacteriorhodopsin at 1.55 A resolution. *J Mol Biol* **291,** 899-911.

Lujan R, Nusser Z, Roberts JD, Shigemoto R & Somogyi P (1996). Perisynaptic location of metabotropic glutamate receptors mGluR1 and mGluR5 on dendrites and dendritic spines in the rat hippocampus. *Eur J Neurosci* **8,** 1488-1500.

Luscher C & Huber KM Group 1 mGluR-dependent synaptic long-term depression: mechanisms and implications for circuitry and disease. *Neuron* **65,** 445-459.

Luthi A, Chittajallu R, Duprat F, Palmer MJ, Benke TA, Kidd FL, Henley JM, Isaac JT & Collingridge GL (1999). Hippocampal LTD expression involves a pool of AMPARs regulated by the NSF-GluR2 interaction. *Neuron* **24,** 389-399.

Malenka RC & Bear MF (2004). LTP and LTD: an embarrassment of riches. *Neuron* **44,** 5-21.

Maletic-Savatic M, Malinow R & Svoboda K (1999). Rapid dendritic morphogenesis in CA1 hippocampal dendrites induced by synaptic activity. *Science* **283,** 1923-1927.

Mank M, Santos AF, Direnberger S, Mrsic-Flogel TD, Hofer SB, Stein V, Hendel T, Reiff DF, Levelt C, Borst A, Bonhoeffer T, Hubener M & Griesbeck O (2008). A genetically encoded calcium indicator for chronic in vivo two-photon imaging. *Nat Methods* **5,** 805-811.

Mao T, O'Connor DH, Scheuss V, Nakai J & Svoboda K (2008). Characterization and subcellular targeting of GCaMP-type genetically-encoded calcium indicators. *PLoS ONE* **3,** e1796.

Markram H, Lubke J, Frotscher M & Sakmann B (1997). Regulation of synaptic efficacy by coincidence of postsynaptic APs and EPSPs. *Science* **275,** 213-215.

Martina M, Schultz JH, Ehmke H, Monyer H & Jonas P (1998). Functional and molecular differences between voltage-gated K+ channels of fast-spiking interneurons and pyramidal neurons of rat hippocampus. *J Neurosci* **18,** 8111-8125.

Mast SO (1916). The process of orientation in the colonial organism, Gonium pectorale, and a study of the structure and function of the eye-spot. *J. Exp. Zool.* **20,** 1-17.

Matsuo N, Reijmers L & Mayford M (2008). Spine-type-specific recruitment of newly synthesized AMPA receptors with learning. *Science* **319,** 1104-1107.

Matsuzaki M, Honkura N, Ellis-Davies GC & Kasai H (2004). Structural basis of long-term potentiation in single dendritic spines. *Nature* **429,** 761-766.

McGaugh JL (2000). Memory--a century of consolidation. *Science* **287,** 248-251.

Morgan JI, Cohen DR, Hempstead JL & Curran T (1987). Mapping patterns of c-fos expression in the central nervous system after seizure. *Science* **237,** 192-197.

Morris RG, Anderson E, Lynch GS & Baudry M (1986). Selective impairment of learning and blockade of long-term potentiation by an N-methyl-D-aspartate receptor antagonist, AP5. *Nature* **319,** 774-776.

Murphy TH, Worley PF & Baraban JM (1991). L-type voltage-sensitive calcium channels mediate synaptic activation of immediate early genes. *Neuron* **7,** 625-635.

Murthy VN, Schikorski T, Stevens CF & Zhu Y (2001). Inactivity produces increases in neurotransmitter release and synapse size. *Neuron* **32,** 673-682.

Nader K, Schafe GE & Le Doux JE (2000). Fear memories require protein synthesis in the amygdala for reconsolidation after retrieval. *Nature* **406,** 722-726.

Nagel G, Brauner M, Liewald JF, Adeishvili N, Bamberg E & Gottschalk A (2005). Light activation of channelrhodopsin-2 in excitable cells of Caenorhabditis elegans triggers rapid behavioral responses. *Curr Biol* **15,** 2279-2284.

Nagel G, Kelety B, Mockel B, Buldt G & Bamberg E (1998). Voltage dependence of proton pumping by bacteriorhodopsin is regulated by the voltage-sensitive ratio of M1 to M2. *Biophys J* **74,** 403-412.

Nagel G, Ollig D, Fuhrmann M, Kateriya S, Musti AM, Bamberg E & Hegemann P (2002). Channelrhodopsin-1: a light-gated proton channel in green algae. *Science* **296,** 2395-2398.

Nagel G, Szellas T, Huhn W, Kateriya S, Adeishvili N, Berthold P, Ollig D, Hegemann P & Bamberg E (2003). Channelrhodopsin-2, a directly light-gated cation-selective membrane channel. *Proc Natl Acad Sci U S A* **100,** 13940-13945.

Nagerl UV, Eberhorn N, Cambridge SB & Bonhoeffer T (2004). Bidirectional activity-dependent morphological plasticity in hippocampal neurons. *Neuron* **44,** 759-767.

Nikolic K, Grossman N, Grubb MS, Burrone J, Toumazou C & Degenaar P (2009). Photocycles of channelrhodopsin-2. *Photochem Photobiol* **85,** 400-411.

Oertner TG, Sabatini BL, Nimchinsky EA & Svoboda K (2002). Facilitation at single synapses probed with optical quantal analysis. *Nat Neurosci* **5,** 657-664.

Oliet SH, Malenka RC & Nicoll RA (1997). Two distinct forms of long-term depression coexist in CA1 hippocampal pyramidal cells. *Neuron* **18,** 969-982.

Papagiakoumou E, Anselmi F, Begue A, de Sars V, Gluckstad J, Isacoff EY & Emiliani V (2010). Scanless two-photon excitation of channelrhodopsin-2. *Nat Methods* **7,** 848-854.

Petreanu L, Huber D, Sobczyk A & Svoboda K (2007). Channelrhodopsin-2-assisted circuit mapping of long-range callosal projections. *Nat Neurosci* **10,** 663-668.

Petreanu L, Mao T, Sternson SM & Svoboda K (2009). The subcellular organization of neocortical excitatory connections. *Nature **457,** 1142-5.*

Pologruto TA, Sabatini BL & Svoboda K (2003). ScanImage: flexible software for operating laser scanning microscopes. *Biomed Eng Online* **2,** 13.

Pozo K & Goda Y (2010). Unraveling mechanisms of homeostatic synaptic plasticity. *Neuron* **66,** 337-351.

Reijmers LG, Perkins BL, Matsuo N & Mayford M (2007). Localization of a stable neural correlate of associative memory. *Science* **317,** 1230-1233.

Rickgauer JP & Tank DW (2009). Two-photon excitation of channelrhodopsin-2 at saturation. *Proc Natl Acad Sci U S A* **106,** 15025-15030.

Ritter E, Stehfest K, Berndt A, Hegemann P & Bartl FJ (2008). Monitoring light-induced structural changes of Channelrhodopsin-2 by UV-visible and Fourier transform infrared spectroscopy. *J Biol Chem* **283,** 35033-35041.

Rose T, Schoenenberger P & Oertner TG (unpublished). Dynamic control of vesicle use at Schaffer collateral boutons.

Scanziani M & Hausser M (2009). Electrophysiology in the age of light. *Nature* **461,** 930-939.

Schoenenberger P, Gerosa D & Oertner TG (2009). Temporal control of immediate early gene induction by light. *PLoS ONE* **4,** e8185.

Schoenenberger P, Grunditz A, Rose T & Oertner TG (2008). Optimizing the spatial resolution of Channelrhodopsin-2 activation. *Brain Cell Biol* **36,** 119-127.

Schroder-Lang S, Schwarzel M, Seifert R, Strunker T, Kateriya S, Looser J, Watanabe M, Kaupp UB, Hegemann P & Nagel G (2007). Fast manipulation of cellular cAMP level by light in vivo. *Nat Methods* **4,** 39-42.

Skeberdis VA, Chevaleyre V, Lau CG, Goldberg JH, Pettit DL, Suadicani SO, Lin Y, Bennett MV, Yuste R, Castillo PE & Zukin RS (2006). Protein kinase A regulates calcium permeability of NMDA receptors. *Nat Neurosci* **9,** 501-510.

Smeyne RJ, Schilling K, Robertson L, Luk D, Oberdick J, Curran T & Morgan JI (1992). fos-lacZ transgenic mice: mapping sites of gene induction in the central nervous system. *Neuron* **8,** 13-23.

Sohal VS, Zhang F, Yizhar O & Deisseroth K (2009). Parvalbumin neurons and gamma rhythms enhance cortical circuit performance. *Nature* **459,** 698-702.

Song I & Huganir RL (2002). Regulation of AMPA receptors during synaptic plasticity. *Trends Neurosci* **25,** 578-588.

Stehfest K, Ritter E, Berndt A, Bartl F & Hegemann P (2010). The branched photocycle of the slow-cycling channelrhodopsin-2 mutant C128T. *J Mol Biol* **398,** 690-702.

Stevens JC & Pollack MH (2005). Benzodiazepines in clinical practice: consideration of their long-term use and alternative agents. *J Clin Psychiatry* **66 Suppl 2,** 21-27.

Stierl M, Stumpf P, Udwari D, Gueta R, Hagedorn R, Losi A, Gärtner W, Petereit L, Eftowa M, Schwarzel M, Oertner TG, Nagel G & Hegemann P (2010). Light-modulation of cellular cAMP by a small bacterial photoactivated adenylyl cyclase, bPAC, of the soil bacterium Beggiatoa. *Journal of Biological Chemistry* **in press**.

Stoppini L, Buchs PA & Muller D (1991). A simple method for organotypic cultures of nervous tissue. *J Neurosci Methods* **37,** 173-182.

Stosiek C, Garaschuk O, Holthoff K & Konnerth A (2003). In vivo two-photon calcium imaging of neuronal networks. *Proc Natl Acad Sci U S A* **100,** 7319-7324.

Suter BA, O'Connor T, Iyer V, Petreanu L, Hooks BM, Kiritani T, Svoboda K & Shepherd GMG (2010). Ephus: multipurpose data acquisition software for neuroscience experiments. *Frontiers in Neuroscience* **4,** 12.

Tanaka J, Horiike Y, Matsuzaki M, Miyazaki T, Ellis-Davies GC & Kasai H (2008). Protein synthesis and neurotrophin-dependent structural plasticity of single dendritic spines. *Science* **319,** 1683-1687.

Tang W, Ehrlich I, Wolff SB, Michalski AM, Wolfl S, Hasan MT, Luthi A & Sprengel R (2009). Faithful expression of multiple proteins via 2A-peptide self-processing: a versatile and reliable method for manipulating brain circuits. *J Neurosci* **29,** 8621-8629.

Tian L, Hires SA, Mao T, Huber D, Chiappe ME, Chalasani SH, Petreanu L, Akerboom J, McKinney SA, Schreiter ER, Bargmann CI, Jayaraman V, Svoboda K & Looger LL (2009). Imaging neural activity in worms, flies and mice with improved GCaMP calcium indicators. *Nat Methods* **6,** 875-881.

Toni N, Buchs PA, Nikonenko I, Bron CR & Muller D (1999). LTP promotes formation of multiple spine synapses between a single axon terminal and a dendrite. *Nature* **402,** 421-425.

Trachtenberg JT, Chen BE, Knott GW, Feng G, Sanes JR, Welker E & Svoboda K (2002). Long-term in vivo imaging of experience-dependent synaptic plasticity in adult cortex. *Nature* **420,** 788-794.

Tronson NC, Schrick C, Guzman YF, Huh KH, Srivastava DP, Penzes P, Guedea AL, Gao C & Radulovic J (2009). Segregated populations of hippocampal principal CA1 neurons mediating conditioning and extinction of contextual fear. *J Neurosci* **29,** 3387-3394.

Tsien JZ, Huerta PT & Tonegawa S (1996). The essential role of hippocampal CA1 NMDA receptor-dependent synaptic plasticity in spatial memory. *Cell* **87,** 1327-1338.

Turrigiano GG, Leslie KR, Desai NS, Rutherford LC & Nelson SB (1998). Activity-dependent scaling of quantal amplitude in neocortical neurons. *Nature* **391,** 892-896.

Ungless MA, Whistler JL, Malenka RC & Bonci A (2001). Single cocaine exposure in vivo induces long-term potentiation in dopamine neurons. *Nature* **411,** 583-587.

van den Pol AN, Ozduman K, Wollmann G, Ho WS, Simon I, Yao Y, Rose JK & Ghosh P (2009). Viral strategies for studying the brain, including a replication-restricted self-amplifying delta-G vesicular stomatis virus that rapidly expresses transgenes in brain and can generate a multicolor golgi-like expression. *J Comp Neurol* **516,** 456-481.

Wang H, Peca J, Matsuzaki M, Matsuzaki K, Noguchi J, Qiu L, Wang D, Zhang F, Boyden E, Deisseroth K, Kasai H, Hall WC, Feng G & Augustine GJ (2007). High-speed mapping of synaptic connectivity using photostimulation in Channelrhodopsin-2 transgenic mice. *Proc Natl Acad Sci U S A* **104,** 8143-8148.

Wen L, Wang H, Tanimoto S, Egawa R, Matsuzaka Y, Mushiake H, Ishizuka T & Yawo H (2010). Opto-current-clamp actuation of cortical neurons using a strategically designed channelrhodopsin. *PLoS ONE* **5,** e12893.

Wilbrecht L, Holtmaat A, Wright N, Fox K & Svoboda K (2010). Structural plasticity underlies experience-dependent functional plasticity of cortical circuits. *J Neurosci* **30,** 4927-4932.

Yang G, Pan F & Gan WB (2009). Stably maintained dendritic spines are associated with lifelong memories. *Nature* **462,** 920-924.
Ye H, Kuruvilla R, Zweifel LS & Ginty DD (2003). Evidence in support of signaling endosome-based retrograde survival of sympathetic neurons. *Neuron* **39,** 57-68.
Zemelman BV, Lee GA, Ng M & Miesenbock G (2002). Selective photostimulation of genetically chARGed neurons. *Neuron* **33,** 15-22.
Zhang F, Prigge M, Beyriere F, Tsunoda SP, Mattis J, Yizhar O, Hegemann P & Deisseroth K (2008a). Red-shifted optogenetic excitation: a tool for fast neural control derived from Volvox carteri. *Nat Neurosci* **11,** 631-633.
Zhang F, Wang LP, Boyden ES & Deisseroth K (2006). Channelrhodopsin-2 and optical control of excitable cells. *Nat Methods* **3,** 785-792.
Zhang F, Aravanis AM, Adamantidis A, de Lecea L & Deisseroth K (2007). Circuit-breakers: optical technologies for probing neural signals and systems. *Nat Rev Neurosci* **8,** 577-581.
Zhang K & Kaufman RJ (2006). Protein folding in the endoplasmic reticulum and the unfolded protein response. *Handb Exp Pharmacol***,** 69-91.
Zhang YP, Holbro N & Oertner TG (2008b). Optical induction of plasticity at single synapses reveals input-specific accumulation of {alpha}CaMKII. *Proc Natl Acad Sci U S A* **105,** 12039-12044.
Zhang YP & Oertner TG (2007). Optical induction of synaptic plasticity using a light-sensitive channel. *Nat Methods* **4,** 139-141.
Zhu P, Narita Y, Bundschuh ST, Fajardo O, Scharer YP, Chattopadhyaya B, Bouldoires EA, Stepien AE, Deisseroth K, Arber S, Sprengel R, Rijli FM & Friedrich RW (2009). Optogenetic Dissection of Neuronal Circuits in Zebrafish using Viral Gene Transfer and the Tet System. *Front Neural Circuits* **3,** 21.

9. ABBREVIATIONS

AAV:	adeno-associated virus
ACSF:	artificial cerebrospinal fluid
AMPA:	α-amino-3-hydroxy-5-methylisoxazole-4-propionic acid
AP:	action potential
CA:	cornu ammonis
CC:	current-clamp
CaMKII:	calcium/calmodulin-dependent protein kinase II
ChR2:	channelrhodopsin-2
DIV:	day in vitro
EPSC:	excitatory postsynaptic current
EPSP:	excitatory postsynaptic potential
GFP:	green fluorescent protein
IEG:	Immediate early gene
LED:	light emitting diode
LFS:	low frequency stimulation
LTD:	long-term depression
LTP:	long-term potentiation
mGluR:	metabotropic glutamate receptor
NMDA:	N-methyl-D-aspartate
STDP:	spike timing-dependent plasticity
wt:	wild-type
VC:	voltage-clamp
VTA:	ventral tegmental area

10. ACKNOWLEDGEMENTS

I am very grateful to Thomas Oertner for exciting projects, constant support, lots of help and many discussions. Working with Thomas I think I have learned to understand the function of neurons really from molecules and potentials to plasticity, which will be a valuable fundament for my future work.

Many thanks also to all current and past members of the Oertner lab, without whom my work would not have been possible and certainly not much fun. Very special thanks to Åsa, Yan-Ping, Nik and Tobias for a lot of help in the first months in the lab and for teaching me the necessary basics to work with neurons. And a big thank-you to Daniela for providing great cultures, help with many things in the lab, and for being an important person in creating a nice working atmosphere.

I want to thank Silvia Arber and Andreas Lüthi for giving me advice and providing ideas in the annual thesis committee meeting. I also thank Dominique Muller being second reader of my thesis.

I thank the many colleagues at FMI for discussions, help, reagents, and for a pleasant and motivating working environment.

Special thanks also to several people from the FMI technical platforms, whose help I needed on many opportunities, especially Sjoerd van Eeden, Alan Naylor, Paul Argast, and Aaron Ponti.

Finally, I am grateful to my mum and my sisters for mental support during my many years of study, and to Stephanie for support, encouragement, understanding, and a place to look forward to.